

UNIVERSITÀ DEGLI STUDI DI PADOVA

DIPARTIMENTO DI INGEGNERIA INDUSTRIALE

CORSO DI LAUREA MAGISTRALE IN INGEGNERIA CHIMICA E DEI PROCESSI INDUSTRIALI

Tesi di Laurea Magistrale in Ingegneria Chimica e dei Processi
Industriali

COMPARISON OF HOMOGENEOUS AND
HETEROGENEOUS HYDROLYSIS OF ALGAL
BIOMASS

Relatore: Prof. Paolo Canu

Correlatore: Prof. Jyri-Pekka Mikkola

Laureando: Andrea Baccini

ANNO ACCADEMICO 2015-2016

*"The Road goes ever on and on,
Down from the door where it began.
Now far ahead the Road has gone,
And I must follow, if I can,
Pursuing it with eager feet,
Until it joins some larger way
Where many paths and errands meet.
And whither then? I cannot say"*

J. R. R. TOLKIEN

Abstract

In the perspective of the future development of bio refinery based on third generation feedstock, the interest towards the algal biomass has recently increased. Algal biomass could provide a renewable carbon neutral feedstock which can be used to produce fuels and fine chemicals. Indeed, algae have several advantages over first and second biomass feedstock. First, biomass derived from algae does not compete with land crop production, consequently the fuel vs food debate will be settled. Moreover, the higher growing rate and the lower amount of lignin that occur in algae will significantly reduce the energy required to pre-treat the raw material in agreement with the bio refinery implementation concept. Notwithstanding, some issues such as the high concentration of water and the seasonality in the chemical composition are challenges that make algae products not yet economically feasible.

The present work was focused on the acid hydrolysis of a carbohydrate called ulvan into its main constituents, rhamnose (Rha) and glucuronic acid (GlcA), which could be further transformed into high value platform molecules. The performance between the traditional homogenous and the heterogeneous acid hydrolysis catalysis were evaluated. Different reaction conditions respectively temperature (90°C-120°C), acidity (50-100mMH⁺eq) and catalyst type (HCl, SMOPEX101, AMB70) were varied in order to evaluate their influence on the monomers yield. The best results in terms of yield were obtained at 110°C and 100mMH⁺eq for both the heterogeneous and the homogenous catalysis, accounting for almost 90% for rhamnose after 48h of reaction. However, these results are referred only to the yield of rhamnose. In fact, an unknown interaction between GlcA and the acid resin was believed to be responsible of the reduction of the yield of GlcA. Eventually, a simple kinetic modelling study was done in order to determine the activation energy (E_a) and the preexponential factor (A) of the reactions involved in the hydrolysis of ulvan according to the suggested reaction mechanism.

This was the first time that the hydrolysis of ulvan was studied in such a way that a high yield of rhamnose was attained and a reasonable model of the kinetics of the hydrolysis reaction was developed. However, more work is needed to give better understanding to the GlcA decomposition phenomena under sulphonic acid bearing resins, and more experimental data to better validate the model hereby proposed.

Riassunto

Negli ultimi decenni, l'interesse verso la biomassa derivante dalle alghe é cresciuto, nell'ottica del futuro sviluppo delle bioraffinerie alimentate da biomassa di terza generazione. La biomassa derivante dalle alghe fornirebbe una fonte di materia prima a base di carbonio a impatto zero, al fine di produrre carburanti e diversi prodotti della chimica fine. Diversi sono i vantaggi che le alghe hanno rispetto alla biomassa di prima e seconda generazione attualmente processate nelle bioraffinerie. In primo luogo, la produzione di alghe non interferisce con i raccolti terrestri, di conseguenza non sussisterebbe l'attuale dibattito carburanti vs cibo. In secondo luogo, il maggior tasso di crescita e i livelli inferiori di lignina presenti nella biomassa derivante da alghe, consentirebbero una sostanziale riduzione dell'energia necessaria per il pretrattamento del materiale grezzo, in accordo con i principi di una bioraffineria. Tuttavia, la stagionalità della composizione chimica delle alghe unita all'alto contenuto di acqua presente nella biomassa rendono i prodotti derivati dalle alghe attualmente economicamente svantaggiosi.

Il presente progetto di tesi si propone di studiare l'idrolisi acida di un polisaccaride, noto come ulvan, nelle sue unità fondamentali, il rhamnosio (Rha) e l'acido glucuronico (GlcA), i quali possono essere successivamente trasformati in prodotti ad alto valore aggiunto. Sono state valutate le prestazioni, in termini di resa di monomero, tra la tradizionale catalisi omogenea e la catalisi eterogenea. Differenti condizioni di reazione quali temperatura (90-120°C), acidità (50-100mMH⁺eq) e tipo di catalizzatore (HCl, SMOPEX101, AMB70), sono state variate al fine di valutarne l'influenza sulla resa di monomero. I valori di resa piú alti sono stati ottenuti a 110°C e 100mMH⁺eq per entrambi gli approcci di catalisi, nello specifico un valore superiore all'80% é stato ottenuto per il rhamnosio in 48h di reazione. Tuttavia, i valori sono riferiti al solo rhamnosio. Di fatto, un'interazione non definita tra GlcA e il catalizzatore solido si ritiene sia responsabile del crollo della resa finale di acido glucuronico. Infine, un semplice studio di modellazione cinetica ha permesso di determinare le energie di attivazione (E_a) e i parametri pre-esponenziali (A) delle reazioni che prendono parte all'idrolisi dell'ulvan, secondo i meccanismi di reazione ipotizzati nello studio. Questo progetto é il primo del suo genere nel quale l'idrolisi dell'ulvan é stata studiata e ottimizzata, al fine di ottenere una considerevole resa in rhamnosio, e un ragionevole modello cinetico della reazione di idrolisi é stato sviluppato. Tuttavia, sono necessarie ulteriori indagini al fine di ottenere una miglior comprensione dei fenomeni di decomposizione dell'acido glucuronico ad opera dei gruppi sulfonici graffiati alla resina. Ulteriori dati sperimentali sono inoltre necessari al fine di consolidare il modello cinetico proposto.

Contents

Introduction	1
1 Basics on algae	5
1.1 Definition	5
1.2 Classification	5
1.2.1 Thallus	6
1.2.2 Nutrition	7
1.2.3 Photosynthesis	7
1.2.4 Reproduction	8
1.2.5 Cell anatomy	8
1.2.6 Nucleus	11
1.3 Green Algae	12
1.3.1 Biochemical composition	12
1.3.2 Production	18
1.3.3 Interesting products and uses	19
1.4 <i>Ulva rigida</i>	21
1.4.1 Chemistry of <i>Ulva rigida</i>	21
2 Theoretical background	29
2.1 Hydrolysis	29
2.1.1 Mechanism of acid hydrolysis	30
2.1.2 Parameters affecting the hydrolysis	31
2.2 Acid catalysis	32
2.2.1 Homogeneous acid catalysis	32
2.2.2 Heterogeneous acid catalysis	33
2.2.3 Enzymatic Hydrolysis	38
2.3 Algae carbohydrates and Hemicellulose hydrolysis state of art	39
2.4 Glucuronic acid decomposition	41
2.5 Analytical techniques	43
2.5.1 Gas chromatography	45
2.5.2 Liquid chromatography	47
3 Materials and methods	49
3.1 Ulvan extraction reactor and procedure	49
3.1.1 Algae washing	50
3.2 Ulvan Hydrolysis reactor and procedure	51

3.2.1	Catalyst pretreatment	53
3.3	Raw materials	53
3.3.1	Algae	53
3.3.2	Catalysts	54
3.4	Analysis	56
3.4.1	Total sugar content	57
3.4.2	Monomer content	57
3.4.3	Gas chromatography	58
3.4.4	HPLC	58
3.5	Experimental matrix	58
3.5.1	Temperature	58
3.5.2	Acidic concentration	59
3.5.3	Reutilization of the catalyst	59
4	Experimental results	61
4.1	Total sugar content t=0	61
4.2	Heterogeneous acid hydrolysis results	63
4.2.1	Temperature effect	63
4.2.2	Acidity concentration effect	65
4.2.3	Catalyst type	66
4.2.4	Catalyst reutilization	68
4.3	Homogeneous acid hydrolysis	69
4.4	Glucuronic acid decomposition	74
4.5	Variability analysis	77
5	Kinetic Modelling	83
5.1	Homogeneous reaction mechanisms	83
5.2	Homogeneous mechanisms of ulvan hydrolysis	84
5.2.1	Parameter estimation results	88
5.3	Heterogeneous reaction mechanisms	93
5.3.1	Heterogeneous mechanisms of ulvan hydrolysis	94
	Conclusions	99
	Appendix A	105
A.1	Total carbohydrates content	105
A.1.1	Methanolysis protocol	105
A.1.2	Silylation protocol	106
A.2	Monomer analysis content (Heterogeneous samples)	106
	Appendix B	109
B.1	Ulvan extraction	109
B.2	HPLC Calibration	109
	Appendix C	113
C.1	TEM results	113
	Bibliography	125

List of Tables

3.1	Sampling Interval	52
3.2	Catalysts properties	56
3.3	Experimental matrix	59
4.1	Total sugar content of samples 0h	62
4.2	Estimation of the degradation rate (equation (4.3)) in the homogeneous catalysis for both Rha and GlcA	72
4.3	Experimental conditions to study the decomposition of glucuronic acid	74
4.4	Variability results in ulvan hydrolysis with HCl at different temperatures. Mean concentration, standard deviation and coefficient of variation are given	78
4.5	Variability results in ulvan hydrolysis with SMOPEX-101 using different acid concentration. Mean concentration, standard deviation and coefficient of variation are given	80
5.1	Degree of explanations for the homogeneous models	91
5.2	95% IC for the homogeneous models parameters	92
5.3	Degree of explanations for the heterogeneous model	96
5.4	95% IC for the homogeneous models parameters	97
B.1	Results for the ulvan (U) mass balance on the washing procedure (fresh, solid, liquid), and values for the liquid phase after 4h of hot water extraction (unpublished data)	109
B.2	Calibration results for the compounds analyze in HPLC	110

List of Figures

1	Diagram of an integrated bio-refinery	2
1.1	Colony of <i>Pediastrum</i> Sp. (a), Portion of the thallus of <i>Acetabularia</i> sp. (b) [4]	6
1.2	Schematic drawing of a simple cell membrane [4]	9
1.3	Chloroplast, cyanobacterium comparison	11
1.4	Pyranosic and furanosic forms of Ribose [93]	15
1.5	Structural heterogeneity of agar (a), and structure of carrageen in the κ form, [96]	17
1.6	Cycloeudesmol structure [41]	20
1.7	Bar graph and table showing different biochemical parameters of general <i>Ulva</i> and <i>Ulva Rigida</i> [85]	21
1.8	Distribution of the different <i>Ulva</i> sp. cell wall polysaccharides in a thallus cross section [96]	22
1.9	Chemical structure of the 4 disaccharides forming Ulvan [72]	23
1.10	Structure of Ulvan gel [12]	24
1.11	Heparyn structure	25
2.1	Mechanism of hydrolytic cleavage of glycosidic bonds	31
2.2	Zeolites (a), Ion exchange resin in beads form (b), superacid fibrous catalyst (c)	35
2.3	Ionic exchange resin structure (a), Amberlyst 15 resin structure [20][71]	37
2.4	Smopex101 structure	37
2.5	Different enzymes and their relative action [38]	39
2.6	Equilibrium between GlcA and GlcL [99]	42
2.7	Acid detected from the hydrothermal decomposition of GlcA [58]	43
2.8	Mechanism of trimethylsilyl silylation [87]	46
3.1	Extraction reactor diagram	50
3.2	Schematic picture of the reactor setup (a), Autoclave vessel section (b)	51
3.3	Monosaccharide content in <i>Ulva Rigida</i> used in this project [72]	54
3.4	SEM images of SMOPEX-101, Scientific Figure on ResearchGate. Available from: https://www.researchgate.net/239156190_fig1_Fig-1-SEM-Image-of-the-Smopex-101-fibres-a-fibre-physical-appearance-b-fibre	55
4.1	Rhamnose yield as a function of time in experiments 1,2,3	63
4.2	Glucuronic acid yield as a function of time in experiments 1,2,3	64

4.3	Rhamnose yield as function of time in experiment 2,4,5	65
4.4	Glucuronic acid yield as function of time in experiment 2,4,5	66
4.5	Rhamnose yield as a function of time in experiments 2,4,6,7	67
4.6	Glucuronic acid yield as a function of time in experiments 2,4,6,7	67
4.7	Rhamnose yield as a function of time in experiments 2,12	68
4.8	Glucuronic acid yield as a function of time in experiments 2,12	69
4.9	Fresh S101 (a), after the first run S101 (b), after the second run S101 (c)	70
4.10	Glucuronic acid yield as a function of time in experiments 8,9,10,11	71
4.11	Glucuronic acid yield as a function of time in experiments 8,9,10,11	72
4.12	Rhamnose yield as a function of time in experiments 2,11	73
4.13	Glucuronic acid yield as a function of time in experiments 2,11	74
4.14	Glucuronic acid and Glucuronic acid- γ -lactone concentrations as function of time in experiment 13,14	75
4.15	Glucuronic acid conversion as a function of time in experiments 13,14	76
4.16	Glucuronic acid and detected calibration compounds concentration as a function of time in experiment 11	77
4.17	Homogenous acid hydrolysis results of ulvan at different temperatures with the relative variability, showing formation of Rha(a) and GlcA(b)	79
4.18	Heterogeneous acid hydrolysis results of ulvan at different temperatures with the relative variability, showing formation of Rha(a) and GlcA(b)	81
5.1	Homogeneous hydrolysis mechanism of hemicellulose in the work of Wärnå et al. [84]	84
5.2	Homogeneous hydrolysis mechanism #1 of Ulvan considered	85
5.3	Homogeneous hydrolysis mechanism #2 of Ulvan considered	87
5.4	Homogeneous hydrolysis mechanism #3 of Ulvan considered	88
5.5	Modelling results for the homogeneous kinetic experimental data of Rha	90
5.6	Modelling results for the homogeneous kinetic experimental data of GlcA	91
5.7	Homogeneous hydrolysis mechanism of hemicellulose in the work of Wärnå [84]	94
5.8	Suggested mechanism based on the work of Wärnå et al. [84]	95
5.9	Modelling results for the heterogeneous kinetic experimental data of Rha	96
C.1	TEM image of the cross section of the fresh SMOPEX101	114
C.2	TEM image of the cross section of the SMOPEX101 after the second run	114

Nomenclature

σ	Standard deviation
σ^*	Coefficient of variation
A	Pre-exponential factor, collision factor
C	Concentration
C_{0i}	Concentration of monomer i in the unhydrolyzed chain
C_{avg}	Mean concentration
cal	calibration
Ea	Activation energy
f_i	correction factor
ID	Internal diameter
IL	Internal length
m_{cat}	Catalyst mass
OAD	Outer autoclave diameter
OAL	Outer autoclave length
OD	Outer diameter
R	Ideal gas constant
R_i	Kinetic rate of reaction i
R_i^2	Degree of explanation of component i
std	Standard
V	Volume
W_{lft}	Water left in the washed catalyst
X	Conversion

x_{wt} weight fraction
 Y Yield
Glc Glucose
GlcA Glucuronic acid
GlcA γ L Glucuronic acid gamma lactone
HMF Hydroxymethylfurfural
Man Mannose
Rha Rhamnose
Xyl Xylose

Introduction

In the last few decades the limited availability, environmental concerns and the critical dependency of global economy on fossil feedstock have created an increasing interest in the research and exploitation of biomass as a commercial source, to supply fuels and a number of valuable products.

First-generation biomass feedstock, such as corn and soybean were first exploited in order to produce alternative transportation fuels. The initial effort was focused on the greenhouse gases mitigation to reduce the carbon dioxide atmospheric concentration, which has risen tremendously over the last decades [89]. In addition to that the higher prices that oil reached during the last decade triggered the investment in this technology. However, the food vs fuel, the low net energy balance and the unknown economic impact debates that have resulted, boosted the research to different type of biomass feedstock to the so called second generation biomass. The second-generation biomass claimed to face the issues according to its nature. Indeed, second generation biomass comes from waste streams of paper and agricultural industries. Furthermore, other non edible crops such as grass straws, puddy ask and other herbaceous materials are considered among the second generation feedstock [88]. Anyhow, second generation biomass does not offer clear advantages in terms of the use of land and water supply. Moreover, the current conversion technologies are either not completely developed or economically profitable. The term third generation biomass feedstock refers to organic matter derived entirely from algae. Formerly, algae were considered as second-generation biomass. However, thanks to their higher growth yield, with less resource input, than the other feedstock, many suggested to create a new feedstock category. Furthermore, algae have no lignin, except for a few exceptions [100]. Indeed, due to their aquatic living environment, they don't need this structural polymer. Therefore, the extraction of carbohydrates, to be further hydrolyzed, should result in an easier process. Moreover, the lower amount of glucan with respect to terrestrial plant, on behalf of a number of different an interesting carbohydrates makes algal biomass very interesting in the bio-refinery scenario. Contrarily to terrestrial biomass, algal biomass is constituted also by a peculiar type of polysaccharides, the so called sulphated polysac-

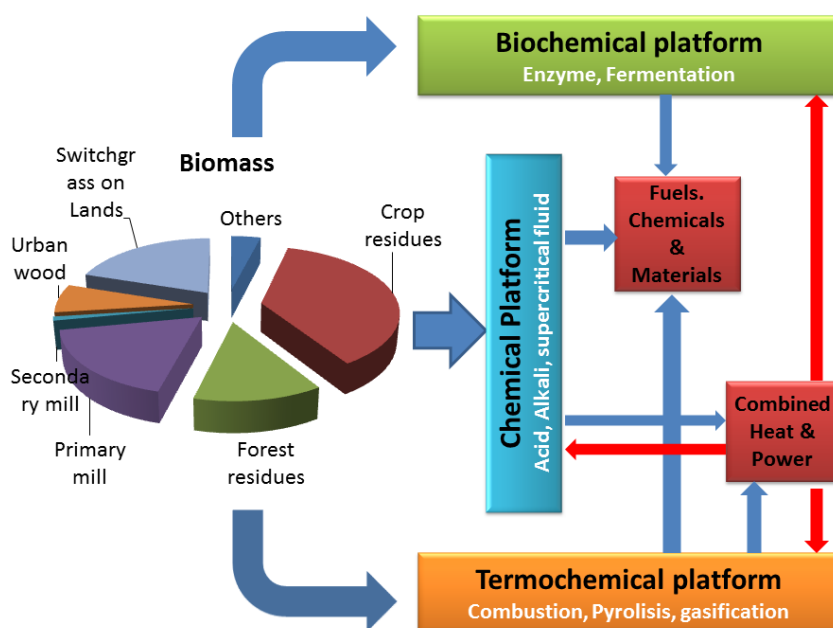


Figure 1: Diagram of an integrated bio-refinery

charides (sPS). These sPS are synthesized by algae due to the marine environment in which they live [69]. Sulphated polysaccharides, such as fucans, ulvan carrageenans and agar, are characterized by the presence of sulphated groups which result in several bioactive properties (antiviral, antitumoral). Moreover, in the backbone of sPS different rare sugars occur, for instance rhamnose and uronic acids. These features make algae very interesting in terms of further valorization of the carbohydrates that can be extracted from their cell wall.

As well the other biomass types, algae could be used as source of feedstock for processing facilities known as biorefineries. The bio-refinery concept is analogous to the current petroleum refinery. An integrated green biorefinery is a system that converts biomass into both materials and energy products, Figure 1 [11]. The aim of these kinds of industries is to gradually replace the traditional petrol based products with bio based ones. In order to simultaneously reduce the dependence on oil and to mitigate the climate change phenomena. The processing structure of a bio refinery is completely different from a traditional petrochemical facility. Biomass composition is not homogeneous, therefore several pretreatments are needed in order to obtain suitable intermediates for a further valorization. This limitation demands from the biorefinery to be an integrated system in which all the resources are used or transformed in order to avoid the large amounts of waste [11].

The interest towards algal biomass has risen since the '70s [89]. Continuing efforts has been done, especially in the fuel industry, in order to developed processes to produce

fuels from algae and equipment to intensify the algae cultivation. Interestingly, the algae are not only a huge source of lipids through which fuels can be synthesized, but algae are also an interesting source of carbohydrates. Polysaccharides, such as cellulose hemicellulose and starch, are molecules with a huge chemical potential, indeed they converted into different platform compounds, which could be further used to synthesize specialties and fine chemicals. The most common chemical pretreatment in the processing of polysaccharides, is the hydrolysis into their sugar components. Hydrolysis is a chemical process that uses acids, alkali or enzymes to depolymerize the long polysaccharides chains. Afterward, the simpler mono or disaccharides obtained can be further treated with several processes in order to increase their value. The main reactions used to process carbohydrates are hydrogenation, oxidation, reforming, dehydration and isomerization. Consequently, all these processes could be integrated into the bio refinery concept. Admittedly, most of these reactions have to be catalyzed in order to achieve high yield, therefore a deep understanding in the kinetic of these processes is fundamental.

The hydrolysis biomass such as cellulose and hemicellulose, via acid hydrolysis and enzymatic hydrolysis, has been widely studied throughout the last years [19][47][105]. The acid hydrolysis of polysaccharides has been traditionally performed via homogenous catalysis, using more or less concentrated solution of inorganic acids. However, the numerous limitation that occur using an homogenous catalyzed reaction, such as the separation of the products from the catalyst and the use of hazardous chemicals, has driven the research to the use of solid acid catalysts.

The aim of this thesis project is to study the hydrolysis of Ulvan, a sulfated polysaccharide, mainly constituted by rhamnose and D-glucuronic acid, extracted from the green seaweed *Ulva rigida*. The hydrolysis via homogenous and heterogeneous catalysis was performed in order to compare the performances of the two different processes. Consequently, the homogenous hydrolysis was catalyzed by HCl, whereas two different polymeric acid resins (SMOPEX-101 and Amberlyst 70) were tested in the heterogeneous catalysis. Additionally, the kinetic modelling of both homogenous and heterogeneous hydrolysis was performed. The study should give a better understanding of the reaction conditions, specifically temperature, acidity and catalyst type, in order to obtain high yield for both monomers that mainly constitute ulvan. However, due to the higher commercial value of L-Rhamnose, the main focus of the work will be on its production. The first chapter will give a brief description on algae, the cell structure and the biochemical composition. An overview on Green algae specifically *Ulva rigida* will be also presented. The theoretical background on the hydrolysis reaction and the analytical techniques used to carry out the project will be discussed in the second chapter. In the third chapter the experimental procedures, the raw materials used and

the experimental matrix will be illustrated. Eventually, chapter four and five will deal with the presentation of respectively experimental and kinetic modelling results.

Chapter 1

Basics on algae

The study of algae is a branch of engineering and biotechnological science which is rapidly expanding according to the recent interest in naturally active compounds as alternatives to synthetics. The open literature is abundant regarding algae valuable biological compounds and the different approaches to assess its extraction and further purification. This chapter aims to give a general description of algae anatomy, biochemistry and the main uses of seaweed extracts. In particular the content will focus on the green algae (*Chlorophyceae*), since this type of biomass has been subject of research in this project.

1.1 Definition

Algae are an important group of living beings which could be found in different natural habitats such as oceans, rivers, lakes, ponds, snow etc. This group of plants is known since ancient times but the term algae was introduced for the first time by Linneus in 1753, and it was at that time that algae were delimited from the plant world. According to the scientific community, algae evolved from cyanobacteria, which are species that contain chlorophyll therefore they are capable to perform photosynthesis to produce energy and oxygen. Consequently, cyanobacteria are considered to be the turning point in evolution of life on earth changing planet's atmosphere due to the production of oxygen [83].

1.2 Classification

Algae are mostly autotrophic organisms, most of them are aquatic and can be classified in two major groups: microalgae and macro algae. The size range varies a lot, from unicellular algae of 1 μ m to large seaweeds up to 60 m of length [4]. Predominantly,

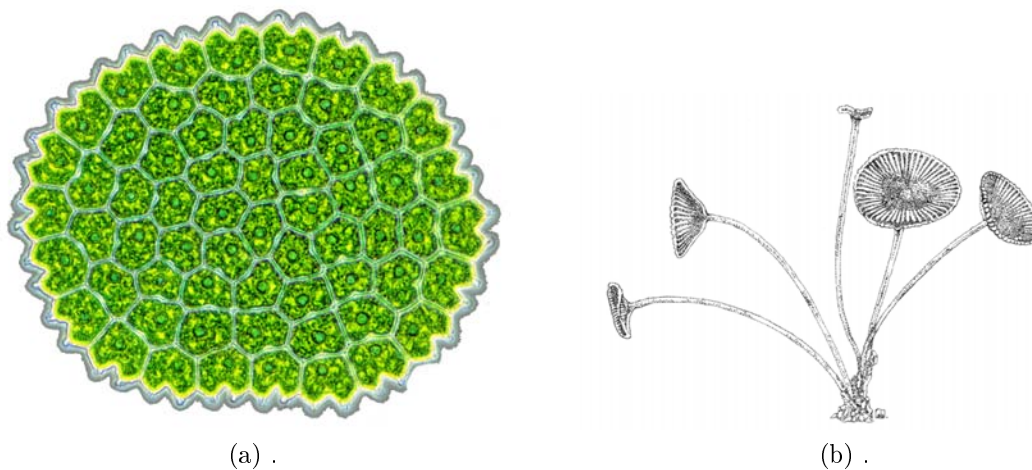


Figure 1.1: Colony of *Pediastrum* Sp. (a), Portion of the thallus of *Acetabularia* sp. (b) [4]

algae are aquatic and can be found either in fresh or marine water. According to their species algae could live in different conditions: aquatic plants may be free floating on water surface, attached to rivers, lakes and oceans depth or even grew either inside or on the surface of aquatic animal bodies (Endozoic, Epizoic).

1.2.1 Thallus

A wide variety of algae thallus (bodies) are present in nature, where the main distinction can be recognized between unicellular and multicellular forms. Unicellular forms are mainly grouped with respect to the presence or absence of flagella accordingly to the ability of motion. When these single cells are held together by a common mucilaginous envelope (matrix) the result form is called colony, which is considered an intermediate between unicellular and multicellular structure (Figure 1.1). A colony might be formed by an indefinite number of cells and this number may have either remained stable during the whole life of the organism or it can change. All the cells forming a colony are independent so they could actually survive on their own. A particular intermediate structure is the filament one, in which cell division is carried out along the filament axis, thus the cells are connected to each other by their end wall.

Among unicellular forms the most characteristic ones is the Siphonous Type which consist of a single giant tubular cell (0.5 – 10cm) that contains thousands of nuclei (Figure 1.1). Multicellular forms, in which a little tissue differentiation may be observed, are the so called *Parenchymatous* and *Pseudo-Parenchymatous* type. Whereas a full tissue differentiation may be found among the so called macro algae (seaweeds). Multicellular algae can be further distinguished in green, brown and red algae.

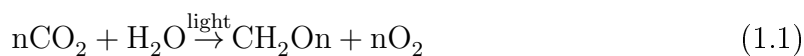
1.2.2 Nutrition

The majority of algae groups are considered photoautotrophs, thus depend entirely on their photosynthetic apparatus to produce nutritional compound, exploiting both sunlight and CO₂ as energy and carbon source. However, it's widely known that algae exploit also different nutritional strategies, combining photoautotrophy and heterotrophy (mixotrophy). For instance, several algae divisions are able to obtain organic carbon from the surroundings environment by picking up either dissolved substances via osmosis or incorporating bacteria and cells by phagotrophy. The nutritional behavior of algae is highly affected not only on the nutritional strategies that the organism may or may not adopt, but even on the environmental conditions. In light limiting conditions heterotrophy can be important, conversely, if particulate food is scarce autotrophy will be the obliged choice.

The main food storages in algae are carbohydrates and fats, whereas the total biochemical composition comprises also proteins and ashes. Sugars and lipids may be either used for bioethanol, biogas and biodiesel production as well as foods additives, pharmaceutical drugs or as intermediates in cosmetic industries.

1.2.3 Photosynthesis

Photosynthesis is the process through which organisms convert carbon dioxide and water into organic molecules exploiting the solar light as energy source [81]. It's however known that not the entire light in the spectrum is useful for the process, only the range between from 700 nm to 400 nm is captured by the organism. All the biochemical mechanisms of the photosynthetic process may be summarized with the following reaction:



Chlorophyll is the molecule on which these reactions are based. Light is captured by special pigments called antenna which carry the light to the photosystem, the reaction center. Light is transported by excitation and relaxation of the electrons inside the chlorophyll a molecules. The final products of this light stage are Adenosine triphosphate (ATP) and Nicotinamide adenine dinucleotide (NADPH), molecules with a high chemical energy content [22]. Subsequently, in the dark step, CO₂ is bounded to ribulose bisphosphate catalyzed by the enzyme ribulose bisphosphate carboxylase. This is the first step of a more complex process that leads to sugars formation [81]. Photosynthesis opposes to cellular respiration, the oxidative process that exploits the photosynthetic sugars as nutrients and in which CO₂ is produced.

1.2.4 Reproduction

Algae reproductive pathways may be vegetative (division of cells), sexual (union of gametes) or asexual (spore production). Binary fission is the simplest way algae have to reproduce; the original organism divides into two equal new cells which have the same genetic information of the parent. This form of reproduction is applied both by unicellular and multicellular algae [4]. Asexual reproduction is accomplished by the formation of either motile or non-motile spores, depending on the type of organisms. These cells are produced within vegetative cell or into specialized one. Motile spores are called zoospores and contain all the components necessary to form a new organism. Aplanospores are aflagellates that begin their development into the parental cell and when released they could develop in zoospores. Similar aplanospores even autospore are aflagellates and they are released by the ancestor cells after the wall rupture. They are a perfect copy of the original organism, but they can't develop to zoospores [4]. Sexual reproduction is characterized by the fusion of two gametes, and it can be classified in line with the structure and behavior of fusing cells. Indeed, gametes may be either morphologically and physiologically similar (Isogamy) or different (Anisogamy). It's further possible to distinguish between other two reproductive strategies oogamy and autogamy. In oogamy, usually, the male partner is motile and female partner is non-motile; whereas in autogamy the gametes are formed by the same mother cell [83].

1.2.5 Cell anatomy

Algae are very ancient organisms, thus both prokaryotic and eukaryotic algae are present in nature. Prokaryotic structures lack bounded organelles. Therefore, respiratory, photosynthetic and genetic apparatus are immersed into the cytoplasmic material without being separated each other by an outer membrane. Conversely, in eukaryotic algae these apparatus are bounded and separated from each other [44]. From the outside structures to the inside components, algae cells can be described as follows.

Cell surface

Algae, besides animal and superior plants, possess a wide variety of cell surfaces. Cell surface is the border between the environment and the internal cell. It has several functions, such as: selective barrier for the transport of molecules, preventing the osmotic free flow of the inner material and protecting the cell against pathogen and desiccation, cell-cell interactions and cell signaling [4].

The primary structure in cell surface is the so called cell membrane. This plasmatic membrane is formed by a lipid bilayer rich in proteins. Several sub-structures are

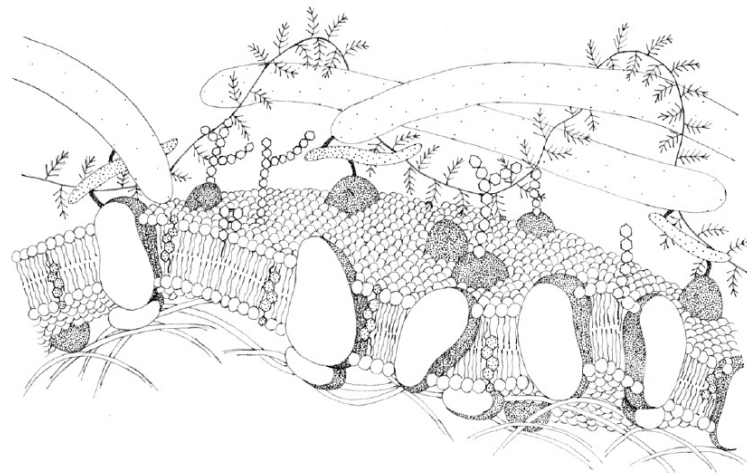


Figure 1.2: Schematic drawing of a simple cell membrane [4]

embedded into the main lipid layer, some of them are surrounded by a carbohydrates coating. Moreover, the carbohydrate sidechains of glycoproteins and glycolipids form an overall carbohydrates coat.

The primary aim of the cell membrane is to protect the cell from the surrounding environment. It is also a center that cells use to regulate the transport of substances and to promote the synthesis of ATP. This first covering layer is always present in both eukaryotic and prokaryotic cells. Either above or beneath this membrane, there may be also additional extra/intracellular matrices.

Additional Extracellular Material Several types of extracellular matrices may surround the plasmatic membrane. As far as this project is concerned, only two of them will be briefly described now: cell wall and mucilages.

Cell wall is a coating of non-living material that surrounds the plasmatic membrane in the majority of algae cells and it represents the largest percentage of the photosynthetically fixed carbon. This wall is mainly formed by carbohydrates either pure or mix, however it may also be entirely silicified or formed by mucopolymeric substances. It's formed by two layers, the outer one is amorphous and readily soluble in hot water, whereas the inner one is mostly crystalline, contains microfibrils and it's more stable than the previous one in boiling water. The microfibrils, typical of cellulosic walls of green algae, may be either composed of pure glucose (cellulose) or glucose plus other related sugars. These fibrous structures are embedded into the amorphous phase. This coating is the first defense that the cell has, and due to its firm texture it is also fundamental for structural support of both unicellular or multicellular organisms [44].

Mucilages are always present in both prokaryotic and eukaryotic algae. In green algae this gelatinous material is the main constituent of the amorphous phase of the

cell wall. In Chlorophyceae, polysaccharides containing rhamnose, galactan sulphate and uronic acid have been found in mucilages. Furthermore, mannose, galactose and arabinose have been hydrolyzed from highly branched polysaccharides isolated from green algae's mucilages [83].

Flagella

Flagellum is a thread like structure that allows the motility of most algae phyla either during their vegetative phase or reproductive one. These appendices originate from cytoplasm and their number, position and length differs from algae species [44]. They are structures of both prokaryotic and eukaryotic cells, and in green algae are typical of unicellular and colonial organisms. They are formed by a protein called flagellin.

Photoreceptor apparatus

Light in aquatic environment is a fundamental factor for both autotrophic and heterotrophic organisms. Photoreceptor could be considered as algae eyes, since light is used by algae to produce nutrients and also for the photoaxis, an alga behavior that allows the optimal positioning of the organism to capture light or to avoid it in order not to damage the apparatus. Photoaxis is also important in some species for reproduction [4].

The photoreceptor centers may have different shapes, colors and contain different kinds of photoreceptive proteins, according to their functions. In prokaryotic algae the photosynthetic pigments are found embedded into lamellar membranes joined at the ends called thylakoids. These sacs like structures are free into the cytoplasm and contain the chlorophyll. Thus they are responsible for light storage during the light dependent reactions [83].

Chloroplasts Chloroplasts are the photosynthetic organelles present in eukaryotic algae. They are by definition plastids containing chlorophyll (a/b) and it's believed that they are originated from endosymbiotic cyanobacteria, Figure 1.3 [64]. These structures are surrounded by a double layer membrane which embeds a fluid called stroma. Ribosomes, a DNA filament and some osmiophilic globules are immersed into this fluidic matrix. Therefore, chloroplasts are able to synthesize the proteins needed for the metabolism of the algae [83]. Thylakoids, inside the stroma, are stacked in groups called grana and organized in stromal thylakoids forming connection between the grana [4].

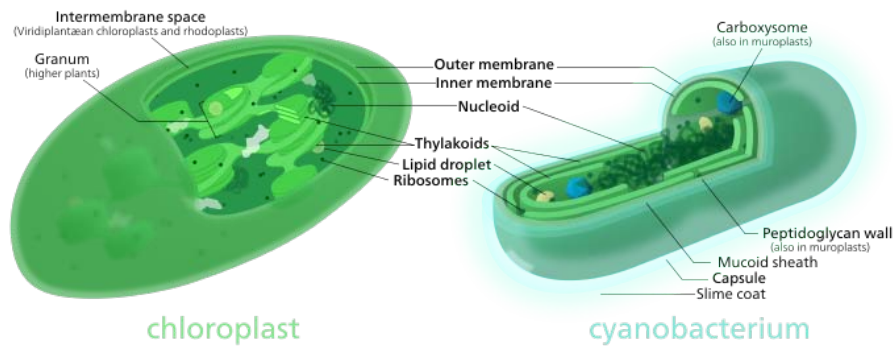


Figure 1.3: Chloroplast, cyanobacterium comparison

Together with chloroplasts, other two important structures in green algae are pyrenoid and eyespot. Pyrenoids are formed by a central granular surrounded by packaged starch plates. They are fundamental in the carbon concentrating mechanism [83].

Eyespot is a small brownish pigmented plate which carries a biconvex hyaline lens. It could be considered as the algae "eye" and it's involved in photoaxis [83].

1.2.6 Nucleus

Cyanobacteria lacks an organized structure to contain the genetic material (prokaryotic algae), featuring a single unbranched molecules of DNA floating freely inside the cytoplasm [4]. In eukaryotic algae instead a membrane bounded genetic apparatus known as nucleus is present. Most of algal cells have only a single nucleus, although some cells are multinucleate [81]. Inside this apparatus DNA is packaged into chromatin, a molecule which is formed by DNA wrapping proteins, which is further condensed into chromosome [64]. The nucleus is surrounded by a two layer membrane which is connected together with the endoplasmic reticulum. This envelope features numerous pores through which macromolecules such as RNA and proteins are transported to the ribosomes inside the cytoplasm [4]. Inside the nucleus there are one or more regions, called nucleoli, which are made of RNA and proteins, and are responsible for the production of rRNA [83].

Mitochondria, Golgi Bodies, Endoplasmic Reticulum and Contractile Vacuules

Endoplasmatic Reticulum (ER), mitochondria and golgi bodies are apparatus that are presented inside the eukaryotic cells, and they have been observed in many members of Chlorophyceae.

Mitochondria are double membrane bounded organelles, containing crista and their own DNA. The folding spots of the inner membrane act as sites for enzyme action

[83]. The infolding of the membrane provides a huge area for the cellular respiration, process in which sugars are broken down to produce energy, water and CO₂ [81].

Golgi bodies, formed by a stack of flat vesicles, are commonly found in the region of nucleus in several green algae. The Golgi body is the center of protein glycosylation and polysaccharide synthesis. It's also responsible for the selection and exportation of cellular products (vesicular transport)[83][64].

The organelle with the largest surface area, in eukaryotic cells, is the so called Endoplasmic Reticulum (ER). The ER network is formed by interconnected membrane tubules and cisternae; the entire membrane is continuous and extends throughout the cytoplasm [64]. This apparatus may be splitted in two sub unit, rough and smooth endoplasmic reticulum. The former, which is covered by ribosomes, is one of the place where proteins are built. The latter, has functions in several metabolic processes.

Most of mature green algae cells possess vacuoles. Vacuoles are membrane bounded apparatus, some of them may be contractile and the periodic contractions are used remove waste products from the cells [83].

1.3 Green Algae

Green algae, mostly known as chlorophyte, are a wide group of eukaryotic algae characterized by the presence of chlorophyll *a* and *b* which give the typical bright grass green color to the tissue. These organisms are the products of an endosymbiotic event, an ancient eukaryotic cell, already containing mitochondria, incorporates a photosynthetic prokaryote that turned into a plastid [83]. The thalluses of this seaweed are very various, including unicellular (*Chlamydomonas*), colonial (*Volvox*), filamentous (*Cladophora*) and tubular (*Ulva*)[40]. Green algae commonly occur in fresh water, attached to rocks or submerged wood, however there are also terrestrial and above all marine species, forming conspicuous and nuisance growth [25]. These organisms play a major role in the structure and function of marine ecosystem being the main constituent of the organic matter flux in the oceans. Green algae generate oxygen, sequester atmospheric CO₂ and provide nutrient for other organism [83].

1.3.1 Biochemical composition

The chemical composition of green macro and micro algae varies; it is mostly dependent on the species, the geographic area of growing and on many external factors such as the light intensity, water temperature and nutrient concentration in water. All these variabilities are reflected into the changeable concentration of proteins, lipids, minerals and carbohydrates within the different genera of algae [41].

Proteins and amino acid

Proteins are large macromolecules formed by chains of connected units of amino acids. They differ from one to another according to the amino acids sequence which is dictated by a particular gene. Like other macromolecules they take part in lots of biological processes within the cell. They may work as catalysts (enzymes) for biochemical reactions, as scaffolding such as inside muscle they could also be important in cell signaling and molecule transportation. The chemical structure of protein is rather complex, most of them are linear polymers built from 20 L- α -amino acids units. All of these monomers possess an α -carbon attached to an amino group, a carboxyl group and variable side chains. The amino acids are bonded one to each other by peptide bonds. Seaweeds like green algae are well known to contain a significant amount of these nitrogen compounds, together with non-protein nitrogen for some compound such as chlorophyll and nucleic acids [41]. Protein content varies according to factors aforementioned and to the determination method applied. Usually protein concentration is determined through Kjeldahl method which is based on a nitrogen-protein conversion factor. For green algae usually this nitrogen-to-protein factor is 5.13, anyhow the fact that algae contain also non-protein nitrogen should be taken into account. Generally, it has been reported that in green algae protein's concentration is between 13-30% of dry matter [41]. Seaweeds proteins contain all the essential amino acids; however they are not full value proteins because of some of these amino acids are present in low amounts. In spite of this lack, algae are increasingly used to improve the amino acid composition in many foods.

Minerals

The mineral content in green seaweeds is particularly high due to the living environment of these organisms. Algae have an intrinsic capability to absorb minerals due to the higher content of carbohydrates and to the ability of predestine different storages inside their tissues, which leads to accumulate ion of minerals in a higher concentration than the concentration in the surroundings. The major minerals that could be found inside algae are Fe, Zn, Mn and Cu together with other linked to macro element such as vitamins, which are Mg, Ca and P. As well as for proteins, the concentration of ashes is mainly dependent on environmental conditions and algae's age. An ion exchange mechanism has been considered responsible for uptake of cationic metals, based on the number of cationic sites, the affinity for positively charge metals may vary. Thanks to the capability of absorbing metals, even the heavy ones (cadmium, chromium) can be adsorbed and thus algae could be used as bio indicators of water pollution, and consequently also as bio sorbents to purify the aquatic environment [41].

Lipids

Concentration of lipids is the lowest one among all the biomolecules, ranging between 1-5% of dry seaweeds and most of them are polyunsaturated ω -3 and ω -6 fatty acids [41]. Anyway, it's also reported that for some microalgae species the lipid content can increase up to 60%, mainly in the form of TAG (Tri acyl glycerol), free fatty acids and phospholipids [89]. A fatty acid is a carboxylic acid attached to a long aliphatic chain, usually unbranched, with an even number of carbons from 4 to 28. They are synthesized by algae to be used for the production of glycerol-based membrane lipids through esterification. However, in case of harsh environmental conditions, algae may modify their biosynthetic lipids pathway toward neutral lipids to be stored as a source of carbon and energy (TAG)[31]. It has been reported that, for green seaweeds, the content of fatty acids is directly linked to light and salinity exposition. It has been observed that the combination of low salinity and high light intensity resulted in decrease of fatty acid content [41]. Oil is mainly extracted from algae by mechanical treatment, solvent extraction or Soxhlet process. Nevertheless, new techniques have been studied, in order to avoid some of the drawbacks such as the low yield of extraction. Therefore, more and more often the old techniques are coupled with microwave, sonication or bead beating [7].

Carbohydrates

Carbohydrates are undoubtedly the main constituent of algae dry mass, their amount can reach up to 76% but usually averages around 50% [96]. Commonly, the carbohydrates contain either 5 or 6 carbons arranged in linear or cyclic form. When the cyclic forms are linked together with covalent glycosidic bond the resulting molecules are known as polysaccharides. These molecules are hydrates of carbon; anyway it is more accurate to define them as polyhydroxy aldehydes and ketones with several hydroxyl groups attached. Carbohydrates may be distinguished by the length of the chain, thus it is possible to recognize: monosaccharides, disaccharides, oligosaccharides and polysaccharides.

Monosaccharides Monosaccharides are the basic unit of carbohydrates. They are usually known as single sugars can be classified in several ways. The simplest one is according to the number of carbons that forms the chain or the ring, generally between 3 and 7. The general elemental composition is $(\text{CH}_2\text{O})_n$ in which n represents number of carbon [71]. In nature different sugar monomers occur, mostly they have six or five carbons and are respectively called hexoses and pentoses. These simple sugars are usually in a ring form which is more stable than the linear one. Therefore, according to

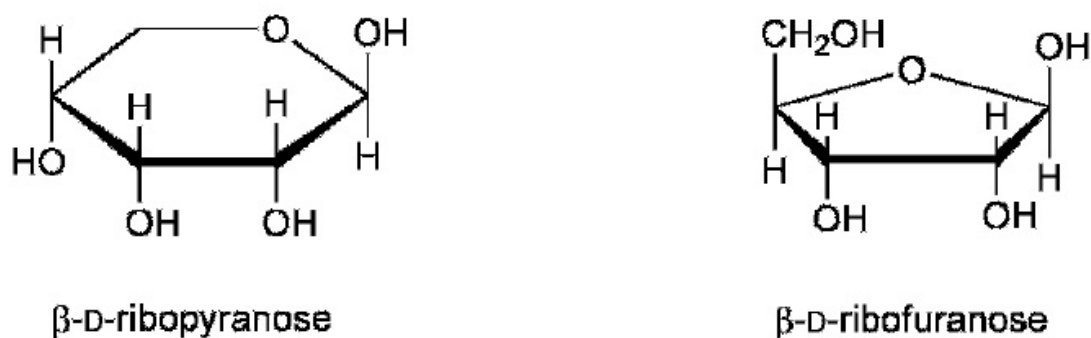


Figure 1.4: Pyranosic and furanosic forms of Ribose [93]

the number of carbons that appear inside the ring they might be known as furanoses (5 carbons) or pyranoses (6 carbons) Figure 1.4 [93].

Whether a terminal hydroxyl group in a monosaccharides has been oxidized to a carboxylic acid an uronic acid is produced. For instance, glucuronic acid is formed after the oxidation of glucose [6]. These kind of sugar acids occur in pectins, and they might be valuable compounds, such as glucuronic acid is a building block of heparin, and it is also a precursor of ascorbic acid, as it will be described later.

Disaccharides and oligomers Oligomers, like the disaccharides, are formed when two or more monosaccharides are linked by a glycosidic bond. According to the stereochemistry, the glycosidic bond may be defined as α or β ; the bond could be also located between different carbons of the ring. Because of these different linkage possibilities commonly in literature the structure of an oligomers is reported as:



where it is indicated that the glycosidic bond type is α and it's between carbon 1 and carbon 4 of the respective glucose units [93]. Generally oligomers are part of a longer chain of polysaccharides.

Polysaccharides Generally, sugars are found in several forms of polysaccharides which may have different structures and metabolic functions. Polysaccharides may be classified according to the monomers that occur inside the chain. Thus, homopolysaccharides are formed from the same repeating unit and heteropolysaccharides might be built by different monosaccharides [71].

Polysaccharides in algae are mostly part of the cell wall which is constituted by different carbohydrates based on the algae phyla. The main structural polysaccharide in green algae is cellulose which accounts for 19-49% of the total content [96].

Cellulose Cellulose is a homopolysaccharide made up of D-glucose units linked via $\beta - 1,4-$ glycosidic bonds [56]. It has been reported that cellulose is the most abundant biomaterial in nature, and it is estimated that a volume of $3.24 \times 10^{11} \text{ m}^3$ exist in the world [71]. It's a semicrystalline polymer containing both amorphous and crystalline regions, the general elementary composition may be represented by $(\text{C}_6\text{H}_{10}\text{O}_5)_n$. The crystalline domain is due to the presence of inter and intra-molecular hydrogen bonds between the chains [56]. The degree of polymerization is strictly dependent on the species and on the growing conditions.

In the industrial scenario the use of cellulose is well established as a source of textile fibers (cotton), for production of paper and several derived polymers (acetate, cellophane). Different transformations of cellulose are still studied because of its application in sustainable bio refineries.

Hemicellulose Hemicelluloses are heterogeneous polysaccharides formed from different sugars monomers such as mannans, xylans, arabinans and galactans [56]. These polymers contribute, together with cellulose, to the cell wall structure of green algae. While cellulose, due to its crystalline structure is very resistant to hydrolysis, hemicellulose with its random amorphous structure, in which side branches are highly likely, is easier to be hydrolyzed. The ease with which hemicellulose can be hydrolyzed may be also explained by the degree of polymerization which conversely to cellulose (thousands of units) is very low, between 50 and 300 monomers [71]. Hemicelluloses like pectines are partially soluble in water, and are a mixture of pentoses (xylose, arabinose), hexoses (glucose, galactose and mannose) and hexuronic acids (galacturonic/glucuronic acid). A common structure in hemicellulose is a backbone made of glucose, xylose or mannose; the monomers are bounded with $\alpha 1 - 4$ bonds. On the main chain several side groups of monomers or short oligomers are grafted.

Sulphated polysaccharides Green algae are well known to contain a large amount of sulphated polysaccharides, between 19 and 41% [96]. These sugars are polydisperse heteropolysaccharides in which, at least, some of the hydroxyl groups have been substituted by half ester sulphate groups [70]. They are very complex branched molecules in which it does not seem to be single unit regularity in the backbone. Many functions have been proposed to these polysaccharides, in vivo they exist as gels or mucilages with different stiffness. They may be used to repel the attack of other organism, and to increase the strength of the cell wall. Further, due to their hygroscopic properties they may prevent the desiccation in plant exposed to tides [70]. In green algae sulphated polysaccharides may be classified according to their chemical composition. Uronic acid-rich polysaccharides mainly contain also rhamnose, xylose

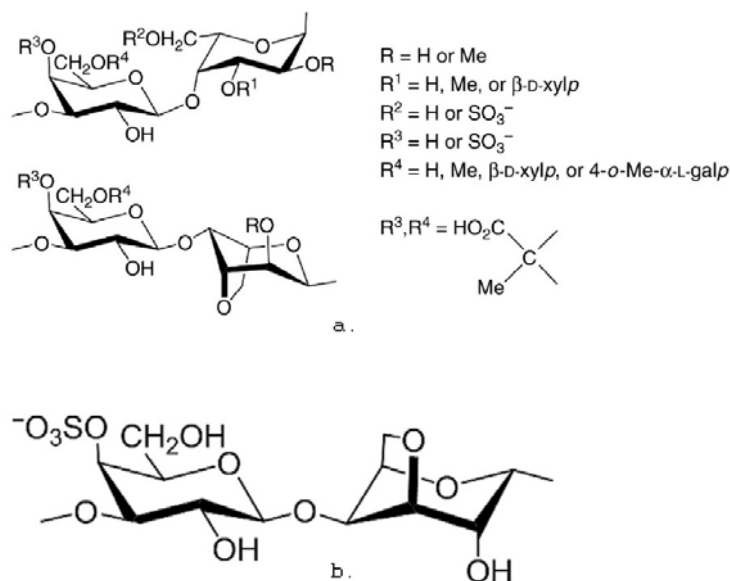


Figure 1.5: Structural heterogeneity of agar (a), and structure of carrageen in the κ form, [96]

and galactose. Uronic acid-limited polysaccharides consist of galactose, arabinose and sometimes xylose [17]. Ulvan is the sulphated polysaccharide commonly present in green algae and it will be describe further.

Sulphated polysaccharides are also constituents of red and brown algae. Red seaweeds are known to produce the so called agar and carrageenan. Those two polysaccharides are galactans made entirely by galactose or modified galactose units. The main difference between the two is that agar contains L- and D- galactose, whereas carrageenans are mainly formed from the D- sugar [70], Figure 1.5. The main forms of carrageenans are ι , κ and γ and they are strictly algae dependent. Agar instead may be divided into two subgroups agarose and agarpectin, an acid polymer carrying sulphate groups [96]. Both, carrageenan and agar, are structural polymer present in the cell wall and thus their functions are probably very similar to those of the sulphated polysaccharides found in green algae [70].

Fucose-containing sulfated polysaccharides (FCSP) are structural polysaccharides present in brown algae cell wall in significant quantities (2-10%)[96]. Their structure is severely dependent on species, indeed among FCSP it is possible to recognize ascophyllan, fucan, fucoidan, galactofucan, fucogalacturonan etc. FCSP are polydisperse heteromolecules containing in addition to fucose variable quantities of galactose, mannose, xylose and glucuronic acid [70]. The well-known fucoidan is composed mainly of L-fucose (50%) and a variable amounts of d-uronic acid, d-galactose, d-xylose, and l-fucose sulfate. As well as the other sulphated polysaccharides, fucans have the property to retain water inside the algae. Indeed, the sulphated ester groups can be associated

with the magnesium ions which are highly hydrated.

1.3.2 Production

An important feature, which makes algae very interesting talking about biorefineries industry, is the speed at which algae can produce biomass if compared to terrestrial plants. It has been reported that microalgae can, under right growing conditions, double its biomass in 24 h [8]. Furthermore, it has been calculated that the biomass production per hectare from algae can be 10 times higher than crops. These data make microalgae the only valid candidate in order to displace fossil carbon from fuels production [13]. Microalgae, aquatic microbial oxygenic photoautotrophs in general, are also more efficient solar converters, which makes them suitable for year-round culturing [16].

In spite of this good characteristics producing microalgal biomass is usually more expensive than crops. Large scale production of microalgal biomass generally is done either in raceway ponds or photobioreactor. Raceway ponds is the first technique that has been studied and evaluated, although has several drawbacks such as potential contamination, low production concentration and low efficiency in carbon dioxide fixation [13]. However, it is definitely less expensive in terms of cost and operation than photobioreactors, making the alternative of choice for raceway ponds commercial microalgae production [83].

As well as microalgae, Macroalgae are much more productive in terms of biomass than terrestrial plant. For instance, *Ulva lactuca* has a growing rate of around 45 t TS ha⁻¹ y⁻¹ and *L. hyperborean* can reach a growing rate up to 90 t TS ha⁻¹ y⁻¹. Conversely, maize has a growing rate of 19.5 t TS ha⁻¹ y⁻¹ which is 57% lower than *Ulva lactuca* [61]. Macroalgae cultivation is typically done through artificially produced seed in greenhouse, until small plantlet size. Afterwards, algae are transplanted to coastal farm to harvestable size [80]. Other option for siting macroalgae could be offshore farms and landed-based ponds.

Moreover, algae offer other important advantages over terrestrial plants. The cellular structure of algae is simpler than terrestrial plants and the content of lignin is almost null, except for a few exception. Therefore, algae are potentially easier to pre-treat and transform into valuable products. Algal biodiversity is another interesting feature. With more than 4000 species, algae can be selected in order to easily adapt to the local available aquifers (marine, fresh, wastewater). Unlike terrestrial plants, algae biochemical composition can be easily altered using either environmental or nutritional stresses [16].

1.3.3 Interesting products and uses

The production of green algae and seaweeds for human uses is a well-established industry. The fields in which algae find a practical utilization are several, from food and dietary supplement to the production of commercial products such as cosmetic, pharmaceuticals and hydrocolloids. They may also be used as soil conditioner, treatment of wastewater and in CO₂ capture. Biomass from green algae and other seaweeds can also be used to produce third generation biofuels such as biodiesel and bioethanol [83][89].

Biofuels

Due to the high level content of lipids and carbohydrates, green algae are of enormous interest in biofuel production. Carbohydrates can be hydrolyzed and fermented through yeast to bioethanol. These polysaccharides are mainly present as starch, cellulose and other sugar molecules, and besides terrestrial plants the absence of lignin overcomes the relatively low alcoholic yield which can be obtained with terrestrial cellulosic material [89]. Algae like *Chlamydomonas reinhardtii* and *Scenedesmus* contain the enzyme hydrogenase. This enzyme may be exploited to produce hydrogen from water [83]. It is also well recognized that, in an ideal biorefinery, after the extraction of lipids, which are further used to produce biodiesel, all the residue can sequentially be introduced into an anaerobic digester for biogas production [89].

Biologically active natural products

A considerable amount of secondary metabolites produced by algae have been considered and studied as bioactive substances for treatment of diseases. The bioactivity of algae extracts has been reported against prevalent worldwide illnesses such as cancer, diabetes and obesity. Moreover, some polysaccharides have been elucidated to inhibit various enzymatic activities inside the life cycle of HIV [40].

Among all the substances that could be extracted from algae the most interesting one for this project, concerning the biological activity are the polysaccharides. The main activities from polysaccharides are antibacterial, antiviral, anticoagulant, antitumor and anti-inflammatory. Many of them like sulfated polysaccharides, which are the most active ones (galactofucans, rhamnan, arabinogalactans), have been isolated from different green algae species [40]. In a recent study, a sulfated polysaccharide (CrSP) extracted from a green algae called *Caulerpa Racemosa*, could be coupled with sPLA2 to enhance its antibacterial activity [73].

Besides the pharmaceutical potential of polysaccharides, the activity of algal proteins is also well known, carotenoids and many other second metabolites that could be

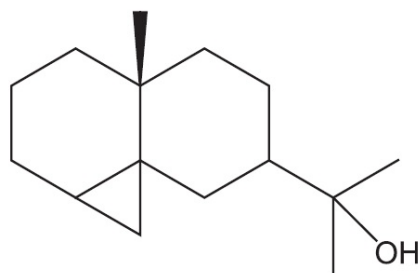


Figure 1.6: Cycloeudesmol structure [41]

extracted. For instance, Cycloeudesmol is isolated from *Chondria oppositoclada* (Figure 1.6) was found to work as an antibiotic against *Staphylococcus aureus* and *Candida albicans* [41].

Extracts derived from several algae, such as *Chlorella*, are known to stimulate the production of collagens, supporting tissue regeneration. Therefore, green algae are widely use in skin care products like antiaging creams, emollient and sun protection lotions [83].

Reducing CO₂ emissions

An interesting feature of green algae is carbon dioxide fixation to reduce the greenhouse effect. Released CO₂ can be directly pumped into an algae bioreactor to feed the algae population; moreover this device might also be installed on a smokestack. Besides this, algae may also be used to provide oxygen to soldiers in war theaters, capturing vehicular emissions and reducing the ocean acidification. *Chlorella* is one of the most used algae for these purposes due to its rapid rate of photosynthesis and high efficiency in using the released CO₂ [83].

Food and dietary supplements

Green algae are worldwide used as food in different form thanks to their high amount content of nutraceutical compounds. Concerning the nutritional content of *Chlorella*, which is rich in protein and lipids, it can be compared to a mixture of soybean and spinach. Some studies have reported that many green algae synthetize omega3 and are rich sources of Vitamin B and C. The proteins synthetized by some green algae contain all the essential amino acids required for human nutrition. Some pigments, such as Astaxanthin, have different health benefits like enhancing eye health and muscular strength, reducing skin ageing from UVA damages, protecting tissues from oxidative degeneration [83].

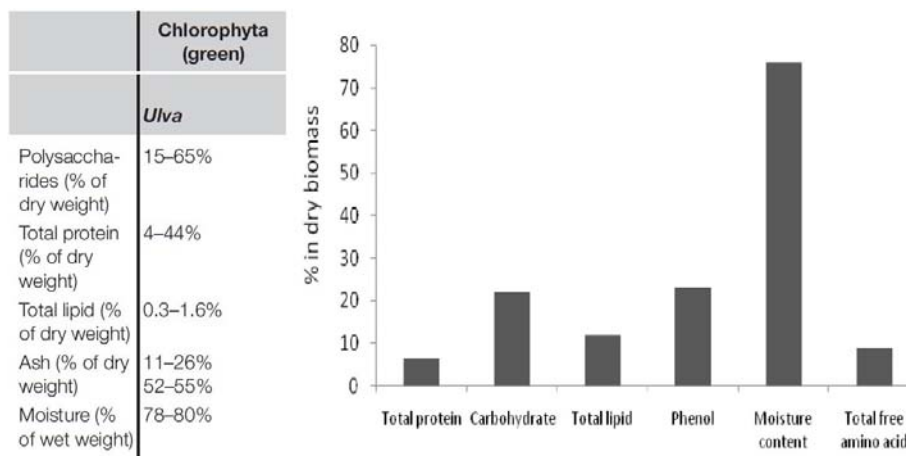


Figure 1.7: Bar graph and table showing different biochemical parameters of general *Ulva* and *Ulva Rigida* [85]

1.4 *Ulva rigida*

The green seaweed studied in this project is the so called *Ulva rigida* from the Ulvaceae family (C. Aghard 1823 Chlorophyta, *Ulvaceae*). *Ulva*, commonly known as sea lettuce, is a marine alga generally found attached to stones in rocky shores. It may also live in brackish water, polluted estuaries or fresh water runoff high in nutrients content. It has a worldwide distribution in warm and temperate seas. *Ulva rigida* may have different types of thallus: generally it is rather thin, sheet-like, as turfs or solitary blades. Therefore the shape of *Ulva rigida* is variable with a height up to 10 cm. The reproduction occurs through all three classical ways: vegetative, asexual as well as sexual. Almost 20-60% of overall algae's biomass is used monthly for reproduction and the reproductive success is mostly due to the photosynthetic ability of the reproductive cells.

1.4.1 Chemistry of *Ulva rigida*

As well as all the other green algae, the main macromolecules that could be found in *Ulva rigida* are carbohydrates, protein lipids and ashes. *Ulva rigida* contains mostly carbohydrates and lipids as shown in Figure 1.7 [85]. The amount of these two major components is highly dependent on the culture medium in which the cells have grown. Moreover, According to the studies of Irkin et al. 2014, the chemical composition is highly variable depending on season, temperature and salinity level [33].

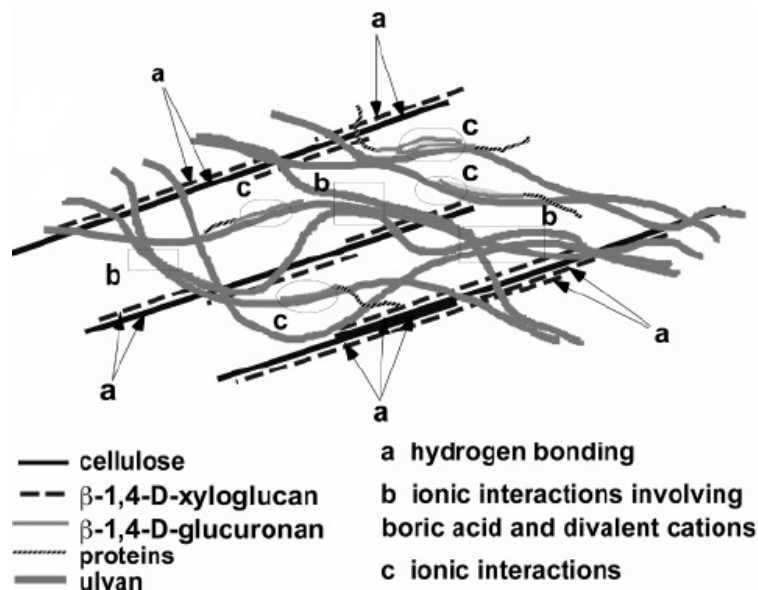


Figure 1.8: Distribution of the different *Ulva* sp. cell wall polysaccharides in a thallus cross section [96]

Carbohydrates

Among all the polymers synthesized by the cell, the carbohydrates that form the cell wall represent the main part of the dry algae matter around 38-54%. These mainly include four families in *Ulva* species: two in major quantities Ulvan (water-soluble) and insoluble cellulose, and the two minor ones, xyloglucans and glucuronan [52]. The model structure of thallus cross section in Figure 1.8 depicts their position and association in the cell wall

Within the cell wall, cellulose and xyloglucans have a regular arrangement, like a skeleton, whereas Ulvan has a microfibrillar shape and it is grafted on the cellulosic structure.

Ulvan Ulvan is a glucuronorhamnoxyloglucan sulfate polysaccharide, typically found in green algae of the order Ulvales. It is a water-soluble carbohydrate and it has been reported that it's mainly formed of sulfate, xylose, rhamnose, glucuronic and iduronic acid [36]. The works of by Brading, Mckinnel and Quemener [57][77], found out that the composition of Ulvan is the following: Rhamnose 16-45%, xylose 2.1-12%, glucose 0.5-6.4% uronic acids 6.5-19% and sulfate 16-23.2%. Rhamnose and uronic acid form the backbone of this polysaccharide and they mainly occur in the form of aldobiuronic acid 3-sulfate types containing either iduronic or glucuronic acid [17][52][79]. Minor repeating units containing sulfated xylose as a branch on O-2 of the rhamnose-3-sulfate have been reported [36][50], Figure 1.9.

The chemistry and the biosynthesis of Ulvan may be affected by ecophysiological

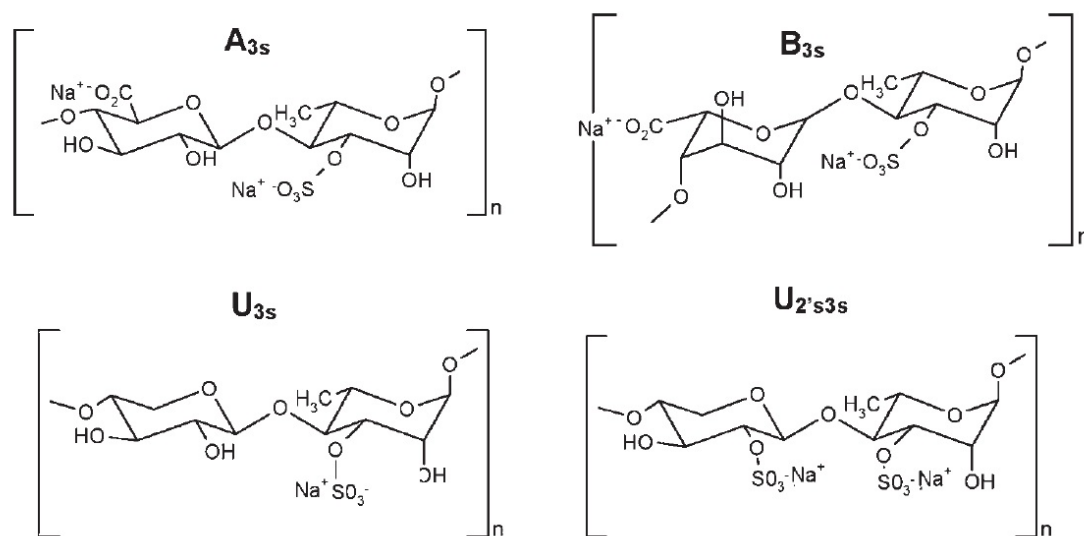


Figure 1.9: Chemical structure of the 4 disaccharides forming Ulvan [72]

growth conditions, season and species. Although, to date, no specific correlations have been determined [52].

Ulvan can be described as a family of branched molecules that may differ in terms of charge, density and molecular weight [32]. Different molecular weight distributions have been reported from sedimentation, osmometry and light scattering measurements, giving weights ranging from $1.7e5$ to $8.62e6$ g/mol depending on the species, the temperature of the extraction and the solvent used [52]. Ulvan solutions are characterized by low intrinsic viscosities ranging from 24 to 285 mL/g, which low viscosity may be explained by the polymolecularity of ulvans with a high number of short chains and/or branched chains [32]. Observations with TEM have showed that ulvan in aqueous solution appears as an aggregate of spherical shapes structure linked to each other by strands and filament material, resembling like a necklace-type structure [79]. Ulvan is an anionic polyelectrolyte due to the presence of carboxyl and sulphate groups within the chain, and its net charge depends on the pH and the ionic strength of the working medium [12]. Although its polyelectrolyte nature, the polysaccharide has also a strong hydrophobic nature. This characteristic is attributed to the methyl group provided by rhamnose, this unusual hydrophobicity for a polyelectrolyte molecule may also explained the characteristic Ulvan necklace-like ultrastructure [79][12].

An interesting feature of Ulvan is its ability to form gels [57][32]. This peculiar property is enhanced by the presence of boric acid and calcium ions [51]. The mechanism through which Ulvan is able to form a gelatinous state has not been completely understood yet, anyway a two-step gelification process, that explains the requirement for calcium and borate ions, has been proposed. First, there is a formation of a borate

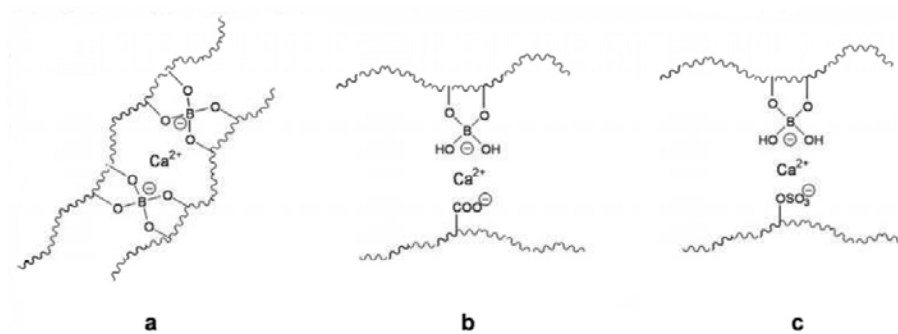


Figure 1.10: Structure of Ulvan gel [12]

ester with Ulvan 1-2 diols which is followed by the linkage with calcium ions, Figure 1.10 [26]. The function of Ca^{2+} ions is then to stabilize the borate ester, later it has been proposed that calcium creates the coordination bridge also with sulfate and carboxylic groups [49].

The gel that may be synthesized from Ulvan is thermoreversible, then the linkage between Ulvan chains can be disrupted by heat. Therefore, the mechanical properties of the hydrogel are poor, and tend to get worse if used with body fluids owing to the ion exchange phenomena between Ca^{2+} and other ions present in the fluids [53]. Hydrogels produced from Ulvan can be tuned by pH and temperature; the chemical crosslinking may be improved by photopolymerization in the presence of photoinitiators (methacryloyl or acryloyl groups) in order to enhance mechanical properties [60]. The gelling properties might be exploited in tissue engineering, food industry, biomedical applications or when molecules have to be trapped/released under specific conditions [12][43].

Due to the complexity of the sulphated structure of polysaccharides, the relation with the biological activity, they have been attributed to have, is not completely understood. However, the presence of the sulfate groups is widely recognized as the reason of the most positive health effect induced by Ulvan (Wijesekara et al., 2011)[101]. The main biological effects reported span from antitumor, anticoagulant, antioxidant, antihyperlipidemic and immunomodulating; all of them have been proved both *in vitro* and *in vivo*.

Probably the best studied bioactivity effect of sulfated polysaccharides from green algae is the heparin-like activity. The heparin-like antithrombotic and anticoagulant activity, may be explained by the direct and indirect activation of thrombin, through the activation of thrombin inhibitors. The molecular weight of the molecules has an effect on the antithrombotic activity, indeed it has been reported that longer chains are needed to achieve the thrombin inhibition [12]. The sulfation level and the position of the sulphate ester groups, along the chain, are other important factors to explain

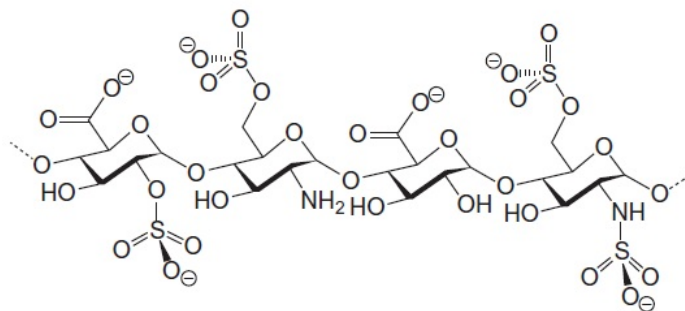


Figure 1.11: Heparin structure

the phenomena[36]. The development of an Ulvan based anticoagulant drugs would overcome the potential with prions or virus that may come from commercial heparin produced from bovins and pigs intestines.

The anticancer activity of sulfated polysaccharides has also been reported. In addition antiproliferative and inhibitory cancer cell grow activity has been confirmed in vitro and in mice [101][21]. For instance, HeLa cell proliferation can be inhibited between 36 and 58% after 72 h of incubation with sulfated polysaccharides from green algae [21].

As dietary fiber, Ulvan resists to the degradation that may occur due to the human endogenous enzymes. Dietary fibers are associated to decrease of the cholesterol level and this ability is enhanced by ion charged groups. Ulvan has the capability to bind and sequester bile acid due to the presence of carboxylic and sulfated negatively charged groups along the chain [101][12]. Therefore, Ulvan is capable of reducing the total (TG) and the LDL/HDL cholesterol concentration in the serum and induce an increase in the bile excretion in mice. The antihyperlipidemic activity has also been linked to the chain length of the sugar, in particular the high molecular weight is more effective on reducing LDL levels, whereas low molecular weight is acting on decreasing TG and HDL levels [68].

Ulvan has been reported for its antioxidant activity against free radicals in vitro and the prevention of oxidative damage in living organism [75]. As all the other Ulvan activities, the antioxidant capability is deeply affected by the amount and the distribution of the sulfated groups along the Ulvan chain [75][101]. The antioxidant activity may thus boost by the introduction of sulfated groups through a sulfur trioxide treatment or by introducing suitable groups acetyl and benzoyl [76].

Rhamnose According to the chemical composition of Ulvan, the biomass may be a source of rare sugars that can be used as precursor for the synthesis of fine chemicals. The main sugar is rhamnose, a rare sugar used mainly for the synthesis of aroma

compounds. Rhamnose is a deoxy sugar that can be classified either as methyl pentose or 6-deoxy hexose. Naturally it occurs in its L-form, conversely to the majority of natural sugars that appear in their D-form. Rhamnose can be extracted from terrestrial plants in the genus *Uncaria*, its production from *Monostroma* has been patented [52] L-Rhamnose is used in cosmetics and pharmaceuticals. As well as L-fucose, it has the property of preserving the skin moisture level. 5-deoxy-L-ribose, which has medical applications, can be produced from L-Rhamnose [56]. It has been reported that deoxy sugars, in particular rhamnose, are effective for the treatment of viral diseases and inhibits the absorption of bacteriophage to cells [39]. Hydrogenation of rhamnose leads to rhamnitol a sugar alcohol. Sugar alcohols are commonly used as sweetener, but recently some studies have reported that they can be used also as intermediate in the production of special ligands and pharmaceuticals [29].

Xylose Xylose occurs in Ulvan either as a branch of the main ulvanbiouronic acid backbone or in minor part as a unit of the ulvanbiose disaccharide. It should be noticed that xylose is present also in the form of xyloglucans (hemicellulose) inside the *Ulva rigida* cell wall, thus its amount is highly variable. D-xylose is a five-carbon sugar, and as well as the other aldopentose, it may occur in several forms such as: pyranose, furanose or free carbonyl group (reducing sugar). The most important utilization for xylose is its hydrogenation to xylitol, a compound widely used in cosmetic, food and in the pharmaceutical industry [55]. Xylose can be also dehydrated to furfural, which represents an intermediate for the solvent industry.

Glucose As well as xylose, glucose is located either as a branch of the main Ulvan chain and/or in the xyloglucans hemicellulose. Glucose is a valuable compound which can be easily transformed into fine chemicals. The most important reaction is its catalytic hydrogenation to sorbitol on Ni or Ru acting as catalyst. Analogously to xylitol, Sorbitol has several applications areas such as sweetener and a starting material for synthesis of vitamin-C synthesis. Glucose can be further hydrogenated into glycols (antifreeze). Sorbitol has also been investigated in the so called APR reaction (aqueous phase reforming), that allows to obtain green fuels with a lower amount of energy with respect to the classical steam reforming [9]. Gluconic acid, a cleansing agent and food additive is produced by oxidation of glucose [55]. As well glucaric acid, an intermediate for green adipic acid production, may be obtained from glucose oxidation. Eventually, glucose alkylation is another route that can be used to obtain intermediate for nonionic surfactants, detergent and food industry [55].

Uronic acids Uronic acids are sugar acids with both carbonyl groups and carboxylic groups which derive from the oxidation of one terminal hydroxyl group. They are either crystalline or amorphous substances, non volatile, relatively high melting and easily soluble in water and poplar solvents. Thanks to the particular structure of uronic acid, they own properties of both monosaccharides (mutarotation, oxidation, reduction, ability glycosides) and hydroxyl acids (formulation of esters and lactones). In nature uronic acids are important constituents of many vegetable and animal biopolymers [74]. Ulvan contains uronic acids in the form of D-glucuronic and L-Iduronic acid which are epimer. D-Glucuronic acid in animals removes toxic substances from blood and urin forming glycosides. It is a starting block from the synthesis of ascorbic acid, hyaluronic acid and can be/has been also found in heparin [74]. The stereoisomer of D-glucuronic acid is also a building block for heparin, hyaluronic acid.

Chapter 2

Theoretical background

Hydrolysis of natural polysaccharides has been widely studied during the years. However, as far as plant polysaccharides are concerned, the scientific community has focused its effort to deepen the understanding about hydrolysis of hemicellulose and lignocellulosic materials. Indeed, Ulvan hydrolysis has been mainly utilized by researchers as a pure intermediate in the Ulvan chemical analysis protocol. Therefore, no significant references has been found in the open literature regarding the optimization and modelling of Ulvan hydrolysis. Accordingly, in this chapter the main characteristics of hemicellulose hydrolysis will be presented. These, anyway may reflect the hydrolysis of Ulvan due to the similarity in the bonding that connects the single monosaccharides units in both the chains. Consequently, the chapter will provide a description of the acid catalysts which has been tested, and the analytical techniques used to the analysis of the samples.

2.1 Hydrolysis

The high amount of rare sugars such as rhamnose, uronic acids and xylose (in minor part), make Ulvan hydrolysis very interesting in order to obtain sugar monomers for further valorization. The production of rare sugars in high yield is going to be a fundamental aspect for the biorefineries economic viability, indeed these sugars have different applications as intermediate and/or platform chemicals in the synthesis of high added-value products.

As already mentioned, the hydrolysis of biomass, especially lignocellulosic materials, has been studied for years with different purposes, like hydrolyzing cellulose to obtain glucose. Similarly, the hydrolysis of hemicellulose has been widely studied and reviewed by different authors [56]. Hemicellulose, like Ulvan is a huge source of rare sugars such as ribose and rhamnose, and moreover several most common sugars like

xylose, mannose, arabinose, galactose. The hydrolysis of hemicellulose is more appealing with respect to the cellulose one due to the variety of units that occur within the chain. Therefore, hemicellulose can be hydrolyzed under milder condition because of its relatively branched and amorphous structure compared to crystalline cellulose. Consequently, the hydrolysis can be carried on at lower temperature and not so concentrated acids, avoiding further monomer degradation. Therefore, the yield to the desired product may be increased, and the process will become environmental friendly.

The hydrolysis of biomass is based on the cleavage of the glycosidic bond linking two consecutive units in the polymeric chain through the catalyzing acid action. The breakage of the bond may be achieved also by alkaline hydrolysis, anyway several side reactions take place, lowering the monomer yield [18]

2.1.1 Mechanism of acid hydrolysis

The mechanism of acid hydrolysis of hemicellulose is well known, and it is based on the cleavage of the C-O-C bond that connects two sugars molecules [18]. Considering that Ulvan polymeric chains are based on the same structure of hemicellulose, this is single monosaccharides units linked by glycosidic bonds, it is reasonable to assume that the mechanism of acid hydrolysis is equal for both hemicellulose and ulvan.

The hydrolysis reaction starts with the protonation of the glycosidic oxygen which is located between two monomeric units. The oxonium macroion formed leads to the activation of the glycosidic bond, which is further broken down as the result of the dissociation of the oxonium ion. The cleavage of the glycosidic bond produces a macromolecule that can be monomer, dimer or oligomer and a carbonium macroion (carbocation). This carbocation is rather unstable and it reacts immediately with water, regenerating the acid catalysts, and another macromolecule [24]. The mechanism of polysaccharides hydrolysis can be illustrated with an example of cellulose hydrolysis shown in Figure 2.1.

The protonation of the bond may occur at any position along the polymeric chain, thus many options can take place. If the bond is broken in an intermediate position, two long oligomers will be released. Otherwise, if the protonation happens at the end of the chain an oligomer and a monomer will be produced (end biting process).

When the glycosidic bond has been broken and the polymer chain has been broken down into single monomers, the reaction can continue to the degradation of these low molecular weight units into a number of side products. At high temperature and low acidity hexoses dehydrate to HMF (5-hydroxymethylfurfural) whereas pentoses are dehydrated to furfural. It is also known that pentoses are decomposed faster than hexoses. The decomposition into low molecular weight units of monosaccharides leads

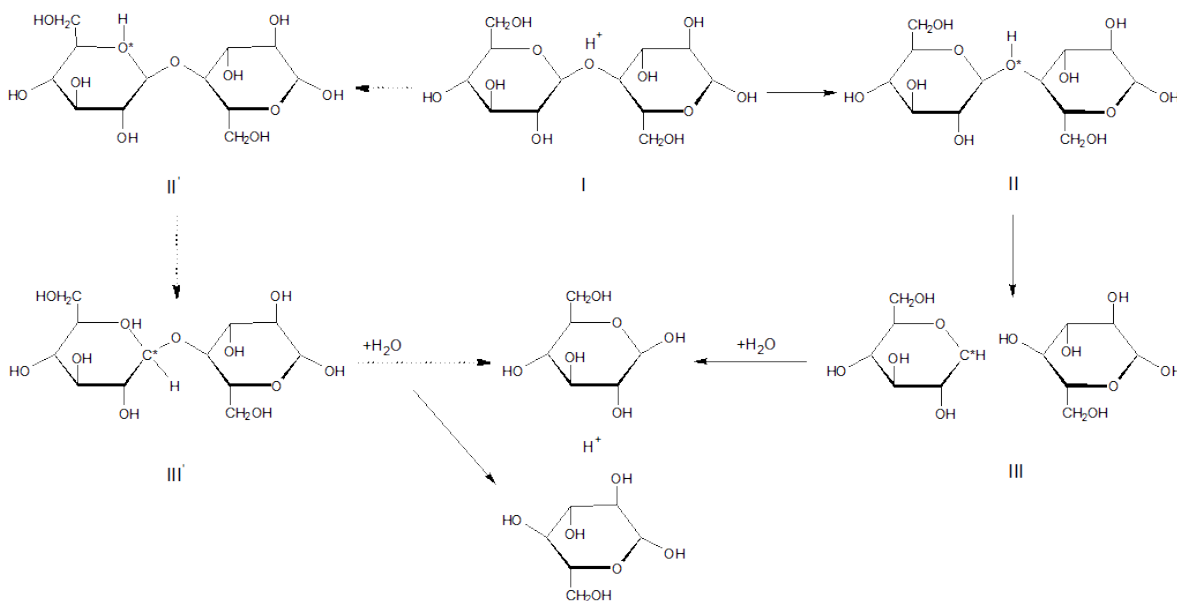


Figure 2.1: Mechanism of hydrolytic cleavage of glycosidic bonds

to a serious decrease in the yield of the expected products.

2.1.2 Parameters affecting the hydrolysis

It is reasonable to assume that, as well as hemicellulose, the depolymerization process of the Ulvan chain goes through several consecutive reactions, which lead to the single monomeric units. In order to develop an industrial scale process to obtain rare sugars from Ulvan, it is important to optimize the parameters that affect the hydrolysis reaction, and it is equally important to develop a kinetic model that describes all the reaction steps. Among all the factors that should be optimized, the most important ones are temperature, acid concentration and type of catalyst. The main purpose for the optimization is to push the productivity towards the desired products avoiding further degradation [56].

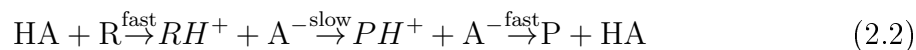
Other important factors affecting the hydrolysis rate are the types of linkage in oligosaccharides. It has been reported that α -glycosidic bonds react almost 2.85 time faster than β -glycosides ones, and this effect is independent on the temperature [59]. Wolfrom et al. also noticed and concluded that α -D linkages hydrolyze much faster than β -D linkages [54].

It should be noticed that the hydrolysis of hemicellulose is also affected by other minor aspects, which might influence partially Ulvan hydrolysis as well. The presence of side chains is important for the reactivity and the stability of the different C-O-C bonds. Uronic acids along the main chain counteract the hydrolysis effect stabilizing the molecules [71]. It has been reported that the hydrolysis of furanoses (5 carbons) is

much easier than pyranoses (6 carbons) compounds, this is due by the angular strain that occurs in five rings saccharides [56][47].

2.2 Acid catalysis

Catalysis provides an increased rate of a chemical reaction by lowering the energy required to obtain the products. This is literally done by changing the pathway of the reaction. Acids can act as catalysts, through two different ways: Specific acid catalysis and general acid catalysis. In the specific acid catalysis, the reaction occurs in the presence of hydroxonium ion (H_3O^+). The rate is proportional to the concentration of the ion and the mechanism is characterized by a two-step process: a fast reversible protonation of the substrate followed by the rate-determining step. Conversely, the general acid catalysis can be catalyzed by any acid that can donate a proton. This time the rate-determining step is the substrate protonation. After both reactions, the catalyst is regenerated. The two reactions mechanism can be summarized as follow:



The equation (2.1) represents the general acid catalysis, whereas equation (2.2) the specific acid catalysis. In both equations HA stands for acid catalyst, R is the reactant and P is the product [2]. According to the studies carried out on hemicellulose hydrolysis [47], the conversion and the yield of Ulvan hydrolysis should also strongly depend on acidity and temperature.

2.2.1 Homogeneous acid catalysis

Homogeneous catalysis is the most common and simple approach for the hydrolysis of hemicellulose. This reaction technique has been widely studied and performed through different acids such as: sulfuric, hydrochloric, nitric, acetic, oxalic trifluoroacetic and maleic acid [56][84][45]. As far as hemicellulose is concerned, studies have shown that the rate of homogeneous acid hydrolysis is affected by pH and temperature. High conversion and yields can be achieved by tuning of those two parameter. The reaction is generally very fast, the conversion of the polymeric chain to single monomeric unit proceeds very rapidly to a maximum after which a drop, due to degradation of the monomers, occurs. The main advantage of homogeneous catalysis, over heterogeneous one, is the absence of mass transfer limitation. Indeed, all the catalyst

is "active" and there is no need for the reagent to diffuse towards the catalytic site. On the other hand, homogeneous catalysis has also several drawbacks. The major one is the separation of the catalyst from the reaction mixture for simple recovery or further product purification. The acid solution, resulting at the end of the reaction, must be neutralized and the precipitated salts have to be removed. This process can be costly. The harsh conditions, in terms of acidity and high temperature, needed to reach a high conversion, can have a negative impact on the yield, because of the dehydration of the released sugars occurs. The formation of by-products drastically reduce the production of the desired monomers. Therefore, a fine-tuning of these two parameters is vital for the process. Eventually, the investment on anti-corrosive materials has to be done due to the low pH at which the homogeneous acid hydrolysis of carbohydrates is carried out.

Some of these problems, such as harsh acidity conditions, elevated temperature and the separation issue, might be solved by using enzyme as catalyst. However, often a mixture of different enzymes has to be used. Additionally even though enzymes operate at low temperature, they are rather temperature sensitive, and deactivation of the molecule can occur, requiring very efficient temperature control systems. Another aspect is that the hydrolysis rates are relatively low, consequently several days are required to achieve total conversion. Finally, since enzymes are very specific catalysts for a particular type of bond, which indeed give several possibilities, the production of enzymes is relatively expensive .

2.2.2 Heterogeneous acid catalysis

In the heterogeneous acid catalysis, the catalyst is supported on a solid which has the function of avoiding the dissolution of the catalyst in the fluid phase. The aim of heterogeneous acid catalysis is the same of homogeneous one, providing a source of protons in order to achieve the protonation of the glycosidic bond. Conversely to homogeneous catalysis, heterogeneous acid catalysis is much more complex. Several intermediate steps are required, including mass transfer and adsorption/desorption of the species on/from the catalyst surface, before to achieve the hydrolysis of the molecules. The entire reaction route can be described as follow. First the reactant should be transferred from the liquid bulk to the solid particle (external mass transfer). Then, the sugar molecules has to reach the active site, which might be located inside the particle (internal mass transfer). Each of these intermediate steps is characterized by its own kinetic, which is usually a function of the thermodynamic equilibrium between the fluid phase and the solid one, the conformation and the density of the active sites and their position inside the particle. This complexity in the reaction pathways is

reflected on the final reaction rate, which is usually slower than the homogeneous one.

Anyhow, the main advantage of using an heterogeneous catalyst is the easiness to control in a more suitable manner the occurrence of side reactions compared to homogenous catalysis. The use of a solid catalyst allows to control better the cleavage of glycosidic bonds, reducing secondary reactions like monomer degradation [47][98]. Therefore, the yield of the process can be improved. Many catalysts have been proposed and tested so far with the hydrolysis of oligosaccharides. The most interesting ones are: zeolites, resins and polymers (Figure 2.2), activated carbon materials, functionalized silica and other inorganic oxides such as sulfated zirconia or phosphates. Nevertheless, some general features can be identified in order to choose or design an active catalyst for the hydrolysis reaction. A solid catalyst suitable for the hydrolysis of oligosaccharides must be acidic, water resistant and it must bear strong Brønsted acid sites. Diffusion can limit the use of microporous materials such as zeolites, which are not the best candidates for hydrolysis of oligosaccharides. Mesoporous catalysts are preferred. The solid particle has to be synthesized or chosen in order to ensure that the reactant will reach the active site, which is not dissolved in the reaction medium but is embedded in the catalytic matrix. Another characteristic enhancing the catalyst activity toward hydrolysis of polysaccharides, is the hydrophilicity of the surface. Materials with $-OH$ groups on the surface make the adsorption of the reactants easier [98]. Using a solid catalyst allows to face and settle the other problems encountered with homogeneous catalysis. The separation of the catalyst may be done by simply filtration and consequently no costly and environmental hazardous neutralization is required. The catalyst can also easily be recycled if its activity is not deeply affected by the reaction media. Anyhow, if it is so, it might be regenerated. The easiness of the separation, and the fact that no more solid waste will be produced, makes the heterogeneous acid catalysis a perfect example of green process. Usually, a solid catalyst may be more expensive than a homogenous acid, however the material cost would be compensated by the fact that there is no need for anti-corrosive materials for process equipment. Heterogeneous acid catalysis have been widely used by the chemical industry especially in petrochemical processes, such as catalytic cracking or isomerization. Nevertheless, the catalyst used for those oil refinery processes were not designed to be water resistant. The development of the concept of biorefineries, set the necessity of new acid catalysts which must be suitable for reactions that involve soluble compounds, such as sugars, at a low temperature.

Different solid catalysts have been studied and proposed as good candidates to hydrolyze oligosaccharides, like hemicellulose and Ulvan. Most of the studies have been focused on the ion exchange resin catalyst, solid beads with big porous or non porous fibers with relatively high specific surface area.



(a) .



(b) .



(c) .

Figure 2.2: Zeolites (a), Ion exchange resin in beads form (b), superacid fibrous catalyst (c)

Ion exchange resins

An ion exchange material can be defined as an insoluble matrix containing labile ions that are exchanged with ions in the surroundings medium, where this exchanging process is done without physical changes in the material structure [10]. Ion exchange resins are organic polymers that can be synthesized in the form of beads, through the so called pearl polymerization (Figure 2.2). They can either be anionic or cationic exchangers, depending on the structure of the matrix and the embedded groups.

The most important and commonly used acid resins are constituted by a crosslinked polystyrene matrix on which are grafted sulfonic acid groups ($-\text{SO}_3\text{H}$). The sulfonic groups are introduced after the polymerization via a treatment with concentrated sulfuric acid. It is possible to synthesize also resins which have a weak acid behavior just by anchoring carboxylic groups ($-\text{COOH}$) instead of the sulfonic ones. It should be noticed that a cation exchange resin is characterized mainly by three parameters. The acidity of the catalyst, which is an indication of the strength of the acidic groups grafted to the chain. Secondly, the capacity of the resin, which represents the amount of active sites available for the reaction, and finally, the specific surface area.

The structure of these resins can be divided into gel and macroreticular. The former are constituted by an homogeneous matrix with no discontinuities. Thus, in order to exhibit a catalytic behavior, these materials must be used with reactants which are capable to swell the matrix to increase the accessibility to the catalytic sites. Consequently, in order to overcome this limitation, macro reticular resins have been synthesized. These types of resins consist of agglomerates of gellular microporous beads, which are fused during the last stage of polymerization [102]. This peculiar double structure of microspheres and macropores among clusters, allows the reactants to move more easily within the beads, through the macropores (10-100nm), to reach the catalytic sites avoiding resin swelling [28]. These materials have been the first ones used as catalyst in order to simulate the action of soluble acid, and also for the hydrolysis of several disaccharides [23]. Ion exchange resins, such as Amberlyst, are able to hydrolyze disaccharides into monomeric units at very low temperature (40-130°C). Moreover, it has been reported that at 80-90°C they are more active than zeolites [98].

The main drawback of ion exchange resins is their poor thermal stability. Generally, the hydrolysis of oligosaccharides is carried on between 90 and 200°C. However, resins like Amberlyst have been designed to operate at temperature lower than 130°C. Moreover, acid resin, functionalized with sulfonic-acid groups operating above 120°C, face to resin desulfonation and deactivation [42]. As well as other solid catalyst, ion exchange resins may be affected by fouling and poisoning caused by impurities. Proteins present in a sugar mixture derived from biomass, can be adsorbed on the resins

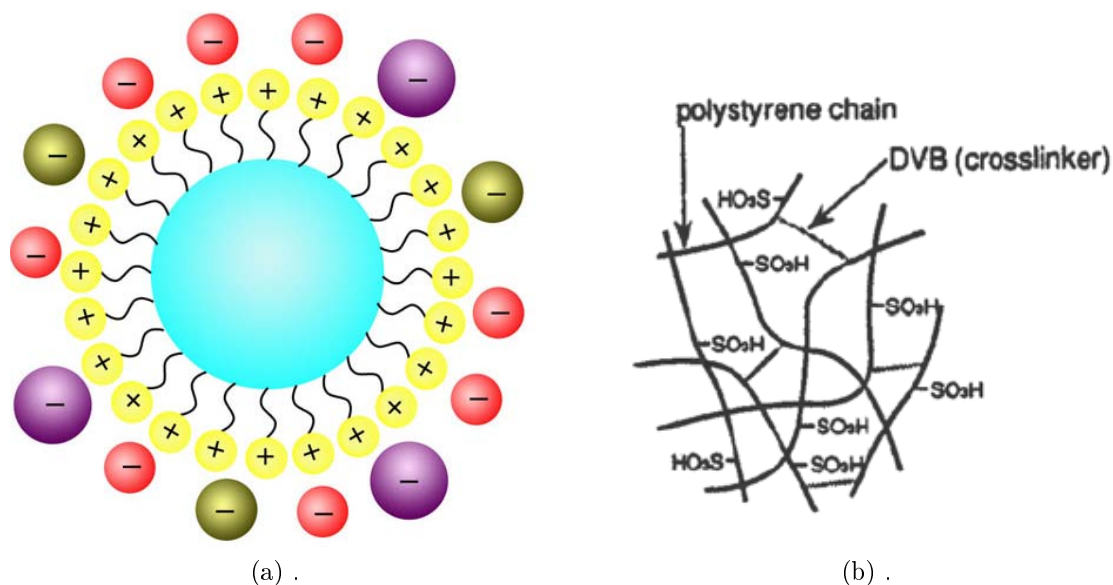


Figure 2.3: Ionic exchange resin structure (a), Amberlyst 15 resin structure [20][71]

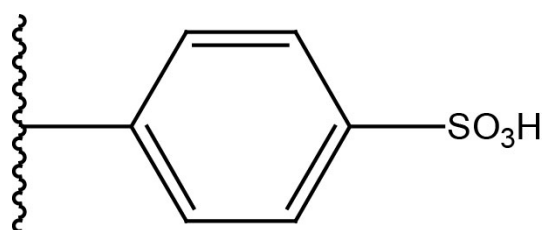


Figure 2.4: Smopex101 structure

polymeric chains, thanks to the interaction between the hydrophobic protein tails and the hydrophobic adsorbent surfaces. Besides, minerals can replace the hydrogen ions of sulfonic groups, deactivating the resin [102]. Polar solvents may lead to the leaching of the sulfonic groups and consequently free catalytic active species will be observed in the liquid bulk, reducing the catalyst selectivity.

Fibrous catalysts

Interesting types of ion exchange catalysts are the so called fibrous catalysts. These catalysts, also known as superacid fibrous catalysts, are non porous fibers bearing sulfonic acid functional groups. The fibrous catalyst used in this study is the SMOPEX-101, Figure 2.4

The structure of this fiber is formed by a scaffold of polyethylene on which polystyrene is grafted and sulfonic group are linked to it, as shown in Figure 2.4. The small size of the fiber allows to have a high specific surface area available for the reaction. This fibrous ion exchange catalyst is very appealing for hydrolysis of polysaccharides. Indeed, thanks to the non porous structure and to the relatively high surface area, the

catalytic sites are easily accessible for the polysaccharides chain. It has been observed that the hydrolysis of arabinogalactan gives an higher yield, in terms of arabinose, when the reaction is catalyzed by SMOPEX-101 rather than Amberlyst-15, even though the latter one has a higher acid capacity [62]. The explanation for that result is based on the diffusion limitation that occurs when Amberlyst is used as a catalyst. Indeed, its structure is porous, which hinders the accessibility of the polysaccharides to the active sites.

2.2.3 Enzymatic Hydrolysis

The enzymatic hydrolysis is another route that could be exploited to convert vegetable into monomeric units. Enzymes are generally proteins of high molecular weight (up to millions of Dalton). They can act as specific and effective biological catalysts in the hydrolysis of cellulose and hemicellulose. Enzymes are very interesting as green catalysts, indeed the reaction rates achievable are much higher than chemically catalyzed reactions. Moreover, enzymatic catalysis may occur even at ambient conditions [38].

Enzymatic hydrolysis of cellulose involves several pretreatment steps. First lignin and hemicellulose have to be removed because they are not digestible by the cellulosic enzymes inducing deactivation. Then the cellulose structure has to be opened up and the crystalline phase has to be broken because it slows down the effect of cellulase [105][103].

Enzymatic hydrolysis of hemicellulose is more complicated to analyze than that of cellulose. Even though, both are influenced by temperature, pH, substrate quality and concentration and enzyme activity, the main issue with enzymatic hydrolysis of hemicellulose is its complex chemical nature and heterogeneity. In order to achieve high yields a cocktail of different enzymes are required, the so called hemicellulases. Some of the enzymes needed to break down the hemicellulose structure are listed in Figure 2.5 [38].

Every enzyme has its own action (Figure 2.5), specificity and range of optimum utilization conditions. A good degree of coordination between all the different enzymes is therefore not so easy to be achieved, since quite often some intermediate products, produced by a particular enzyme, inhibit the action of other enzymes.

As far as Ulvan is concerned, the enzymatic hydrolysis has not so been deeply studied. Nevertheless, it has been reported that bacteria found inside some marine gastropod have an efficient capability to degrade Ulvan. Two of the enzymes, participating in the reaction, have been isolated, from the supernatant medium in which the bacteria grew in presence of ulvan, and classified in the CAZy glycoside hydrolase

Enzyme	Mode of action
Endo-xylanase	Hydrolyzes mainly interior β -1,4-xylose linkages of the xylan backbone
Exo-xylanase	Hydrolyzes β -1,4-xylose linkages releasing xylobiose
β -xylosidase	Release xylose from xylobiose and short chain xylo-oligosaccharides
α -arabinofuranosidase	Hydrolyzes terminal non reducing α -arabinofuranose from arabinoxylans
α -glucuronidase	Release glucuronic acid from glucuronoxylans
acetyl xylan esterase	Hydrolyzes acetyl ester bonds in acetyl xylans

Figure 2.5: Different enzymes and their relative action [38]

family (carbohydrate-active enzymes) [27].

Enzymatic hydrolysis is though very interesting in terms of reaction conditions (mild pH and low temperature), yields (close to 100%) and environment friendly features and benefits (no toxic vapour compounds or very strong dangerous acids). However, the very low concentrated solutions obtainable from an enzymatic hydrolysis and the problem of catalyst separation and re utilization required due to the relatively high cost of some particular enzymes, makes this route yet non-suitable for large volume of production.

2.3 Algae carbohydrates and Hemicellulose hydrolysis state of art

The aim of this work was, as mentioned in the introduction, to study the best conditions for ulvan acid hydrolysis in order to obtain high yield for both its constituents, rhamnose and glucuronic acid. Moreover, the work wanted to give a comparison between the traditional homogenous catalyzed hydrolysis with the heterogeneous catalyzed hydrolysis, in order to verify if the latter process would give comparable results to the former. Indeed, as mentioned in Section 2.2.2 the use of a solid acid catalyst for the hydrolysis of biomass would results in a simpler and environmental friendly process.

A brief description of the state of art regarding carbohydrates hydrolysis will be given, in order to provide a better understanding on the choices that were made to carry out the experiments. The works that were examined to obtain information about hydrolysis of carbohydrates were mainly focused on the hydrolysis of cellulose and hemicellulose. However, due to the heterogeneity of the ulvan chain only the works

regarding the hemicellulose hydrolysis were mainly taken into consideration.

In the work of Kusema et al. 2013 [45], the hydrolysis of O-acetyl-galactoglucomannan (GGM), derived from terrestrial biomass, has been studied both via homogenous and heterogeneous catalysis. The raw material hydrolyzed had an average molecular weight of 20kDa and the ratio of *Gal* : *Glc* : *Man* was equal to 0.5 : 1 : 4. In addition to that, the backbone of GGM was linear and the monomers were randomly distributed. The hydrolysis experiments were performed at 90 °C in the pH range of 0.5 to 2. It turned out that no side products were detected and the hydrolysis via SMOPEX-101 was faster than Amberlyst 15 due to SMOPEX-101 fiber structure. The initial rate of formation of galactose resulted faster than the other two monomers. This was explained according to the side position of galactose in the GGM backbone.

The hydrolysis of arabinogalactan (AG) has been studied in the work of Kusema and co-workers 2010 [47]. The performances of SMOPEX-101 were compared to Amberlyst 15 in the selective heterogeneous hydrolysis of arabinose. The hydrolysis experiments were performed at 90 °C and 0.01 M concentration of H⁺. The relatively milder conditions were needed to selectively hydrolyze the arabinose which is a side substituent in the AG backbone. The raw material had an average molecular of 20-100kDa. The study demonstrated that the selective hydrolysis of arabinogalactan is possible via heterogeneous catalysis. The yield in Arabinose was 95% when SMOPEX-101 was used as catalyst, thus the result was comparable in term of final production yield to the traditional homogeneous hydrolysis. No further degradation products such as HMF and furfural were detected.

The work of Hilpmann et al. (2014) [30] comprised the hydrolysis of glucuronoxylan was compared, in terms of performances, to the heterogeneous acid hydrolysis catalyzed by SMOPEX-101. The reusability of the solid catalyst was also tested. The results of the study demonstrated that for the same reaction conditions (90 °C, 0.01 M [H⁺]) the heterogeneous hydrolysis of xylans performed better than the homogenous one. Higher yield of xylose were obtained, however the catalyst deactivation, due to the leaching of sulfonic groups, deeply affected the performances of the catalyst in the following test. An autocatalytic behavior was also observed.

Notwithstanding, the open literature is scarce on works regarding *Ulva rigida* hydrolysis, there are some works dealing with algae hydrolysis which have used heterogeneous catalysis for the production of monomers.

The hydrolysis of biomass residue, derived from the extraction of κ -carrageenan from *Eucheuma cottonii*, was studied in the work of Tan et al. 2015 [94]. The cellulosic residues were pretreated in order to be further hydrolyzed via enzymatic conversion into glucose. The pretreatment was carried out with a solid acid catalyst, Dowex™Dr-G8. The results shows that at high temperature (120 °C) the cellulosic fiber were dissolved

faster and this had a positive effect on the further enzymatic hydrolysis. However, an increment to 140 °C for the pretreatment process lowered down the glucose final yield, because side degradation reaction may occur.

The performances of Amberlyst 15 was tested in the hydrolysis of marine macro algae in the study of Jeong et al. 2015 [34]. The biomass hydrolysed was derived from the *Gracilaria verrucosa*, and it was mainly constituted by glucose and galactose. Different reaction parameters were studied, however is important to notice that the range of temperatures tested was higher than in the hemicellulose hydrolysis works mentioned. Indeed, the temperature was ranged from 100 to 140 °C. Evidently, more extreme conditions are required to hydrolyze the backbone compared to the side chain monomers. The study concluded that the biomass was efficiently hydrolyzed, though some further degradation products, specifically 5-HMF and levulinic acids were also detected.

In the work of Jeong and Park 2015 [35], the factors affecting the production of reducing sugar from *Enteromorpha intestinalis* were investigated. The hydrolysis was performed via heterogeneous route using Amberlyst 15 as catalyst. The optimized parameters, in order to obtain the highest concentration in reducing sugar, were 140 °C, 15%wt. catalytic amount and a liquid to solid ratio of 7.5. Low concentration of 5-HMF was also detected.

The works that has been summarise in this section were taken into account in order to built the experimental matrix in Section 3.3.

2.4 Glucuronic acid decomposition

According to the experimental results that will be presented in Section 4, glucuronic acid decomposition is more severe than rhamnose decomposition under acidic conditions evaluated in this work for the hydrolysis of ulvan. Therefore lower glucuronic acid yields were obtained by the hydrolysis experiments. Consequently, a review of the open literature was conducted, in order to figure out what happens to glucuronic acid, after its cleavage from the ulvan backbone under acidic conditions and high temperature. Uronic acids are defined as aldose derivatives, which have the same carbon structure of the original sugar and the pseudoaldehydic group in position C-1, but they feature a carboxylic group in position C-6. D-Glucuronic acid is one of the three most abundant uronic acids in nature, together with D-galacturonic and D-mannuronic acids [3]. Uronic acids, together with their corresponding lactones, are the oxidation product of the hexoses. In the case of glucuronic acid the corresponding hexose is glucose, whereas the lactone is glucuronolactone. It has been reported that glucuronic acid is usually

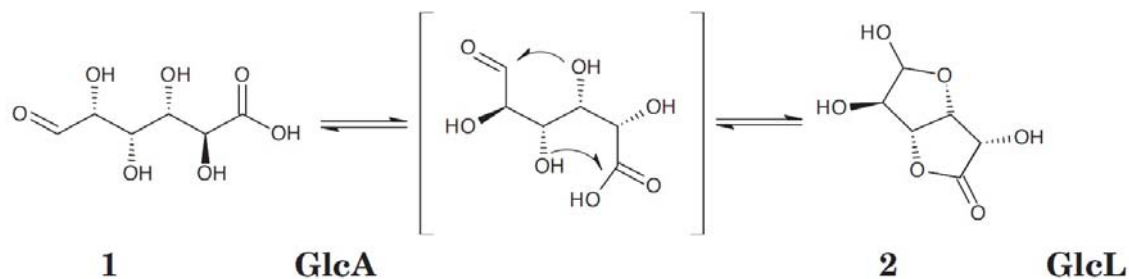


Figure 2.6: Equilibrium between GlcA and GlcL [99]

in equilibrium, in aqueous solution, with glucuronolactone (D-glucurono- γ -lactone), which is its dehydration product [99][3].

Figure 2.6 shows the mechanism on which the equilibrium, between glucuronic acid (GlcA) and glucuronolactone (GlcL), is based. The aldehydic group is hemiacetalized by nucleophilic addition of the C4 hydroxyl group, whereas the C3 -OH group is esterified by the carboxylic group [99].

The degradation kinetics of glucuronic acid, has been studied in subcritical water in the work of Rongchun et. al 2010 [99][97]. The use of subcritical water has several advantages since the concentration of protons is higher due to the increase of the temperature. Therefore, supercritical water is capable to act either as an acid or a base catalyst for hydrolysis or degradation of polysaccharides. It has been concluded that the degradation of glucuronic acid goes through three steps which include the equilibrium between GlcL that is further decomposed. Moreover, GlcA may also go straight to its decomposition products. The decomposition of GlcA is an endothermic process, exhibiting a faster rate if the heat supply is higher [99].

It has been studied that the organic acids obtained from hydrothermal treatment of alginate are the same as the ones obtained from the hydrothermal treatment of glucuronic acid [58]. Alginate is composed from D-guluronic acid and D-mannuronic acid which is the C2 epimer of GlcA. In the work of Aida et. al 2012, glucuronic acid has been hydrothermally treated at 300 °C and 20 MPa, to study its decomposition products. The GC-MS analysis detected the presence of formic, acetic, malic, lactic, succinic, glycolic and 2-hydroxybutyric acids and glucuronolactone, Figure 2.7.

The degradation of monosaccharides has been studied in the work of Novotny et al. 2008, [65]. In the case of glucose oxidation via $K_2S_2O_8/H_2O$ several acids and lactones were identified among which glucuronic acid and glucurono lactone were detected. It has also been reported that the recombination of the free radicals, produced from the intermediates of the monosaccharides degradation, lead to the formation of several C3 and C4 organic acids such as acetic, propionic, butyric and succinic acids [65].

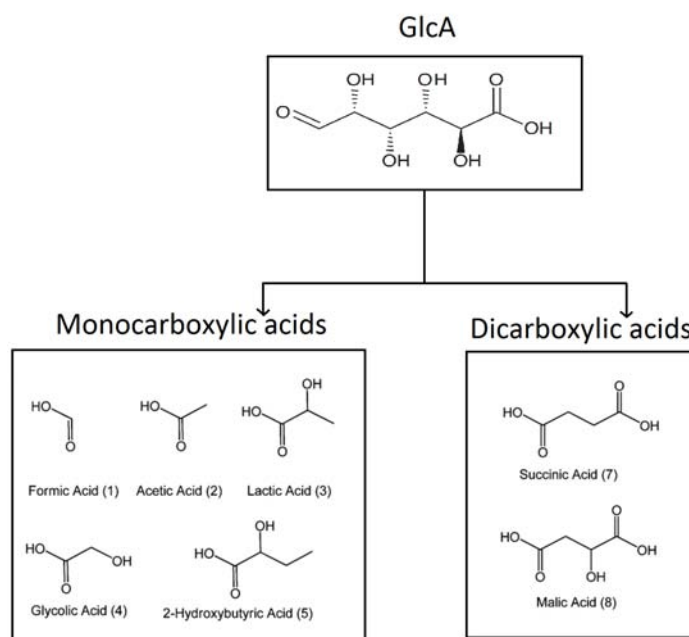


Figure 2.7: Acid detected from the hydrothermal decomposition of GlcA [58]

2.5 Analytical techniques

Chromatography is a powerful tool of analytic chemistry that allows the separation, the identification and the quantification of the different components from a complex mixture [92]. The simple method scheme consists of the dissolution of the sample into a mobile phase (gas, liquid or supercritical fluid), which is further forced to go through a stationary phase which, in the latest equipment, is commonly fixed inside a column [86]. The two phases are chosen in order to have different degree of affinity towards the components in the sample mixture.

In spite of the fact that many chromatographic methods are currently developed and established, the equipments that allow to carry out a chromatographic analysis are characterized by the same parts, i.e injection section, mobile phase, stationary phase and detector [78]. The injection system has the task of introducing the sample inside the chromatographic equipment. This is usually the most delicate part of the equipment, since the injection flux must be kept constant in order not to disturb the system. In turn, the mobile phase is the phase where the sample must be diluted before entering the column. The chromatographic techniques are divided into: gas, liquid and supercritical fluid chromatography, according to their nature. Generally, the mobile phase is just a passive carrier for the sample. Therefore, it is in charge of solubilizing the sample and moving it along the column towards the exit (eluate). The stationary phase, which is commonly put inside a column, is the one that usually

interacts more with the substances. Those interactions may have different nature such as: adsorption, size exclusion, ionic exchange, biochemical affinity and distribution. The immobilized phase can be either a solid or a liquid and it represents the key element for a good chromatographic analysis, indeed it has to be carefully chosen to obtain a good separation. Eventually, the detector is the element which stands at the end of a chromatographic equipment. Its role is to measure the signal coming from the end of the column and record it on a chromatogram. There are several types of detectors, some of them are built to destroy the sample in order to reveal the compound, therefore they are not designed for a further analysis of the mixture.

The basic principle, which is exploited in chromatography, is the different affinity that occurs among the compounds in the mixture and the two phases. A molecule, which interacts more with the stationary phase, will take more time to elute through the column than a less interactive molecule. As a result of this interaction, the separation of the two species is obtained, which can be identified by different retention or elution times [86]. Elution time is defined as the time taken for a specific compound to travel from the injection point to the detector [14]. This parameter is affected by several factors such as the length of the column, the operation temperature, the nature of the mixture. But mostly, as already said, retention time is deeply affected by the different forces that attract the compounds to the stationary phase.

The output of a chromatographic analysis may be visualized as a plot signal vs time in which the different peaks at different times are shown. Each peak represents a compound in the analyzed mixture, and the peak area is proportional to the amount of the corresponding compound. In order to carry out a quantitative analysis, it is important to relate somehow the peak area to the concentration. This may be done in two ways. At first it can be assumed that the concentration is proportional to the area of the single peaks divided by the sum of the areas of all the peaks. This method has a strong limitation, indeed it assumes that the signal is independent on the compound and the number of peaks is equal to the number of compounds inside the mixture.

A more sophisticated way is to adopt an internal standard in order to calculate a response factor, which allows to relate the area of the standard to the area of the component. This method can be summarized in the following equation:

$$C_i = \frac{(A_i/A_{std})}{(V_{std}C_{std})/V_i} f_i \quad (2.3)$$

$$f_i = \frac{1}{\frac{A_i^{cal}}{A_{std}^{cal}}} \quad (2.4)$$

where A stands for area, V stands for volume and C is the concentration, i is the i_{th}

compound that has to be analyzed whereas std is the internal standard. The correction factor f_i is calculated for every component in the mixture through a calibration sample in which the concentration of i and std are known.

Both gas chromatography and liquid chromatography are very well established techniques in the analysis of sugar mixtures. During the years, several methods have been designed in order to obtain information about the chemical composition and the structure of the different compounds in the sample [91]. In this project, gas chromatography has been used to quantify monomer concentration in the samples which have been hydrolyzed via heterogeneous catalysis, and the total sugar content in the starting mixture before the hydrolysis, whereas, the monomer content of the samples hydrolyzed via homogeneous catalysis has been quantified using High pressure liquid chromatography (HPLC).

2.5.1 Gas chromatography

In the gas chromatography the distribution equilibrium of the species is achieved between an inert gas mobile phase and a stationary phase, which may be either a solid or a liquid. Usually, the gas phase does not interact with the species, thus it is a pure carrier [92].

Usually, the columns used for a chromatographic analysis are filled up with a solid (packed column), on which a liquid is adsorbed forming a thin layer. This structure forms the so called stationary phase. Through this column the mobile phase flow and the entire device behave alike a distillation column. The different substances are separated according to their boiling point and to the different affinities each of them has with the stationary phase. Both of these parameters affect the retention time thus the degree of separation. In order to increase the effectiveness of the separation, the so called capillary columns have been designed. Capillary columns are formed by a very thin glassy wire, in which the solid immobile phase is coated on the internal wall of the capillary, in order to keep a very tiny hole in the center of the device. This design allows to reduce the pressure drops of the flowing phase, therefore longer column, up to 100 m, can be used.

Capillary columns are used to analyze high volatile organic compound, where the compounds before entering the device have to be dissolve into the gas phase. Nevertheless, it might be that the species to be analyzed are not volatile enough. For instance, if the molecules bear very polar groups such as hydroxyl ($-OH$) or amine group ($-NH$), they will form hydrogen bonds that increase the boiling point of the molecules. For that reason, they need to be pretreated in order to reduce their polarity, so that the volatility will increase.

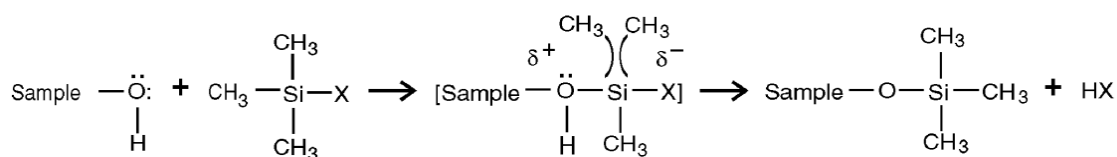


Figure 2.8: Mechanism of trimethylsilyl silylation [87]

Derivatization

The pretreatment, required to reduce the polarity of the molecule, is the so called derivatization and it falls into three reactions: alkylation, acylation and silylation. Alkylation allows to replace an active hydrogen with an aliphatic or aliphatic-aromatic groups (esterification). Acylation is meant to replace the active hydrogen with acyl group, whereas through silylation a silyl group is introduced [66].

The derivatization, through silylation, has been widely studied and successfully used by several research groups, in the analysis of carbohydrates mixtures [1]. It has also been reported that commonly, in the presence of sugar acids such as glucuronic acid, a very effective way of silylation is the so called Trimethylsilyl derivatization [82]. This technique is carried on coupling two standard silylation reagents, which are the hexamethyldisilane (HMDS) and the trimethylchlorosilane (TMCS). The action of HMDS, which is the silylation reagent, coupled with TMCS and pyridine increases the rate of the reaction [87].

The mechanism of silylation, as shown in Figure 2.8, occurs through a nucleophilic attack (SN2), which leads to the replacement of the active hydrogen in the hydroxyl group with a trimethylsilyl group. The reaction is driven by the goodness of the leaving group X. Efficient leaving groups are weak bases which are more capable to stabilize the negative charge in the transitional state [66].

In this project the derivatization, through trimethylsilyl reagents, has been used to analyze both the monomeric composition of the hydrolyzed mixture and the total sugar content of non-hydrolyzed mixtures, which are going to be further called as sample "0".

Methanolysis A technique used to determine the basic constituents of complex polysaccharides, total sugar content analysis, is the analysis of a non hydrolyzed mixture of those polysaccharides. The polysaccharide chains must at first be cleaved to monomer units, and then the sample can be derivatized. Consequently, the sugar and sugar acids, released from the carbohydrate, further react with methanol to form the respective methylglycosides, by replacing a methyl group for the hydrogen bonded to the oxygen coupled to the anomeric carbon. In the case of sugar acids their carboxylic groups are esterified with methyl group. Accordingly, the monomers are "locked" to

further react to form decomposition compounds. There are several ways to hydrolyze the sugar mixture, anyway acid methanolysis has proven to be the most efficient method for this task [1][5].

In the analysis of hemicellulose, the hydrolysis via methanolysis has several advantages with respect to the classical acid hydrolysis. The milder conditions, at which methanolysis is performed, does not degrade the crystalline structure of cellulose, thus the glucose obtained can be attributed only to be originated from hemicellulose. At the same time, uronic acids are esterified, otherwise they may easily undergo to rapid decarboxylation at severe conditions. Therefore, acid methanolysis allows to take into account for both neutral and sugar ring acid [5][82]. Consequently, it can be concluded that this method could be successfully applied to Ulvan as well, as already reported by other authors [15]

2.5.2 Liquid chromatography

Liquid chromatography (LC) is one of the most widely used analytical techniques, to separate a liquid mixture. This analytical method is rather sensitive, it is more accurate than GC for quantitative analysis and it is suitable to separate non volatile or thermally labile components [92]. In this chromatographic technique a liquid is used as a mobile phase, whereas a double structure liquid supported on a solid is used as the stationary one. The solid powder is commonly made by silicons materials in order to chemically bound the liquid.

As well as in GC, the separation is based on the distribution of the analytes between the two phases. The separation is visible as different elution times of different compounds from the column. In LC the equilibrium may be achieved through adsorption (good for low polar compounds) on ion exchange resins or gel permeation (size exclusion chromatography). This last mechanism is used in the analysis of average molar mass of polymers. Shorter molecules are trapped into the pores whereas larger ones cannot fit inside the pores thus they directly take the shorter path through the exit. Ligand exchange (ion exchange resins), is the primary mechanism in the separation of carbohydrates. Hydroxyl groups in the carbohydrates molecules are bounded by the fixed counterion in the resin. The binding is affected by the nature of the counterion, and by the spatial orientation of the of the hydroxyl group in the molecules [48].

To further improve the performance of liquid chromatography the so called High performance liquid chromatography (HPLC) has been developed. In HPLC the liquid mobile phase is forced through the column by pressure up to 350 bar. This allows to use smaller sorbent particles than standard LC, in which the driving force to flow the mobile phase is gravity. The use of high pressure increases the resolution power of

the technique, i.e. the ability to distinguish among compounds [92]. HPLC is anyway much more delicate than gas chromatography and the solvents used must have a high degree of purity. Moreover, the conditioning of the instrument, in case of variation in the method (column packaging, solvent), takes time.

In the current study HPLC has been used in the analysis of monomer content of samples hydrolyzed via homogeneous hydrolysis. Therefore, the pretreatment through derivatization has not been necessary. Moreover, as a side task, HPLC has also been used in the study of glucuronic acid decomposition to identify the decomposition products and to verify the reported equilibrium with glucuronolactone [99].

Chapter 3

Materials and methods

This chapter is focused on the description of the materials and methods used to carry out the project's tasks. The first part of the chapter deals with an overview of the equipments used, in particular the reactors setup and the procedures for extraction and hydrolysis of Ulvan. Also technical information about raw materials and catalysts will be given. Then, a brief description of the analysis, and the equipment used to carry out them, will be done. Eventually, the characterization of the experimental matrix will be explained.

3.1 Ulvan extraction reactor and procedure

Extraction of Ulvan, from fresh or freeze algae, can be done through several experimental procedures. According to literature, the common procedures involve the use of various solvents for the extraction, such as hot water, acid solutions, organic solvents or ionic liquids [72][15][67][104]. However, among all these methods, the one that is characterized by a good compromise between simplicity, effectiveness and time, is the extraction via hot water.

The extraction experiments were performed in an isothermal batch reactor, sketched in Figure 3.1, kept at 90 °C for 4 h, with a mixture of 37.5 g freeze algae and 600 mL of MilliQ water. The reactor was a 1 L glass surrounded by an ISOPADTM -LG2/ER heating mantle which was connected to the ISOPADTM TD-2000 temperature controller. The thermocouple of the temperature controller was not in direct contact with the mixture of water and algae, thus the temperature was also checked with an analogic thermometer in direct contact with the extraction solution. The temperature inside the reactor stayed within $\pm 3^\circ\text{C}$ during the experiments. The experiments were carried out at atmospheric pressure under air. To avoid the loss of liquid by evaporation from the reactor, a reflux condenser, with cooling water, was connected to the experimental

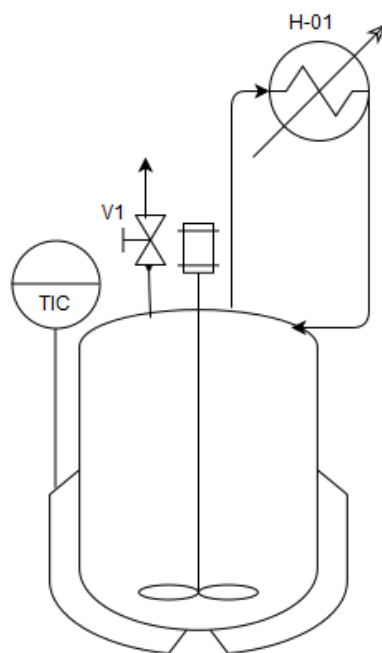


Figure 3.1: Extraction reactor diagram

device. A polypropylene blade was rotating at the stirring speed 650 rpm inside the reactor. The stirring was needed to guarantee the homogeneity of the bulk, avoiding that the algae particle might lie on the bottom of the reactor. From the top of the reactor, samples could be extracted at different time in order to verify the degree of extraction. Anyway, according to the experience of the staff working in the laboratory, a time of 4 h guarantees a high yield in rhamnase and glucuronic acid, up to 80% (Appendix B.1). After 4 hours the extracted Ulvan was centrifuged at 4000 rpm for 30 min, in order to settle the solid phase. The liquid phase was then vacuum filtered with Whatman 589/1 filter paper. Afterwards, 100 mL of extract were measured with a volumetric flask and stored in VWR™ borosilicate bottle in a freezer (-20°C). This protocol allows to recover between 350 to 400 mL of Ulvan extract with a concentration around 8 mg mL^{-1} .

3.1.1 Algae washing

Before the extraction of ulvan, the algae powder (37.5 g) was washed for 20 min in 750 mL of MilliQ water stirred at 650 rpm, at room temperature. After 20 minutes, the mixture was centrifuged at 4000 rpm for 20 min, and then the water was discarded and substituted with fresh one. The centrifugation step was repeated for two more times. This procedure was done to remove the ash from the algae mass as much as possible and to obtain extracted ulvan as pure as possible. According to TGA analysis done by the research group, algae loses ca. 20wt.% of its mass during this washing procedure.

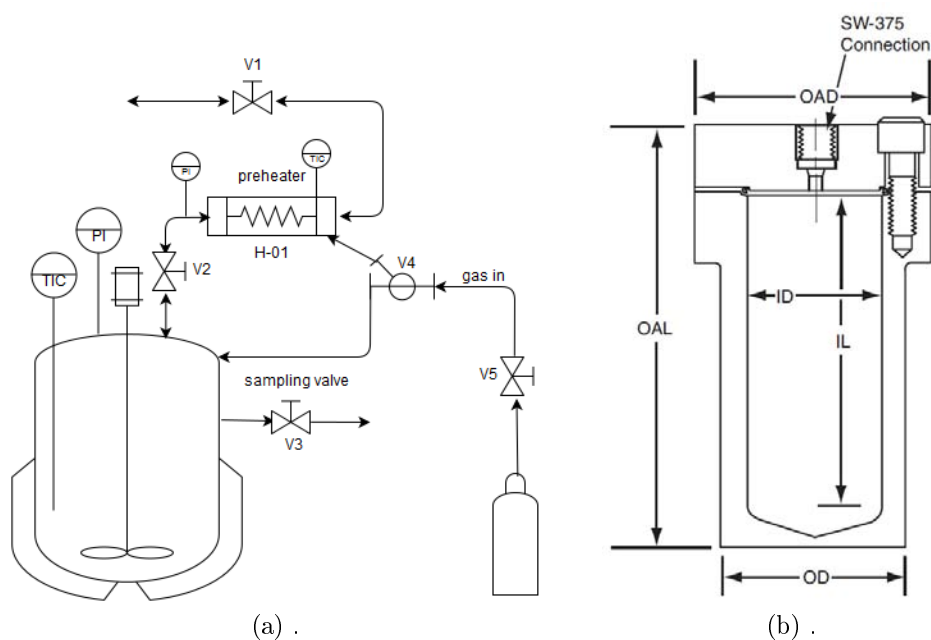


Figure 3.2: Schematic picture of the reactor setup (a), Autoclave vessel section (b)

3.2 Ulvan Hydrolysis reactor and procedure

Ulvan hydrolysis was performed in an isothermal batch autoclave produced by Autoclave Engineers[©]. The system, sketched in Figure 3.2, featured by a 316 stainless steel 300 mL (nominal capacity) vessel. The vessel was designed for high pressure processes up to 423 bar. The dimension of the vessel were: ID=46 mm, OD=65 mm, IL=181 mm, OAL=241 mm, OAD=105 mm. The reactor was equipped with an electric heating mantle, an internal copper coil used to cool it down the reactor at the end of the reaction for the cleaning stage.

On the top of the autoclave there was an additional electrical heat exchanger (pre-heater) which was used to preheat part of the reaction mixture, which was actually just water used to reach the desired reaction volume. The pressure inside the reactor may be increased exploiting an external source of nitrogen, which could flow either directly to the reactor or through the external heat exchanger. Nitrogen was also used in the starting stage of the reaction to help the water flow from the external heat exchanger to the reactor. Eventually, increased the pressure helps even in the sampling stage to increase the sampling flow if needed. Alternatively, the reactor was purged through the external heat exchanger line.

The autoclave was coupled to a CT-2000 control tower through which the temperature was controlled (PID) whereas the pressure was just indicated. The experiments were performed at different temperatures, Table 3.1, while the pressure was maintained

Sample #	Time (h)
0	0
1	1
2	2
3	4
4	7
5	12
6	24
7	36
8	48

Table 3.1: Sampling Interval

between 1-2 bar. The temperature was also recorded, during the whole experimental time, using the software Picolog[®] with 30 s intervals sampling.

The Ulvan extract (100 mL) was taken from the freezer and placed in a fridge (6 °C) overnight to melt it. Afterwards, the extract was poored into the reaction vessel together with the catalyst. The flange is then closed and a pressure test was done to verify the seal of the system. The external heat exchanger was filled with the additional water needed to reach the 200 mL reaction volume, so it was turned on. A simple weighted mean was used to estimate the temperature at which the external heat exchanger and the vessel should be set, in order to reach a temperature as much close as possible to the effective reaction temperature at the moment of mixing. The mixing moment was considered the time 0. Therefore, when the two preset temperatures were reached, the valve V2 (Figure 3.2) was opened to allow the hot water to flow to the reactor in order to trigger the reaction. Then, the vessel is set to the experimental temperature. During the experimental time, of 48 h, the reactor was manually purged, if needed, to keep the pressure in the experimental range.

During the experiment 2 samples of almost 1.5 mL each were taken according to the sampling time showed in Table 3.1

Several extraction experiments were carried out to produce enough ulvan to be used in the hydrolysis experiments. Consequently, the first sample was taken at time 0, right after the mixing between Ulvan -catalyst mixture and additional water, in order to quantify the initial sugar contain of the mixture and to be able to compare the results obtained from experiments, evaluated at different conditions. The samples were store in Eppendorf tubes kept inside a freezer (−18 °C). After 48 h the heating was shut down and the reactor was cooled down for the cleaning stage. The reaction mixture was vacuum filtered with Whatman 589/1 filter paper in order to recover the catalyst which was afterwards dried in an oven at 60 °C. Samples were further stored

at room temperature in PE tubes.

3.2.1 Catalyst pretreatment

In the heterogeneous hydrolysis experiments the solid catalyst was previously treated in order to wash out the sulfonic groups that were not bounded to the resin. Additionally, the leaching of those groups inevitably occurs in water at the reaction temperature. The catalyst was weighted accordingly to the desired equivalent H^+ concentration. Therefore, the catalyst was washed at room temperature with 150 mL of MilliQ water for 30 min. The washing was performed in a becher glass stirred with a magnetic stirrer at 500 rpm. Afterwards, the catalyst was let completely to settle down to the bottom of the glass, and the water was discarded as much as possible. According to the weight of the catalyst and the weight of the empty becher, the calculation of the water leftover into the becher (W_{lft}) was straightforward. This water amount was taken into account in order to calculate the amount of water that must be added ($100\text{ mL} - W_{lft}$) in order to reach the 200 mL reaction volume.

In the case of homogeneous catalysis the above mentioned procedure was not needed. The amount of catalyst, needed to have the desired H^+ concentration, was calculated assuming its complete dissociation.

3.3 Raw materials

3.3.1 Algae

The starting material used for this project was *Ulva Rigida* donated by Prof. Mario Edding from the Research and Technological Center in Applied Phycology CIDTA-Northern Catholic University of Chile. The algae were collected from the area of La Herradura de Guayacàn Bay, city of Coquimbo, Región de la Coquimbo in northern Chile. Algae were first removed from marine rocks, and then spread on plastic film to dry for 48 h in air, avoiding contact with sunlight. Afterwards, the algae sample was further dried at for 40°C overnight and finally milled to 90%-# 30 mesh in a cross beater mill Restch SK10. The samples were stored in a freezer prior to the hot water extraction [72].

In Figure 3.3, the carbohydrate composition of the *Ulva Rigida*, used in this study, is reported. The data are referred to the work of Pezoa-Conte 2015 [72].

Monosaccharide	Value mg/g of dry alga
Arabinose	0.7 ± <0.1
Fucose	0.1 ± <0.1
Galactose	11.7 ± 0.1
Galacturonic acid	1.4 ± 1.5
Glucose	183 ± 7.8
From acid hydrolysis*	183 ± 7.8
From acid methanolysis**	184 ± 1.1
Glucuronic acid	62.3 ± 0.9
Fructose	1.4 ± 0.1
Mannose	ND ± ND
Mannitol	0.9 ± 0.8
Mannuronic and guluronic acids	18.0 ± 6.1
Rhamnose	81.2 ± 2.5
Xylose	38.5 ± 1.1

Figure 3.3: Monosaccharide content in *Ulva Rigida* used in this project [72]

3.3.2 Catalysts

One of the tasks of this project was to test the performance of different solid catalysts in hydrolysis of Ulvan. The catalysts have been selected according to the works which have already widely tested them in the hydrolysis of hemicellulose, and on the characteristic of the catalyst [63][45][84][47].

The performance of heterogeneous acid hydrolysis have been compared with the homogeneous acid hydrolysis. For the homogeneous hydrolysis the catalyst chosen was HCl furnished by J.T Baker™, purity 37.5%. To calculate the amount of HCl needed, in order to achieve the desired concentration of protons in the reaction mixture, the complete dissociation of the acid has been assumed. The assumption is supported by the value of the $pK_a = -6.3$, which means that the acid is strong.



SMOPEX-101

The first solid catalyst chosen for this project was a fibrous catalyst from the family of SMOPEX furnished by Jhonson Matthey®. Among all the SMOPEX catalysts the one which has the features suitable for this project is the SMOPEX-101, Figure 3.4 . SMOPEX-101 (S101) was selected because of its sulfonic groups which give a strong acid behavior. It has relatively high capacity, thus the high concentration of sulfonic groups is needed in order achieve low pH needed for the cleavage of the glycosidic bonds. Eventually, the non-porous structure of SMOPEX-101 is able to minimize the mass transfer limitation from the liquid bulk to the active sites of the molecules.

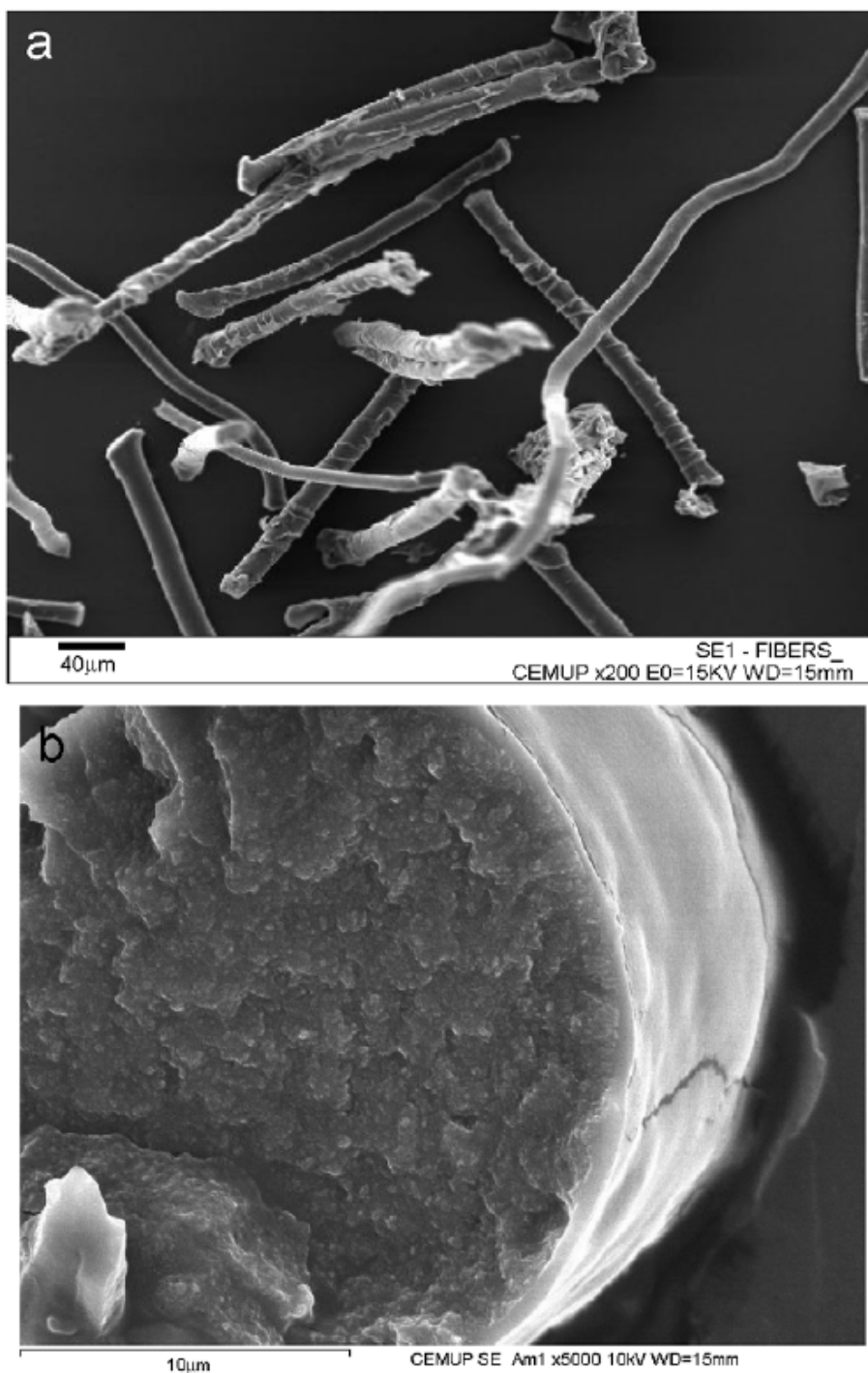


Figure 3.4: SEM images of SMOPEX-101, Scientific Figure on ResearchGate. Available from: https://www.researchgate.net/239156190_fig1_Fig-1-SEM-Image-of-the-Smopex-101-fibres-a-fibre-physical-appearance-b-fibre

Catalyst	SMOPEX-101	Amberlyst 70
Type	fibrous	beads
Diameter (mm)	0.01	0.5
Average pore diameter (Å)	-	220
Length (mm)	4	-
Backbone structure	Polyethylene-graft polystyrene	Polystyrene cross linked DVB- halogenated
Acid Functional Group	-SO ₃ H	-SO ₃ H
Humidity Content (%)	48	48
Surface Area (m ² g ⁻¹)	-	36
Capacity (mmoleqH ⁺ g ⁻¹)	3.2	2.55
Density (g L ⁻¹)	300	770

Table 3.2: Catalysts properties

Amberlyst 70

A regular ion exchange resin has also been tested, Amberlyst 70 (AMB70) from by Rohm and Haas Company was chosen. Polystyrene sulfonic acid resins, in the form of beads, have been widely tested in the hydrolysis of hemicellulose [45][47]. These resins have been commonly utilized in the form of Amberlyst 15, a relatively high specific surface area resin (36 m² g⁻¹), with an acid capacity of 4.7 mmol H⁺ g⁻¹. This resin catalyst has shown to work under mass transfer limitation in the hydrolysis of hemicellulose due to its porous structure although it features more temperature tolerance.

In this study, Amberlyst 70 was tested. This ion exchange resin has the same structure of Amberlyst 15, but the chain has been halogenated. This treatment reduces the cation exchange capacity by weight, but it has been claimed that the halogenation increases the thermal stability [90].

In Table 3.2 the characteristics of both SMOPEX-101 and Amberlyst 70 are listed.

3.4 Analysis

The analyses, performed on the hydrolyzed samples, were meant to analyze the evolution of the main monomeric units versus time from the cell wall of *Ulva rigida* (glucose, xylose, rhamnose and glucuronic acid), which are cleaved from the polysaccharide backbone catalyzed by acid hydrolysis. The attention has been focused on rhamnose and glucuronic acid, since they are the main constituents of ulvan.

3.4.1 Total sugar content

The total sugar content is fundamental in order to obtain the yield versus time of the hydrolyzed monosaccharides. Indeed, the analysis allows to obtain the concentration of the single sugars in the starting mixture (sample 0) prior to the hydrolysis. To measure the total sugar content, in the unhydrolyzed samples, it is necessary to breakdown the cell walls composed of polysaccharides to their monomeric forms by a pretreatment called acid methanolysis (see Section 2.5.1). The samples were treated with a solution of HCl/methanol 2M, for 3 hour in an oven at 100°C. Afterwards, the methanolized samples were neutralized with pyridine, and the internal standards were added (Resorcinol, Sorbitol). Eventually, samples were derivatized via silylation. Together with the samples at time zero, also two calibration samples were prepared. Those two calibration samples were needed to calculate the correction factor for the single species. The calibration samples contained a mixture with known amounts of the singles monomeric units, the internal standard was also added also. The calibrations samples are further methanolized and derivatized. Eventually, both samples at time zero and the calibration ones were analyzed via gas chromatography. The detailed protocol for acid methanolysis is included in Appendix A.1.

3.4.2 Monomer content

The monomer content analysis allows to determine the amount of sugars that has been cleaved from the polysaccharide chains through the acid hydrolysis. The results of the analysis are therefore the concentrations of the single monosaccharides in the samples withdrawn at different times. Therefore, monomer content analysis gives the change of the concentration of monosaccharides in the liquid phase, as a function of time.

The samples subjected to heterogenous acid hydrolysis were treated as follows. The samples taken at different times were derivatized through silylation (Section 2.5.1). Besides, two calibration samples were prepared as in the total sugar content, and derivatized. Xylitol was used, this time, as an internal standard. The samples and the calibration standard are further analyzed with GC. The entire protocol can be found in Appendix A.2.

As far as homogeneous acid hydrolysis' samples are concerned, those ones were analyzed directly using HPLC. Indeed, the fact that the silylation procedure would underestimate the content of monomers has been noticed. The monomers concentrations were further estimated through calibrations curve. The calibration curves have been prepared analyzing four mixtures with the monomers at different known concentrations. The description of the calibration curves fit could be found in Appendix

B.2.

3.4.3 Gas chromatography

The gas chromatography equipment PerkinElmer Autosystem XL, used to analyze the heterogeneous hydrolyzed samples, was equipped with a Hewlett Packard HP1 column. This column has a length of 30 m and an internal diameter of 0.32 mm. The capillary column is coated with a film of dimethyl polysiloxane, 0.17 μm thickness. About 1 μL of silylated sample was injected into the column, the carrier gas was hydrogen. The column temperature was increased with a ramp ($4\text{ }^{\circ}\text{C min}^{-1}$) from 100 to 175 $^{\circ}\text{C}$, and then another ramp from 175 to 290 $^{\circ}\text{C}$ with a rate of $12\text{ }^{\circ}\text{C min}^{-1}$. The GC was equipped with a FID detector, at temperature of 290 $^{\circ}\text{C}$.

3.4.4 HPLC

The HPLC device used to analyze the homogeneous hydrolyzed samples is the HP-1100 series furnished by Agilent Technologies. The HPLC system is equipped with the AminexTMHPX-87H column. The column is packed with a polymer based matrix (polystyrene-DVB), the length is 300 mm and the diameter is 7.8 mm, particle size was 9 μm . A combination of size exclusion and ligand exchange (binding of $-\text{OH}$ with resins counterion) mechanism is used to separate the mixture. The producers claimed that the column is efficient for analyzing carbohydrates in solution with carboxylic acids. The mobile phase was a solution of H_2SO_4 (0.005 M). The injection volume was 10 μL and the column temperature was set at 55 $^{\circ}\text{C}$. The HPLC was equipped with a refractive index detector, HP-1047A.

3.5 Experimental matrix

Hereby, the experimental matrix is presented, Table 3.3

3.5.1 Temperature

The temperature choice was done according to the previous works described in Section 2.3. Notwithstanding, the temperature used to hydrolyze the hemicellulose was below 100 $^{\circ}\text{C}$, the higher molecular weight and the relatively linear structure of ulvan imposed to use higher temperature than the ones used by the previous studies. Three temperatures have been chosen in order to test the performance of SMOPEX-101 in the hydrolysis of Ulvan. The maximum reaction temperature was set to 120 $^{\circ}\text{C}$ because of the relatively low thermal stability of the resins used, and to reduce the further

Experiment #	catalyst	acidity (mM H ⁺ eq)	T (°C)	Batch V (mL)	Sugar conc (g L ⁻¹)	Mass catalyst (g dry)
1	SMOPEX-101	100	100	200	3.851	6.25
2	SMOPEX-101	100	110	200	4.133	6.25
3	SMOPEX-101	100	120	200	5.132	6.25
4	SMOPEX-101	50	110	200	4.601	3.13
5	SMOPEX-101	75	110	200	3.431	4.69
6	Amberlyst70	50	110	200	3.896	3.76
7	Amberlyst70	100	110	200	4.176	7.84
8	HCl	100	90	200	4.250	0.729
9	HCl	100	100	200	5.121	0.729
10	HCl	100	105	200	4.650	0.729
11	HCl	100	110	200	4.422	0.729
12	SMOPEX-101	-	110	200	4.139	-

Table 3.3: Experimental matrix

degradation of sugars. The other two additional temperatures, 100 and 110 °C, were used to study the activation energy of the reaction. Once the screening of temperatures with SMOPEX-101 was accomplished, the temperature that gave the most promising results was chosen as the temperature to test the other resin (Amberlyst-70), and different concentrations of acidic groups. A complete screening of temperature was performed for the the homogeneous acid hydrolysis.

3.5.2 Acidic concentration

The concentration of protons was carefully chosen in order to study the dependency of the hydrolysis on acidity. In the case of heterogeneous hydrolysis using a high solid to liquid ratio, it may lead to limitations in the mass transfer due to the problem with stirring. Therefore, a maximum concentration of 100 mM H⁺eq was set.

3.5.3 Reutilization of the catalyst

An interesting feature of solid acid catalysis is the possibility to recover the catalyst after the reaction, in order to further reutilize it. Consequently, the re-usability of the catalyst, was studied performing a further acid hydrolysis using the recovered catalyst. For this test the optimun reaction parameters, temperature, catalyst type and acidity, were chosen.

The catalyst chosen was SMOPEX-101 which catalyzed the reaction at 110 °C and 100 mM H⁺eq (experiment 2, Table 3.1). It can be noticed that, in Table 3.3, the mass and the catalyst for experiment 12 are not reported. The reason why, those values are

missing, is because the mass balance for the catalyst recover after experiment 2 was not fulfilled. According to Table 3.2 the dry content of SMOPEX-101 is 48%, therefore the total mass of catalyst utilized in experiment 2 was 13.02 g (Table 3.1). After the vacuum filtration of the catalyst and its drying, the recovered mass was around 10 g. This value is higher than the dry mass of the catalyst, used in experiment 2, Table 3.1. There are no clear explanations for this result; the most accepted one was that the catalyst was not completely dry. Accordingly to this non-descriptive result, the experiment to test the re-usability of the catalyst has been performed with the total mass of the catalyst recovered from experiment 2.

Chapter 4

Experimental results

In this section the results of the experiments are presented and discussed. The first part reports the outcome of the total sugar content analysis in the samples at time zero. Afterward, the monomer analysis results of the heterogeneous acid hydrolysis and the performance comparison between the two solid catalysts, are introduced. The second part of the chapter is focused on the homogeneous hydrolysis results and the comparison with the heterogeneous ones. Additionally results regarding the glucuronic acid decomposition and the variability analysis of the methods used for the quantification of monomers are displayed.

4.1 Total sugar content $t=0$

In Table 4.1, the results for the total sugar content analysis are reported. The analysis were performed on the samples withdrawn at time zero, thus before the beginning of the reaction. The concentration for only glucose (Glc), xylose (Xyl), rhamnose (Rha) and glucuronic acid (GlcA) are reported, since they are the main constituents of the *Ulva rigida* cell wall. Indeed, minor quantities of galactose, arabinose and galacturonic acid have been revealed by the analysis. Anyway, the concentration of latter sugars were at least one order of magnitude lower than the ones reported for the main constituents of *Ulva rigida* in Table 4.1 According to the total sugar content analysis, which accounts for the total carbohydrate content in the sample, the average total carbohydrate content, among all the experiments, accounted for 4.33mg/mL. GlcA and Rha were the major constituents of the cell wall of *U. rigida*. Indeed, an average value of 80 wt.% was calculated from the data in Table 4.1, according to the following equation:

$$x_{wt} = \frac{C_{Rha}^0 + C_{GlcA}^0}{C_{Rha}^0 + C_{GlcA}^0 + C_{Glc}^0 + C_{Xyl}^0} 100\% \quad (4.1)$$

Experiment #	Glc [mg/mL]	Xyl [mg/mL]	GlcA [mg/mL]	Rha [mg/mL]	TC [mg/mL]
1	0.419	0.273	1.476	1.964	3.851
2	0.782	0.312	1.786	2.252	4.133
3	0.550	0.244	1.362	1.739	5.132
4	0.745	0.278	1.686	1.892	4.601
5	0.413	0.237	1.201	1.579	3.431
6	0.465	0.272	1.701	1.984	3.896
7	0.446	0.187	1.637	1.869	4.176
8	0.564	0.255	1.536	1.894	4.250
9	0.671	0.252	1.466	1.788	5.121
10	0.758	0.258	1.846	1.787	4.650
11	0.344	0.263	1.577	1.667	4.422
12	0.981	0.317	1.861	1.962	4.139

Table 4.1: Total sugar content of samples 0h

The average ratio between rhamnose and glucuronic acid (C_{rha}^0/C_{GlcA}^0) in the samples was 1.12. This value indicates that the rhamnose content in the extract occurs in a slightly higher amount than glucuronic acid. This feature may be due to the ulvan structure; indeed according to Section 1.4.1 rhamnose occurs in all the different disaccharides, which constitute ulvan. In turn, glucuronic acid occurs only in the aldobionuronic acid 3-sulfate type A (Figure 1.9). Glucuronic acid is also more reactive than rhamnose due to its carboxylic group. Therefore, it's reasonable to assume that a minor part of the glucuronic acid, cleaved by the methanolysis, could further degrade into decomposition products. This might reduce its amount in the analysis of sample at $t = 0$. However, it should be noticed that the methanolysis method is better for accounting uronic acids units than acid hydrolysis [5].

This preliminary data will be taken into account in the modelling of the kinetic data. Indeed, the homogeneous kinetic model is based on the assumptions that only Rha and GlcA constitute Ulvan and that their ratio in the backbone is 1 : 1.

The total concentration of the monomers in the sample at time zero, allows to calculate the yield of the products, namely rhamnose and glucuronic acid, which is defined according to the following equation.

$$Yield = \frac{C_i^t}{C_i^0} \quad (4.2)$$

where C_i^t is the concentration of the i species at time t , whereas C_i^0 is the total concentration of the i species at time zero, considering monomers oligomers and polysaccharides. It is important to provide the final data in terms of yield in order to compare

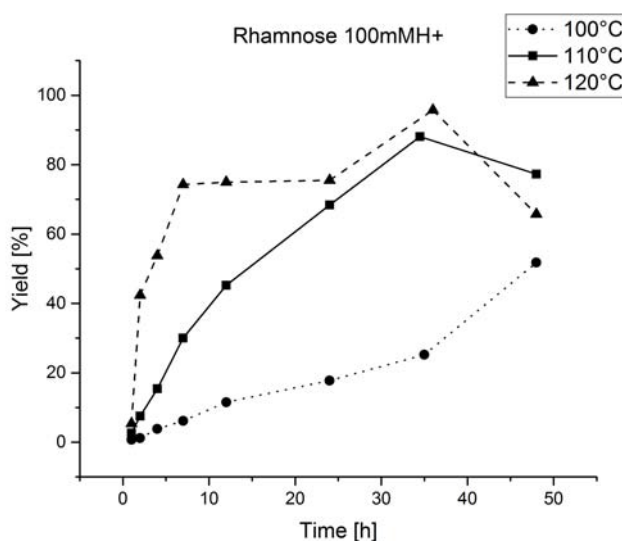


Figure 4.1: Rhamnose yield as a function of time in experiments 1,2,3

the results of different experiments, because the concentration of the samples at time zero are different from one to another experiment, due to the preparation of different ulvan batches for the hydrolysis experiments, as shown in Table 4.1

4.2 Heterogeneous acid hydrolysis results

Hereby, the results for the heterogeneous acid hydrolysis, performed at different temperature, equivalent concentration of H^+ and using different type of catalyst, are reported. The performance of the reused solid acid catalyst in experiment 2 is also reported.

4.2.1 Temperature effect

In Figure 4.1, the yield of rhamnose as function of time is shown. The data are referred to experiment 1,2,3 (Table 3.3), in which the catalyst tested was SMOPEX-101 at the same acid site concentration ($100mMH^+eq$) and temperature between the range 100-120°C. According to the time scale, it is clear from the results reported in Figure 4.1, the heterogeneous hydrolysis of Ulvan, at the experimental conditions hereby evaluated, is a relatively slow reaction. The maximum yield was reached after 7h at 120°C, whereas at 110C the maximum yield was observed after 34h. Eventually, at 100°C after 48h the reaction was not over yet. The temperature had a positive effect on the reaction rate in the initial phase of the reaction, as expected. No further noticeable degradation of rhamnose was observed, even though it seems that at 110

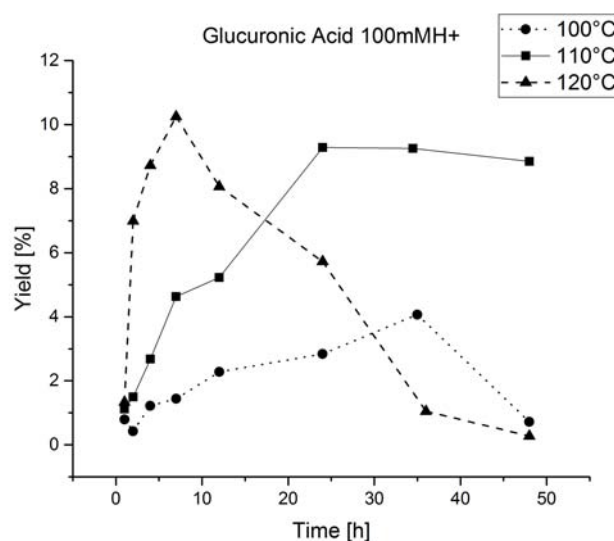


Figure 4.2: Glucuronic acid yield as a function of time in experiments 1,2,3

and 120°C the experimental trend is a combination of a positive ascending curve (production) with a slightly negative descending one (degradation). Opposite to the results reporting autocatalytic kinetics for heterogeneous acid hydrolysis of hemicellulose [84], no autocatalysis was observed in the current case. This might be due either to the higher reaction temperature tested in this study, or to the relatively coarse measurement sampling interval in the first hours of the reaction, which did not allow to prove the occurrence of this phenomenon. According to the last point at 48h, the hydrolysis performed at 110°C seems to have the best performance in terms of final yield achieved. The second last point in the trend at 120°C could not be considered as a reliable point due to its deviation from the general trend. The curves in Figure 4.2 represents the glucuronic acid yield as a function of time for the hydrolysis of ulvan carried out at 100mMH⁺eq at different temperatures. As far as the production step is concerned, the trends seem to behave in a similar way as observed for rhamnose formation. However, for glucuronic acid the degradation reaction occurred in a larger extent decreasing the yield of the monomer. Accordingly, yield for rhamnose was to fold higher the yield of glucuronic acid. Since the most abundant repeating unit in ulvan is this disaccharide, it was expected to obtain relatively similar yields for both Rha and GlcA due to the cleavage of the glycosidic bond. The very low yield of GlcA may be due to its high reactivity. It could react immediately after its formation with the sulfonic groups of the resin. The best performances in terms of yield were achieved at 120°C, even though it has to be taken into account that the kinetic trend at 120°C is severely affected by the decomposition reactions. Additionally, this temperature is very near the threshold thermal stability of the resin.

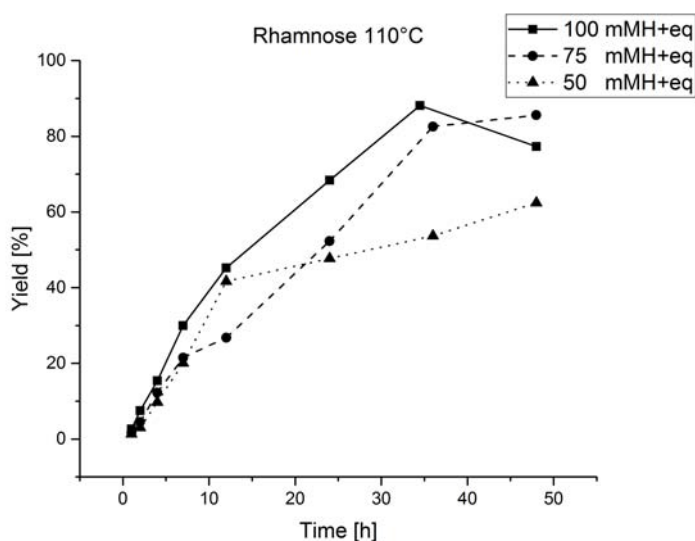


Figure 4.3: Rhamnose yield as function of time in experiment 2,4,5

A common remark for both the experimental trend of Rha and GlcA should be done in order to explain the relatively high scattering phenomenon which occurred on the kinetic experimental trend reported in Figure 4.2 and Figure 4.1. As reported in Section 2.5.1 the heterogeneous samples were first pretreated through derivatization in order to be analyzed with the GC. The reactants used to perform this procedure are very moisture sensitive. Moreover, the relatively multi-step complexity of the protocol may lead to increase the chance of spoiling the samples shattering the final analytical results.

4.2.2 Acidity concentration effect

The results for the experiments at constant temperature (110°C) and different acidity concentration are depicted in Figure 4.3 for Rha and Figure 4.4 for GlcA, respectively. All the experimental curves exhibit the same production rate in the first hours, accordingly to the fact that the experiments were carried out at the same temperature. As far as rhamnose is concerned (Figure 4.3), the yield increased by increasing of acidity.

The results concerning glucuronic acid are shown in Figure 4.4. The decrease on the acidity concentration seemed to have a positive effect in the case of glucuronic acid yield. A lower equivalent H⁺ concentration (50mMH⁺eq) allowed to reach a higher yield, even though the degradation phenomenon is still severe at these experimental conditions. The experimental trend for the experiment at 75mMH⁺eq was rather singular. Indeed, the decomposition was expected to occur in between 100 and 50 mMH⁺eq

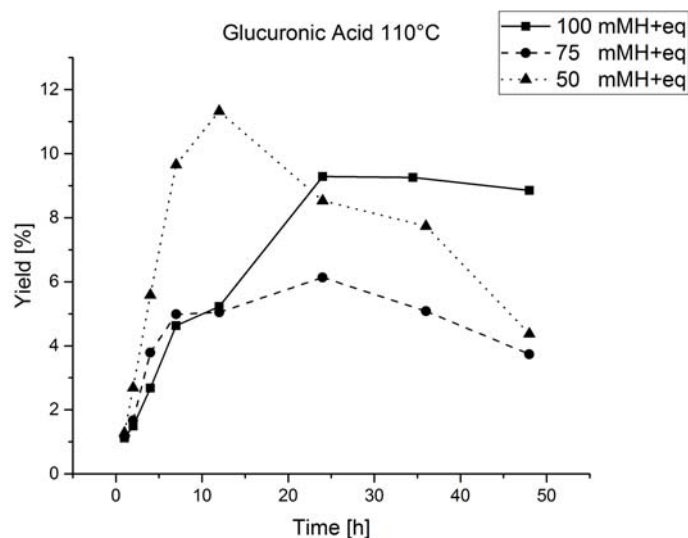


Figure 4.4: Glucuronic acid yield as function of time in experiment 2,4,5

concentration. This observation may be explained by differences in the rates of the several reactions that took place in the degradation of GlcA, which will be discussed in the following sections

4.2.3 Catalyst type

The kinetics of the hydrolysis carried out at 110°C using Amberlyst 70 as catalyst are reported in Figure 4.5 for Rha and Figure 4.6 for GlcA, respectively.

It is evident from the kinetic trends that the hydrolysis catalyzed by Amberlyst 70 is deeply affected by the mass transfer if compared to the SMOPEX-101 results. As described in Section 3.3.2, the porous structure of Amberlyst 70 results in internal mass transfer limitations. Indeed, before reaching the catalytic site, Ulvan molecules have to diffuse inside the mesoporous matrix of the catalyst. Therefore, the production rate was detrimented down by diffusion phenomena, which was consistent with the observation of Kusema and co-workers, for the hydrolysis of arabinogalactans in the presence of SMOPEX-101 and Amberlyst 15 [47].

Indeed, the molar weight of arabinogalactan is around 20-100kDa, whereas in the case of extracted ulvan at 90 °C is around 280kDa (unpublished data). Consequently, the complete hydrolysis takes longer time, and the accessibility to the active sites of the resins is increasingly hindered [46].

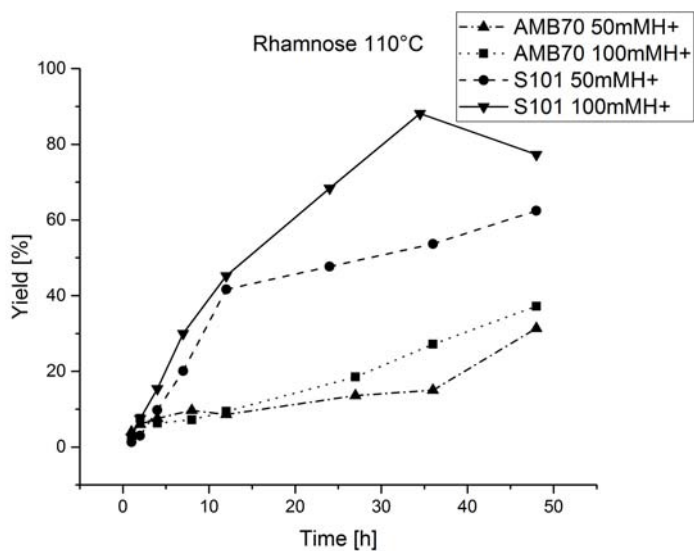


Figure 4.5: Rhamnose yield as a function of time in experiments 2,4,6,7

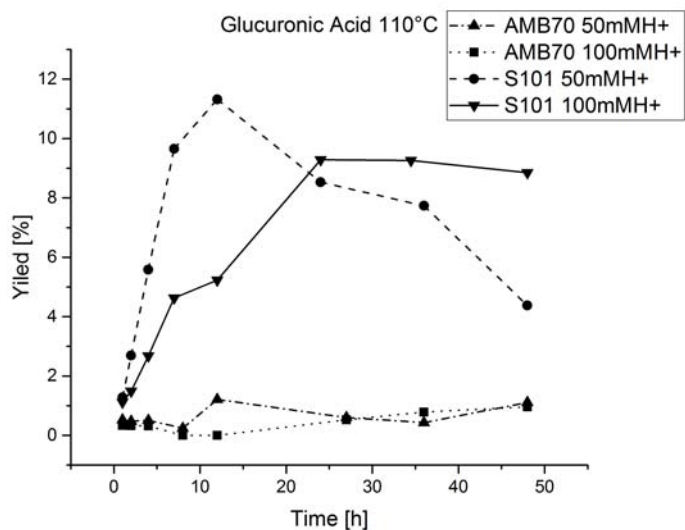


Figure 4.6: Glucuronic acid yield as a function of time in experiments 2,4,6,7

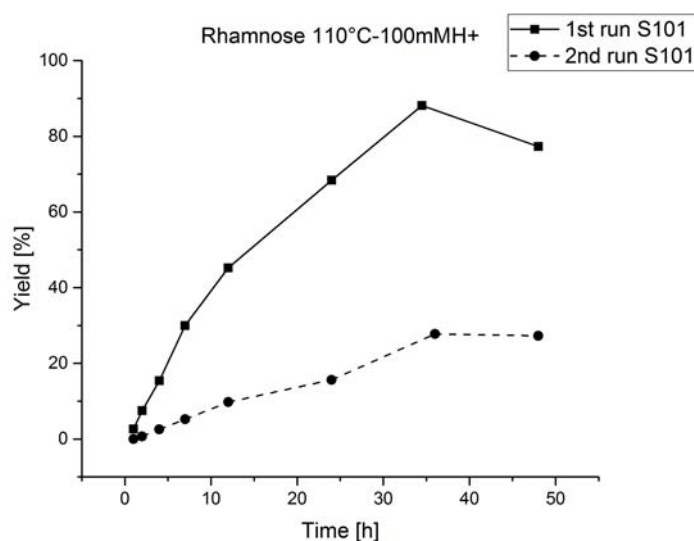


Figure 4.7: Rhamnose yield as a function of time in experiments 2,12

4.2.4 Catalyst reutilization

The catalyst used in experiment 2 (SMOPEX-101) was reutilized to perform experiment number 12. The aim of this experiment was to prove the concept of the resin reutilization for subsequent ulvan hydrolysis batches. In this regard, the temperature used to test the reutilization of the catalyst was the same of experiment 2, in order to compare the results. As far as the concentration of acid sites is concerned, as explained in Section 3.5.3 the mass balance of the catalyst before and after the recovery protocol was not fulfilled. Therefore, the equivalent concentration of H^+ was not available. Accordingly, the yields of Rha and GlcA are shown in Figure 4.7 and Figure 4.8, respectively.

Both rhamnose and glucuronic acid formation kinetics were slowed when the hydrolysis reaction was catalyzed by the recycled catalyst.

This results in a lower yield achieved throughout the reaction time. On an average base, the yield of rhamnose was 5 times lower, whereas the production of glucuronic acid was 2 times lower, than the one obtained with the fresh catalyst. The poorer performance of the recycled catalyst may be due to the leaching of the sulfonic groups that may have occurred during the reaction. This phenomenon would reduce the number of active sites available for the catalysis of the reaction. The leaching phenomenon was not directly quantified in terms of protons concentration in the liquid phase per sample. However, some heterogeneous samples were analyzed with HPCL and an unknown first eluting compound was detected. According to the experience of the personnel working in the laboratory, that first peak matches the sulfonic group peak. Another hypothesis to explain the deactivation of the catalysis, could be the coating

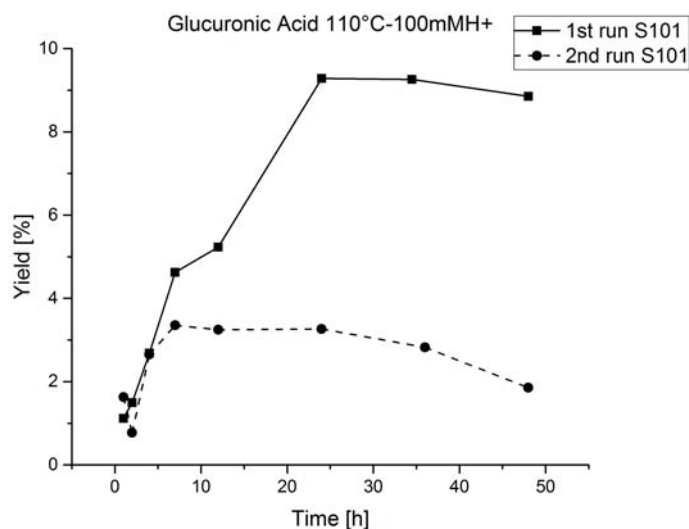


Figure 4.8: Glucuronic acid yield as a function of time in experiments 2,12

of the fibers by a layer of carbon coming from the decomposition products of the monosaccharides in the experiment 2. This carbon layer may deposit on the catalytic sites reducing the availability of sites for the hydrolysis of the ulvan molecule. This hypothesis could be corroborated by Figure 4.9, in which it is shown a comparison between the appearance of the fresh and the recovered catalyst after experiment 2 and the catalyst recovered after experiment 12. Accordingly, the catalyst after the first run looks definitely darker than the fresh one, moreover the catalyst recovered after the second one is even darker. This may indicate that carbon deposit may have been created. However, the temperature used to performed the experiments were relatively low, thus the carbon layer hypothesis it's very rough. In order to find evidence to support the carbon coating hypothesis, some TEM analysis were performed on the catalyst surface. The size of the catalyst were not compatible with the instrument. Therefore, a non well established technique was used in order to overcome the dimension issue. The fiber was dissected in a very thin slice in order to see if an outer layer surrounding the fiber core occurred. Unfortunately, the instrument didn't manage to properly distinguish between the resin carbon structure, the polymeric support on which the slice was laid and the carbon coating which the analysis was meant to find. The picture of the TEM analysis are reported in Appendix C.1

4.3 Homogeneous acid hydrolysis

The results of the homogeneous acid hydrolysis are reported in Figure 4.10 and Figure 4.11. Homogenous acid catalysis was performed in order to compare the per-



(a) .



(b) .



(c) .

Figure 4.9: Fresh S101 (a), after the first run S101 (b), after the second run S101 (c)

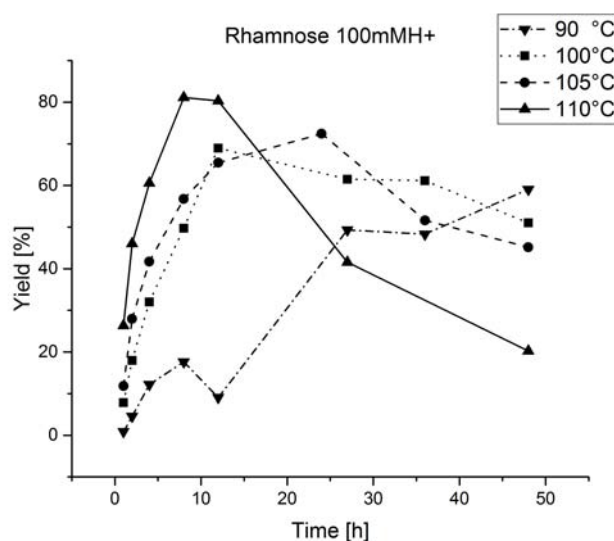


Figure 4.10: Glucuronic acid yield as a function of time in experiments 8,9,10,11

formance of the solid acid catalysis to the traditional hydrolysis catalyzed by strong inorganic acids, described in Section 2.2.2. According to the theory and literature, the hydrolysis performed via homogeneous catalysis should drastically reduce the mass transfer limitations, in particular the internal mass transfer. Indeed, the catalytic "sites" are solubilized in the reaction media and they are allowed to free floating within it. Therefore, the only limitation for the molecules to reach the active site is the external mass transfer from the liquid bulk to the actual position of the protons inside the bulk. Anyway, this limitation can be avoided by a proper mixing of the reaction mixture to enhance the collision between the protons and the glycosidic bonds. Furthermore, proper mixing was used in this study to exclude possible external mass (from the liquid bulk to the protons) transfer issues. Additionally, the reaction time was long enough to study the whole kinetic profile of the reaction.

For both rhamnose and glucuronic acid the experimental trends show a production curve followed by a further decomposition of the monosaccharides (Figure 4.10 and Figure 4.11). The production rates increase if the temperature increases as well as the decomposition rates did. As expected, performing the experiment at the highest temperature (110 °C) allowed to obtain a high yield for both the studied components, in a shorter reaction time if compared with the heterogeneous catalysis. However, the production at the highest temperature is followed by a severe decomposition of the products. According to the experimental trends, it can be noticed that the decomposition of glucuronic acid is more severe than rhamnose decomposition, therefore glucuronic acid is more reactive than rhamnose.

If both the results in Figure 4.10 and Figure 4.11, are normalized with the respective

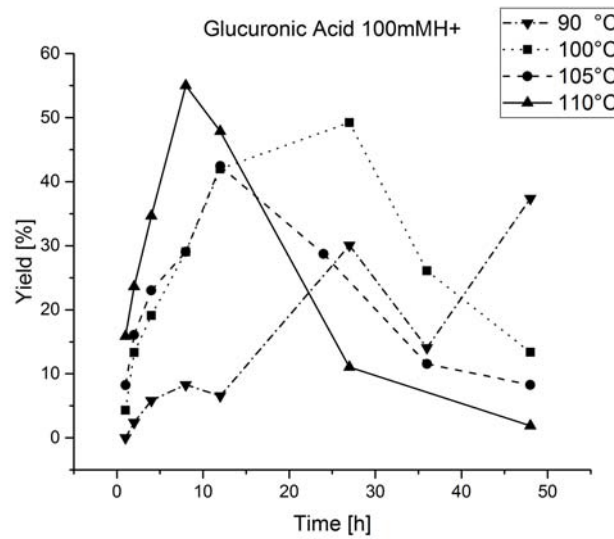


Figure 4.11: Glucuronic acid yield as a function of time in experiments 8,9,10,11

	GlcA (h^{-1})	Rha (h^{-1})	GlcA/Rha
hcl100	-0.0300	-0.00723	4.80
hcl105	-0.0224	-0.0157	1.43
hcl110	-0.0241	-0.0188	1.29

Table 4.2: Estimation of the degradation rate (equation (4.3)) in the homogeneous catalysis for both Rha and GlcA

highest value of the yield, is possible to estimate a rough value of the decomposition rate as follows.

$$\frac{\Delta Y}{\Delta t} = \frac{Y_{48h} - Y_{max}}{(t_{Y_{max}} - 48h) Y_{max}} \quad (4.3)$$

In Table 4.2 the results of the decomposition rate estimation are summarized, showing that glucuronic acid is clearly much more reactive than rhamnose. As already mentioned, it is highly likely that this higher reactivity, of glucuronic acid, may be due to its carboxylic group. The instability of uronic acids has been already reported by other authors [99][97].

In Figure 4.12 and Figure 4.13, the experimental trends of the heterogeneous acid hydrolysis, for both rhamnose and glucuronic acid, are also reported in order to compare the performance of the two hydrolysis routes. As far as rhamnose is concerned (Figure 4.12), the heterogeneous acid hydrolysis allowed to slightly increase the yield. However, the reaction time to obtain the maximum yield was 4 times longer than the homogeneous one. The increment of the reaction time can be explained with the increasing difficulty for the glycosidic bonds to collide with the active site in order to be protonated and further hydrolysed. In the heterogeneous catalysis, indeed, the active

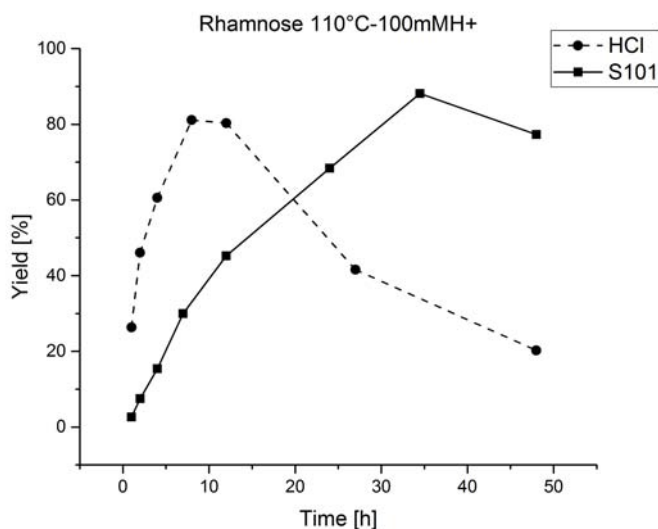


Figure 4.12: Rhamnose yield as a function of time in experiments 2,11

sites are not free floating in the reaction media but they are stuck to the resin. Therefore, a proper orientation of the chain is needed in order to be attacked by the free protons of the sulfonic groups.

The kinetic of glucuronic acid formation and consumption is compared between homogeneous and heterogeneous catalysis in Figure 4.13. The performance of the heterogeneous hydrolysis is definitely poorer if compared to the homogeneous hydrolysis. The yield obtained with the acid resin is almost 6 times lower than the one obtained with HCl, as well as it was for rhamnose, the production rate was slower for the solid acid catalysis. According to the ulvan composition in Table 4.1 the rhamnose to glucuronic acid ratio is almost 1 : 1, which means that for every molecule of rhamnose cleaved from the backbone of ulvan also a molecule of glucuronic acid is cleaved as it was mentioned earlier. The ratio between rhamnose and glucuronic maximum yield, produced via homogenous catalysis (110°C-100mMH⁺eq), was 1.45. In turn, the same ratio with heterogeneous results was almost 10. Therefore, rhamnose was produced ten times more with heterogeneous catalysis than glucuronic acid due to the further decomposition of the latter. It can be concluded that there is an unknown interaction between glucuronic acid and the sulfonic groups of the resin. glucuronic acid was produced but it immediately further reacts with the sulfonic groups of the resin, therefore its yield was much lower than in the homogeneous hydrolysis.

As well as described for the heterogeneous samples in the previous sections, the scattered behavior of the kinetic experimental data was also observed for the homogeneous samples. However, in this case the samples were not derivatized. Therefore the scattering should be due to other reasons. It has been hypothesized that the manual

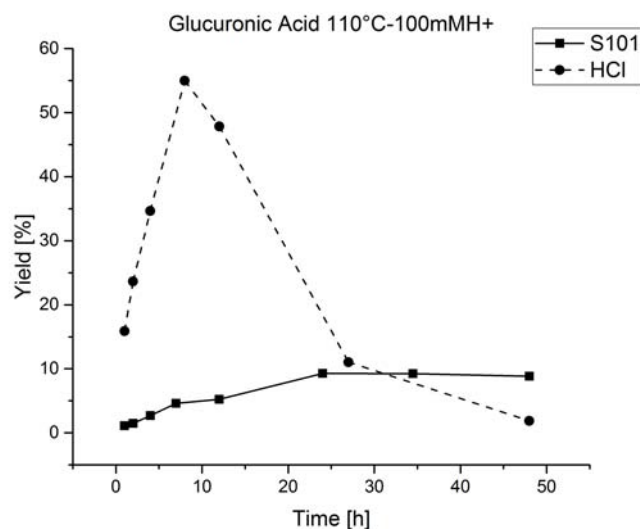


Figure 4.13: Glucuronic acid yield as a function of time in experiments 2,11

Experiment #	Catalyst	T [°C]	Acidity [mMH ⁺ eq]	Conc GlcA [mg/mL]	Batch V [mL]	Time [h]
13	SMOPEX-101	110	100	1.5	200	48
14	HCL	110	100	1.5	200	12

Table 4.3: Experimental conditions to study the decomposition of glucuronic acid

integration that had to be performed on the HPLC chromatograms, which was caused by the peaks overlapping that will be further described in the next section, might be a possible cause for the scattering phenomenon.

4.4 Glucuronic acid decomposition

In order to figure out whether the rate of glucuronic acid decomposition is affected by the presence of the sulfonic groups in the resin, as speculated in Section 4.3, thus two extra experiments were carried out. Two hydrothermal treatments catalyzed by the SMOPEX-101 and the HCl were performed. The reactor utilized was the autoclave presented in Section 3.2. The reaction conditions are reported in Table4.3

The samples were withdrawn according to the sampling interval in Table 3.1, and they were further analyzed with HPLC.

The results of the analysis of both experiments are reported in Figure 4.14. It can be noticed that when glucuronic acid was treated with SMOPEX-101 its decomposition was definitely faster than the hydrothermal treatment with HCl, supporting the observation for GlcA in the ulvan hydrolysis experiments. The conversion (X) of glucuronic

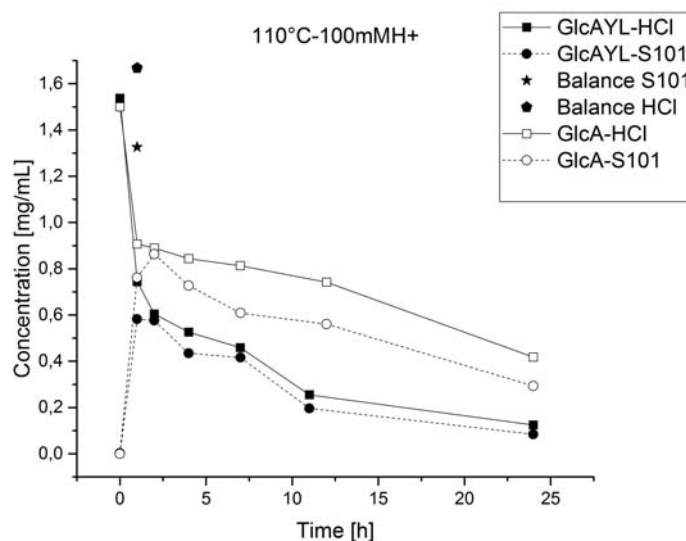


Figure 4.14: Glucuronic acid and Glucuronic acid- γ -lactone concentrations as function of time in experiment 13,14

acid is reported in Figure 4.15. In the case of SMOPEX-101, the conversion was 1.3 higher than HCl in the first hour of reaction. Subsequently, after 11h of reaction the conversion of GlcA in S101 was 1.65 times higher than in the case of HCl. Consequently, it can be claimed that glucuronic acid decomposition was heavily affected by the resin through an unknown mechanism.

The interaction of GlcA with the resin and its decomposition would explain why the yield of glucuronic acids produced from heterogeneous ulvan hydrolysis was much lower than the yield of rhamnose, in spite of their ratio in ulvan backbone is almost 1 : 1. According to Section 2.4, glucuronic acid- γ -lactone, one of the dehydration products of GlcA, was also detected. Moreover, in Figure 4.14, the mass balances ($C_{GlcA} + C_{GlcA\gamma L}$) of both treatment after one hour are almost fulfilled. The closure of the mass balance upholds again the equilibrium that exists between the two species. This observation was also reported by Wang and co-workers [99].

In the chromatograms from the samples analyzed in HPLC, obtained after homogeneous hydrolysis, several unknown peaks were detected. These peaks have been attributed to the degradation products of the different sugars that occur in ulvan backbone and in *U. rigida* cell wall, which are rhamnose, xylose, glucose and glucuronic acid. Several substances were analyzed in HPLC to confirm the nature of those unknown compounds. Therefore, it was possible to verify whether the unknown peaks have the same retention time of the calibration compounds. For each substance was also calculated a calibration curve from the analysis of different solutions at known concentration. According to Section 1.3.1, the degradation of pentoses and hexose lead

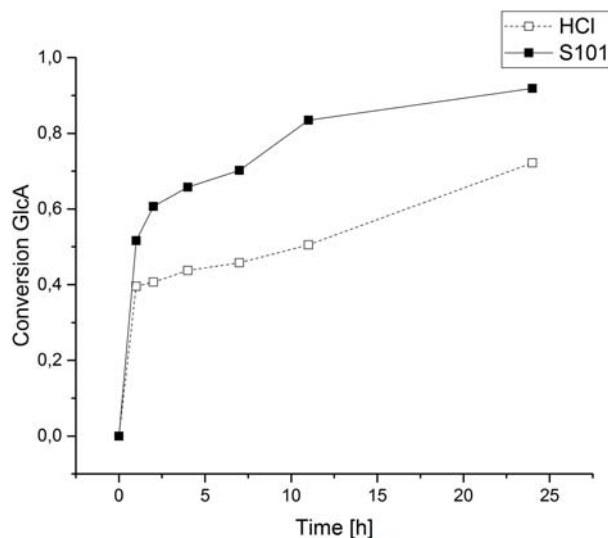


Figure 4.15: Glucuronic acid conversion as a function of time in experiments 13,14

repectively to furfural and HMF. Moreover, furfural and HMF are further decomposed to formic and levulinic acid, thus these four compounds were used as calibration substances. Furthermore, several organic acids have been tested, based on the compounds found for different authors regarding degradation of uronic acids (in agreement with Section 2.4), in order to identify some degradation products of glucuronic acid. Therefore, succinic, glycolic and lactic acid analysis were performed with HPLC. Eventually, according to Section 2.4 malic acid an 2-hydroxybutyric acid have been detected in the hydrothermal treatment of glucuronic acid. However, those last mentioned compounds were not available, thus it was decided to test similar molecules such as maleic acid and butyric acid.

The chromatograms obtained from the HPLC analysis of the homogeneous hydrolyzed samples were characterized by overlapping peaks. Therefore, the manual integration has been an arduous task. In order to overcome this problem and to obtain reliable data in the overlapping zone, the calibration curve has been produced using mixtures at known concentration of the testing substances including the monosaccharides.

Figure 4.16 depicts the results for the experiment 11 (Table 3.3). It should be noticed that glucose and xylose have not been plotted because the experimental yield obtained in the case of homogeneous hydrolysis was higher than 100%. Most likely the overestimation of the concentration for xylose and glucose was due by the overlapping of degradation compounds. Therefore, some unknown substances (typically organic acids), with the same retention time of Glc and Xyl, mislead the integration of the area under the corresponding peaks, leading to a higher value of the area. The compounds

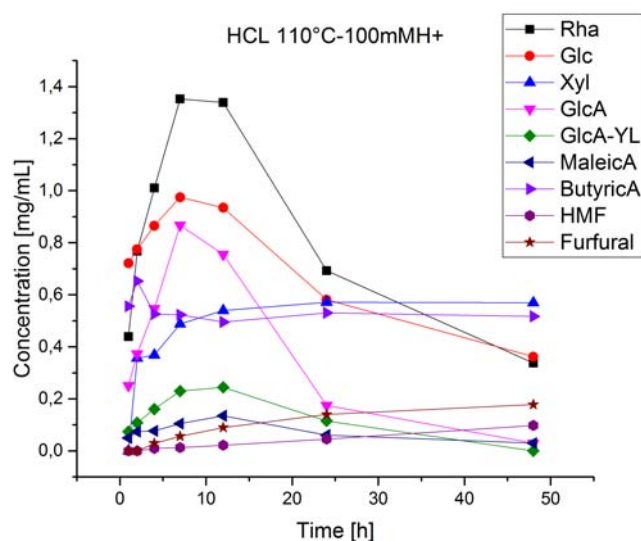


Figure 4.16: Glucuronic acid and detected calibration compounds concentration as a function of time in experiment 11

that have been detected from the analysis are GlcA γ L, HMF, furfural, butyric acid and maleic acid. Furfural should derive from the decomposition of xylose (pentose), whereas HMF was produced from the degradation of rhamnose, glucuronic acid and glucose (hexose). Butyric and maleic acids have also been detected. In spite of the fact that they are not claimed to be degradation products of glucuronic acids it seems reasonable to assume that they derived from GlcA, since their structure is rather similar to butyric and malic acids. Moreover, the retention times of such compounds might be rather similar so it is recommended to use GC-MS instrument in order to determine which compound was present in the hydrolysate. According to the equilibrium in Figure 2.6, glucuronolactone has been detected. It could be noticed that none of the organic acid, which according to Section 2.4 would have been degradation products of glucuronic acid, were detected. This result may be due to the overlapping issue, which did not allow to clearly distinguish those peaks. Since the main focus of this study was the production of L-Rhamnose due to its commercial value, the degradation of GlcA was not deeply studied further. However, to give a complete understanding of the phenomena occurring with GlcA more analysis with the help of different techniques should be used.

4.5 Variability analysis

A variability analysis has been performed on the analyzed samples in order to figure out how precise were the quantification of monomers. The analysis was carried

	C_{avg}		σ		σ^*	
HCl _{T4}	GlcA	Rha	GlcA	Rha	GlcA	Rha
90	0.068	0.165	0.0128	0.0386	0.190	0.234
100	0.303	0.551	0.0161	0.0237	0.0530	0.0430
105	0.454	0.809	0.0286	0.0497	0.0629	0.0614
110	0.512	1.055	0.0237	0.0457	0.0462	0.0433

Table 4.4: Variability results in ulvan hydrolysis with HCl at different temperatures. Mean concentration, standard deviation and coefficient of variation are given

out only on one sample per experiment due to the limited amount of time available. As far as the homogeneous samples are concerned, the samples withdrawn at four hours of reaction were analysed again in triplicate. Consequently, the 3/4 analysis performed to each sample allowed to calculate the mean (C_{avg}), the standard deviation (σ) and the coefficient of variation (σ^*) for both rhamnose and glucuronic acid, according to the following equations.

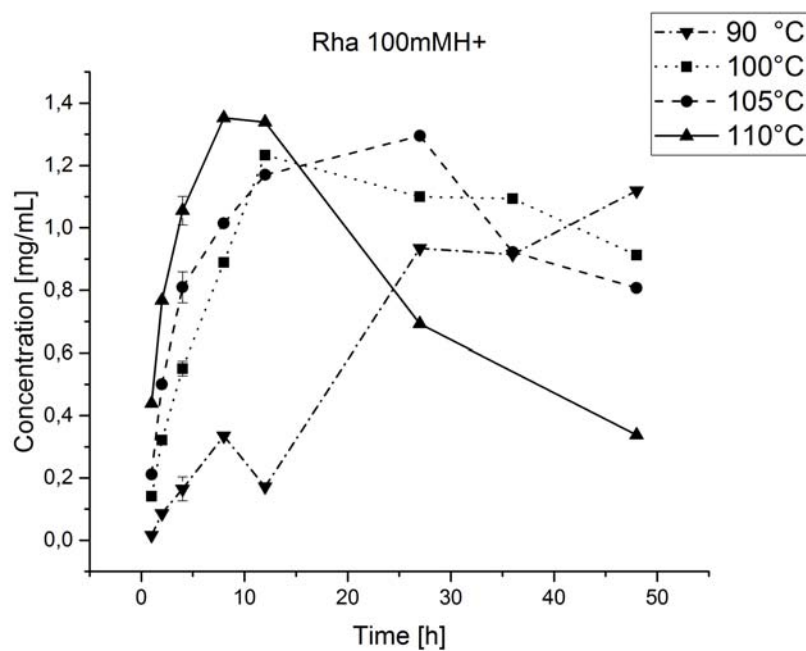
$$C_{avg} = \frac{\sum_{i=1}^n C_i}{n} \quad \sigma = \sqrt{\frac{\sum_{i=1}^n (C_i - C_{avg})^2}{n}} \quad \sigma^* = \frac{C_{avg}}{\sigma} \quad (4.4)$$

where n is the number of analysis repeated to each sample, which are respectively 4 and 3 for the homogeneous and the heterogeneous ones.

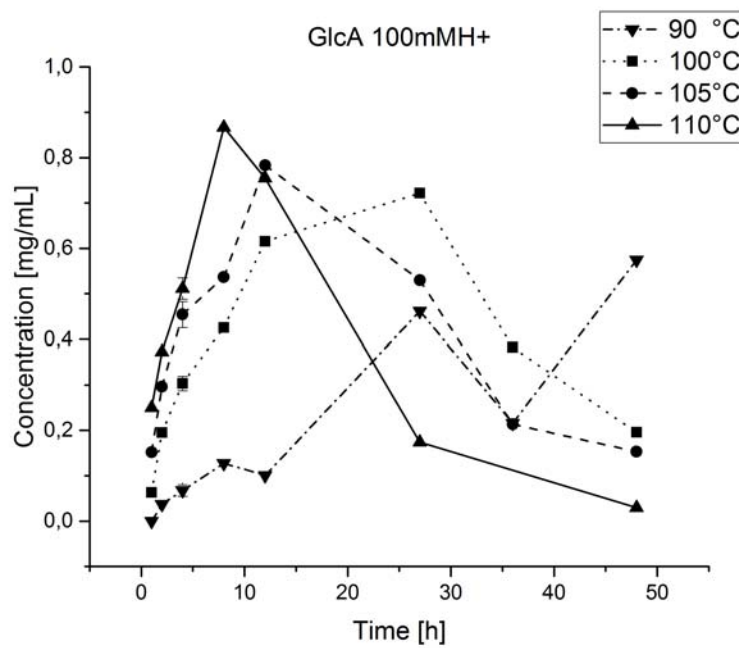
The results for homogeneous acid hydrolysis samples are reported in Table 4.4. It can be noticed that the coefficient of variation is higher for the sample at 90°C. Indeed, the concentrations of both GlcA and Rha were much smaller compared to the other samples. Therefore, the concentration values were more scattered around the mean value than those in the higher temperature samples.

In Figure 4.17, the average concentrations at 4 hours are reported with the relative error in terms of standard deviation ($\pm\sigma$). It can be concluded that, in spite of the HPLC analysis suffers of peaks overlapping, the data obtained from the quantitative analysis are rather reliable due to the relatively low standard deviation values. It must be underlined that this is just an indication of the global error of the trends. As a matter of fact, the variability analysis should be performed on all the experimental data.

The heterogeneous samples were analyzed, according to the monomer content protocol presented in Section 2.5.1 and in Appendix A.1, twice; in order to calculate the average concentration, the standard deviation and the coefficient of variation. Unfortunately, due to non-availability of the samples at 12h for the 110°C-100mMH⁺eq series this analysis was replaced with the sample at 48h. Every analysis was performed



(a) .



(b) .

Figure 4.17: Homogenous acid hydrolysis results of ulvan at different temperatures with the relative variability, showing formation of Rha(a) and GlcA(b)

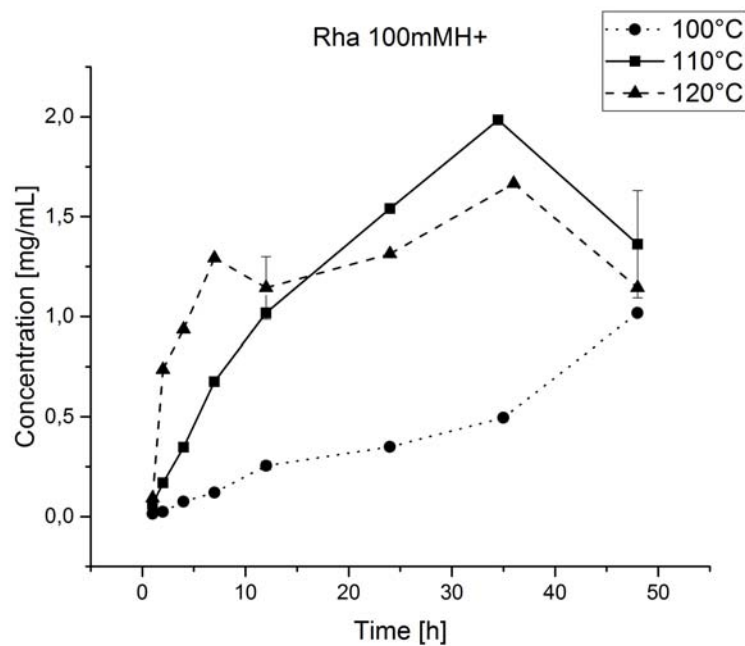
	C_{avg}		σ		σ^*	
	GlcA	Rha	GlcA	Rha	GlcA	Rha
S101						
100mMH ⁺ eq -100°C-T12	0.024	0.255	0.00762	0.0214	0.322	0.0839
100mMH ⁺ eq -110°C-T48	0.108	1.362	0.0361	0.268	0.335	0.197
100mMH ⁺ eq -120°C-T12	0.092	1.143	0.0138	0.157	0.150	0.137
75mMH ⁺ eq -110°C-T12	0.082	0.714	0.00317	0.150	0.0385	0.210
50mMH ⁺ eq -110°C-T12	0.125	0.790	0.00896	0.0942	0.0716	0.119

Table 4.5: Variability results in ulvan hydrolysis with SMOPEX-101 using different acid concentration. Mean concentration, standard deviation and coefficient of variation are given

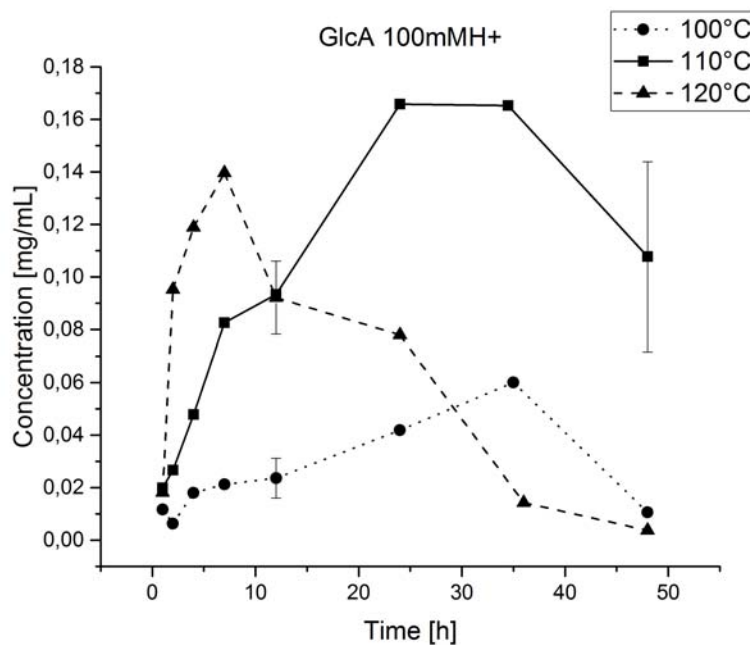
on samples which had been silylated in separate times. Therefore, the results of the variability will not give information only on the precision of the equipment used to analyze the samples, but the results will be representative also of the variability that the silylation treatment implies. According to Table 4.5, the coefficient of variation is higher for the sample at 100°C-100mMH⁺eq. This condition is once again due to the low concentration measured among all the different selected points.

Figure 4.18 depicture the average values with the relative standard deviations for the concentration, of the heterogeneous samples. Conversely to what observed from the homogeneous data, the heterogeneous variability results are much more affected by the analytical method used to estimate the concentration. Indeed, the values of the standard deviation were higher for the heterogeneous samples. According to the experience of the staff working in the laboratory the equipment precision can be approximated with the $\pm 5\%$ of the actual measured value for the concentration. This estimation is definitely much lower than the values obtained for the standard deviations. Therefore, it can be claimed that the silylation procedure might affect the measured concentration of the monomers. However, the peak definition of this analysis is much more defined compared to HPLC where the different degradation compounds, eluting from the column, might also affect the quantification of sugars. To conclude, this variability results cannot be considered neither in a first approximation as a general indication of the global error of the trend. A further analysis on every single data would be needed.

In conclusion, according to the results presented in the above sections, the hydrolysis of Ulvan into its building blocks was affected by both temperature and acidity. From the experiment that had been carried out, it turned out that the yield of rhamnose was definitely much higher than the glucuronic acid yield in the case of heterogeneous hydrolysis. This unexpected results, according to the ulvan backbone structure, has



(a) .



(b) .

Figure 4.18: Heterogeneous acid hydrolysis results of ulvan at different temperatures with the relative variability, showing formation of Rha(a) and GlcA(b)

required to deepen the chemical reasons that hardly affected the yield of glucuronic acid. Therefore, some analysis and experiments were performed. The results suggested that glucuronic acid may react with an unknown mechanism with the sulphonic groups of the resins.

Chapter 5

Kinetic Modelling

One of the task of this project was to attempt to model the experimental kinetic data obtained from the hydrolysis of Ulvan, for both the homogenous and the heterogeneous datasets. The modelling of the experimental data will result in a mechanism, and a value for both the activation energy and the pre-exponential factor of all the supposed reactions that occur in the ulvan hydrolysis. The chapter will describe the reaction mechanisms assumed to model the phenomena occurring in the experiments performed in this project, aiming to obtain good correlation to the experimental data

5.1 Homogeneous reaction mechanisms

The kinetic modelling of hydrolysis of heteropolysaccharides, such as hemicellulose has been studied and reviewed in different works [84][46][45][56]. The common approach used to write down the rate equations for the hydrolysis of hemicellulose is mainly based on the intrinsic structure of the raw materials that were used in these studies and on the shapes of the kinetic curves. In the work of Kusema et al. [46], the branched structure of arabinogalactan was subjected to hydrolysis to study its depolymerization kinetics. Consequently, they suggested to model the hemicellulose as composed by two different structures. This assumption was in agreement with the kinetic trends which showed that the side substituent in the chain (Arabinose) was hydrolyzed faster than the main backbone (Galactose). Therefore, the rates of cleavage, thus the kinetic constants, of the two monomers were considered to be different, even though they were part of the same hemicellulose macromolecule.

As described in Section 2.1.1, the mechanism of acid hydrolysis of the glycosidic bond in polysaccharides is well known. The breakage is based on the protonation of the the glycosidic bond, which is followed by the water hydrolysis, where further degradation of the monomers may also occur under severe reaction condition, Figure 2.1.

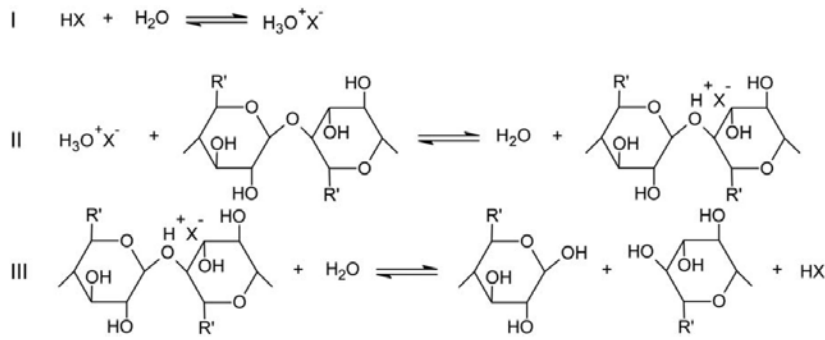


Figure 5.1: Homogeneous hydrolysis mechanism of hemicellulose in the work of Wörnå et al. [84]

The mechanism depicted in Figure 5.1. was used in the work of Wörnå and Kusema et. al [84][46] to set the rate equation of hemicellulose hydrolysis. The steps I and II were considered as rapid equilibria whereas step III which involves the cleavage of the glycosidic bond was considered as the rate determining step. The quasi equilibrium hypothesis applied to the steps I and II allows to obtain the rate of the hydrolysis reaction according to the following equation.

$$r = k_i C_{i0} C_{H^+} C_{H_2O} \quad (5.1)$$

where C_{i0} represents the concentration of the unhydrolyzed monomer i , C_{H^+} is the concentration of protons and C_{H_2O} is the water concentration, both C_{H^+} and C_{H_2O} are assumed to be constant. Therefore, equation (5.1) was used to model the production of every monomer i that was present in the studied hemicellulose chain, according to the following mass balance for batch reactor:

$$\frac{dC_i}{dt} = k_i C_{i0} C_{H^+} C_{H_2O} \quad (5.2)$$

where the concentration of the unhydrolyzed monomer C_{i0} was expressed according to the monomer mass balance, assuming that no further degradation occurs.

$$C_{0i} = C_{i0} + C_i \quad (5.3)$$

Where C_{0i} represents the initial concentration of monomer i in the hemicellulose chain.

5.2 Homogeneous mechanisms of ulvan hydrolysis

According to the relatively linear structure of Ulvan and to the Table 4.1 in which it is claimed that the Rha to GlcA ratio is almost 1 : 1, due to the occurrence of the

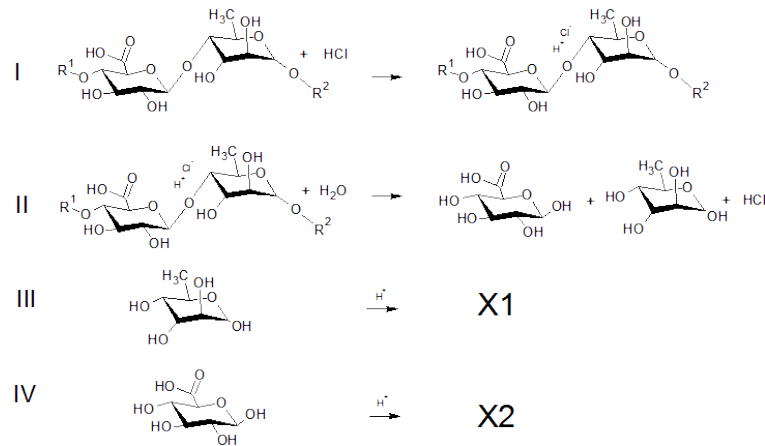


Figure 5.2: Homogeneous hydrolysis mechanism #1 of Ulvan considered

ulvanobiose dimer. Consequently, the assumption of different production rate for the single monomers seems to be less consistent in the case of Ulvan homogeneous hydrolysis. Moreover, the kinetic curves reported in Section 4 indicate that a further degradation of Rha and GlcA occurred. Therefore, the mechanism depicted in Figure 5.1 has to be modified in order to take into account the linearity of the ulvan chain and the decomposition of the monomers. Several mechanisms have been tested in order to find which ones resulted in the best fitting of the kinetic data. Accordingly, the confidence interval of the best fitted kinetic parameter was calculated in order to quantify the variability of the parameters optimized by the software.

Mechanism 1

The first hydrolysis mechanism, proposed to model the kinetic data of ulvan homogeneous hydrolysis, is depicted in Figure 5.2. The suggested mechanism recalls the theory that is behind the glycosidic bond cleavage described in Section 2.1.1. Accordingly, the glycosidic bond is at first protonated to form the so called "activated ulvan" (U^*). The U^* is then hydrolyzed into monomeric Rha and GlcA which are afterwards decomposed into their decomposition products, which are indicated in Figure 5.2 with X1 and X2 for Rha and GlcA, respectively.

The mechanism represented in Figure 5.2 allows to set the rate equations for the 4 suggested steps involved in the hydrolysis of ulvan as follows.

$$\begin{aligned}
 R_I &= k_I C_U C_{H^+} \\
 R_{II} &= k_{II} C_{U^*} C_{H_2O} \\
 R_{III} &= k_{III} C_{Rha} C_{H^+} \\
 R_{IV} &= k_{IV} C_{GlcA} C_{H^+}
 \end{aligned} \tag{5.4}$$

where, in equations (5.4), k_i represents the kinetic constant of the i_{th} step, in Figure 5.2, and C_U is the ulvan concentration. The mechanism sketched in Figure 5.2 is based also on the experimental observations described in Section 4.1. The molecule of Ulvan (U) was considered to be composed only of rhamnase and glucuronic acid in an alternating linear structure. Above all, the ratio $Rha : GlcA$ is assumed to be 1 : 1, in agreement with the experimental results described in Section 4.1. According to the step II in Figure 5.2, both Rha and GlcA are produced at the same rate. Furthermore, the acid concentration (C_{H^+}) is considered to be constant assuming that per every molecule of the activated ulvan (C_{U^*}) that is hydrolyzed one molecule of acid is formed again. Water concentration (C_{H_2O}) is also considered to be constant throughout the reaction, since it is in excess as the reaction media.

The kinetic rates in equation (5.4) can afterwards used to write the following batch (isothermal, constant volume) mass balances to represent the evolution of the reactants and products throughout the reaction time.

$$\begin{aligned}
 \frac{dU}{dt} &= -R_I \\
 \frac{dU^*}{dt} &= R_I - R_{II} \\
 \frac{dC_{Rha}}{dt} &= R_{II} - R_{III} \\
 \frac{dC_{GlcA}}{dt} &= R_{II} - R_{IV}
 \end{aligned} \tag{5.5}$$

Mechanism 2

Due to the limited amount of experimental data available, in particular the lack of knowledge of the experimental evolution of ulvan and its protonated form, a simpler mechanism was also tested. The second mechanism recalls the work of Wörnå et al. [84], Figure 5.1. Similarly to mechanism 1 (Figure 5.2), ulvan has been considered to be a linear molecule formed by alternated unit of GlcA and Rha.

According to the second model, sketched in Figure 5.3, the following rate equations can be derived.

$$\begin{aligned}
 R_I &= k_I C_U C_{H^+} C_{H_2O} \\
 R_{II} &= k_{II} C_{Rha} C_{H^+} \\
 R_{III} &= k_{III} C_{GlcA} C_{H^+}
 \end{aligned} \tag{5.6}$$

Similar mass balances to mechanism 1 can be obtained using the new rate equations

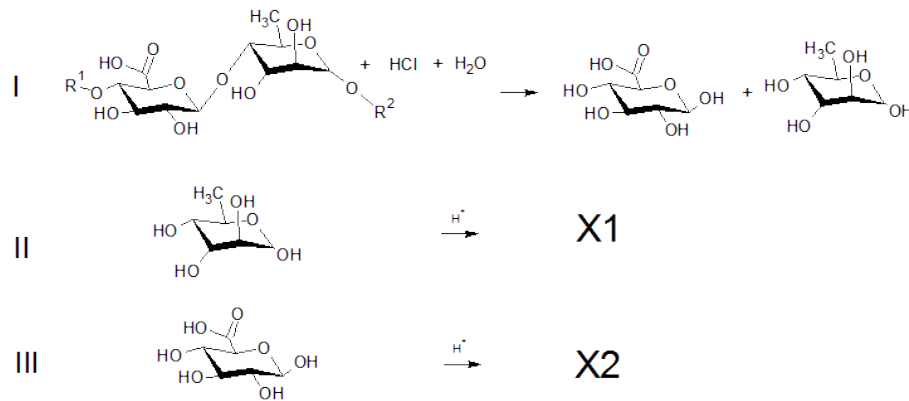


Figure 5.3: Homogeneous hydrolysis mechanism #2 of Ulvan considered

and the pssa hypothesis on U^* .

$$\begin{aligned}
 \frac{dU}{dt} &= -R_I \\
 \frac{dC_{Rha}}{dt} &= R_I - R_{II} \\
 \frac{dC_{GlcA}}{dt} &= R_I - R_{III}
 \end{aligned} \tag{5.7}$$

The differential equations and the kinetic parameter were estimated as mentioned for mechanism 1.

Mechanism 3

Eventually the third mechanism is once again based on the work of Wörnå et al. [84]. Ulvan was considered as formed by two separate homopolymers entirely composed one of rhamnose and the other one of glucuronic acid. This approach decoupled the formation of the two monomers (Rha and GlcA) therefore it seems to be the easiest one but also less representative for hydrolysis reaction of ulvan.

Therefore, the rate equations can be expressed in accordance to the third mechanism depicted in Figure 5.4, as follow

$$\begin{aligned}
 R_I &= k_I C_{R0} C_{H^+} C_{H_2O} \\
 R_{II} &= k_{II} C_{G0} C_{H^+} C_{H_2O} \\
 R_{III} &= k_{III} C_{Rha} C_{H^+} \\
 R_{IV} &= k_{IV} C_{GlcA} C_{H^+}
 \end{aligned} \tag{5.8}$$

where, in equation (5.8) C_{R0} and C_{G0} represent the concentration of unhydrolyzed rhamnose and glucuronic acid in the ulvan chain, respectively. The unhydrolyzed

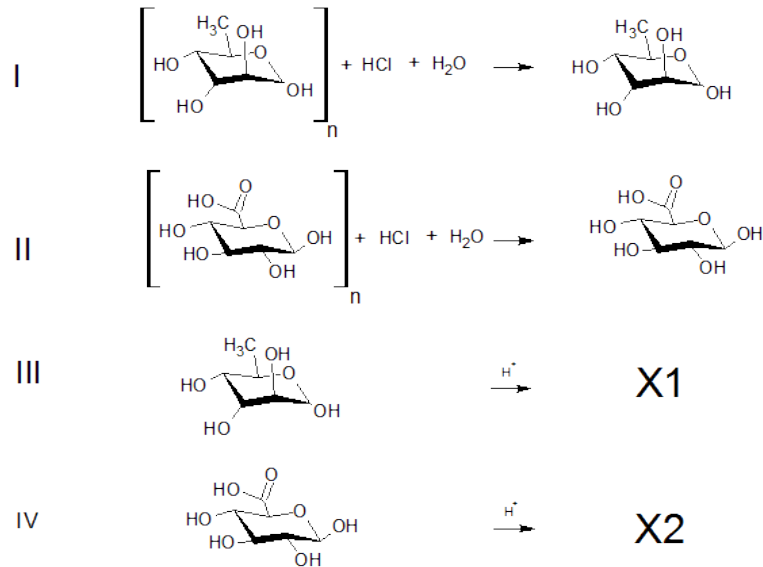


Figure 5.4: Homogeneous hydrolysis mechanism #3 of Ulvan considered

concentration can be expressed at every time instant with the following mass balances

$$\begin{aligned} C_{R0} &= C_{0R} - C_{Rha} - C_{X1} \\ C_{G0} &= C_{0G} - C_{GlcA} - C_{X2} \end{aligned} \quad (5.9)$$

where C_{0i} is the concentration at time 0 of the unhydrolyzed monomer i according to Table 4.1. The differential mass balances for an isothermal, constant volume batch reactor obtained, are expressed by the following equations.

$$\begin{aligned} \frac{dC_{Rha}}{dt} &= R_I - R_{III} \\ \frac{dC_{GlcA}}{dt} &= R_{II} - R_{IV} \\ \frac{dC_{X1}}{dt} &= R_{III} \\ \frac{dC_{X2}}{dt} &= R_{IV} \end{aligned} \quad (5.10)$$

The solution of the differential equations and the estimation of the kinetic parameter were performed both for mechanism one and two.

5.2.1 Parameter estimation results

Hereby, it will be reported the results for the parameter estimation of the three homogeneous models tested. The kinetic parameters (k_i) of the reactions were estimated for each experimental temperature by nonlinear regression analysis. The strategy for

the estimation was the minimization of the objective functions (*FOB*) given by

$$FOB = \sqrt{\sum_t (Y_t - Y_{exp,t})^2} \quad (5.11)$$

where Y_t is a matrix which contains the calculated values for Rha and GlcA yield at the t time step, respectively. Accordingly, $Y_{exp,t}$ contains the experimental values for Rha and GlcA yield at each t time step. The objective function was minimized in MATLAB using the *Levenberg-Marquardt* algorithm (*lsqnonlin* function). This function allows to solve nonlinear least-squares (nonlinear data-fitting) problems. The differential equations (5.5) were also solved in MATLAB using the *ode15s* solver routine. The four experimental kinetic data-set, obtained at different temperatures, were used all together to optimize the kinetic parameters. The results of the optimization were checked by the degree of explanation (R^2) as well as by the intervals of confidence (*IC*) of the parameters. The degree of explanation is defined by:

$$R^2 = \frac{\sum (Y_{iexp,t} - Y_{i,t})^2}{\sum (Y_{iexp,t} - Y_{iavg,t})^2} \quad (5.12)$$

where $Y_{iavg,t}$ is the average value for the experimental yield values of the dataset. The *lsqnonlin* function returned as output the new optimized parameters (*par*), the jacobian matrix (*J*) and the residuals (*res*), which eventually allowed to calculate the IC_s .

$$\begin{aligned} var_{par} &= \frac{\sqrt{\sum (res)^2} (J^T J)^{-1}}{N} \\ Std_{par} &= \sqrt{diag(var_{par})} \\ IC &= Std_{par} t_{95\%} \end{aligned} \quad (5.13)$$

where, in equation (5.13), var_{par} is the variance of the parameters, Std_{par} is their standard deviation $diag(var_{par})$ stands for the diagonal values of the *varp* matrix, N is the number of experimental data and $t_{95\%}$ is the 95% T of student [95]. The values of the parameters are therefore reported with their *IC* according to: $par \pm IC$.

The rate constant k in the rate equations was expressed according to the Arrhenius equation:

$$k = A e^{-\frac{Ea}{RT}} \quad (5.14)$$

where A indicates the frequency factor and its unit of measurement is strictly dependent on the reaction order of the rate equation, whereas Ea stands for the activation energy and its unit of measurement is [J/mol]. Consequently, R stands for the universal gas constant and T is the reaction temperature.

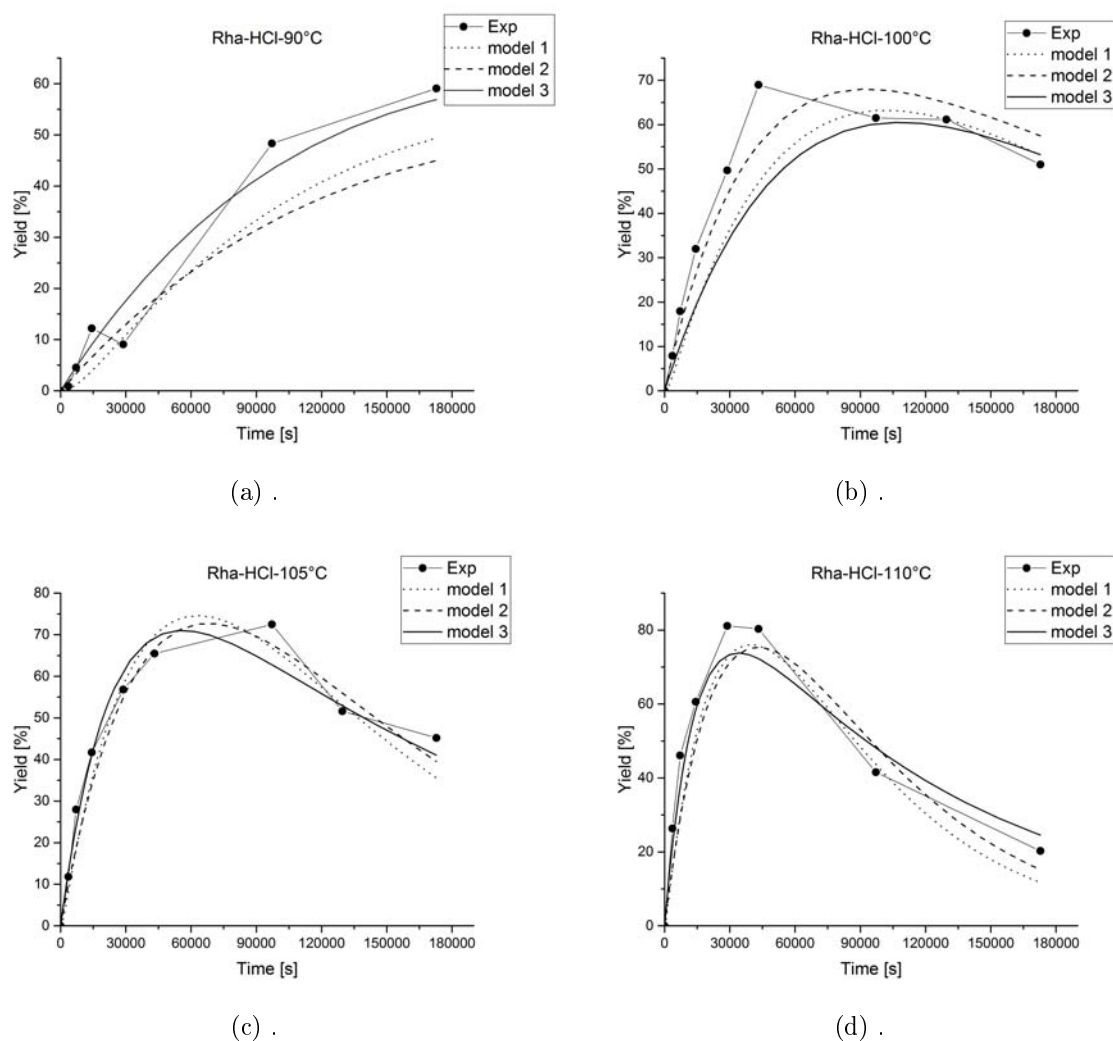


Figure 5.5: Modelling results for the homogeneous kinetic experimental data of Rha

The frequency factors and the activation energies were first estimated from the linear form of the Arrhenius equation. Therefore, the logarithm of the kinetic constants estimated were plotted versus $1/T$. The slope of the straight line is $-Ea/R$, whereas the intercept is $\ln(A)$. This simple estimation was used as the first guess to optimize Ea and A in the code, which used the kinetic dataset at different temperature all together to optimize the kinetic parameters. The results of the three homogeneous models are reported in Figure 5.5 and Figure 5.6 for rhamnose and glucuronic acid, respectively.

The results of the degree of explanation calculations are reported in Table 5.1. The values reported, for R^2 , suggest that all the three tested models give a rather good representation of the kinetic experimental data. Indeed, the values for R^2 are typically above 85% except for a few exceptions. It can be noticed from the results, in Table 5.1, that all the three models have difficulty to represent the glucuronic acid kinetic dataset at 90°C. The R^2 values for the aforesaid experimental data are indeed the

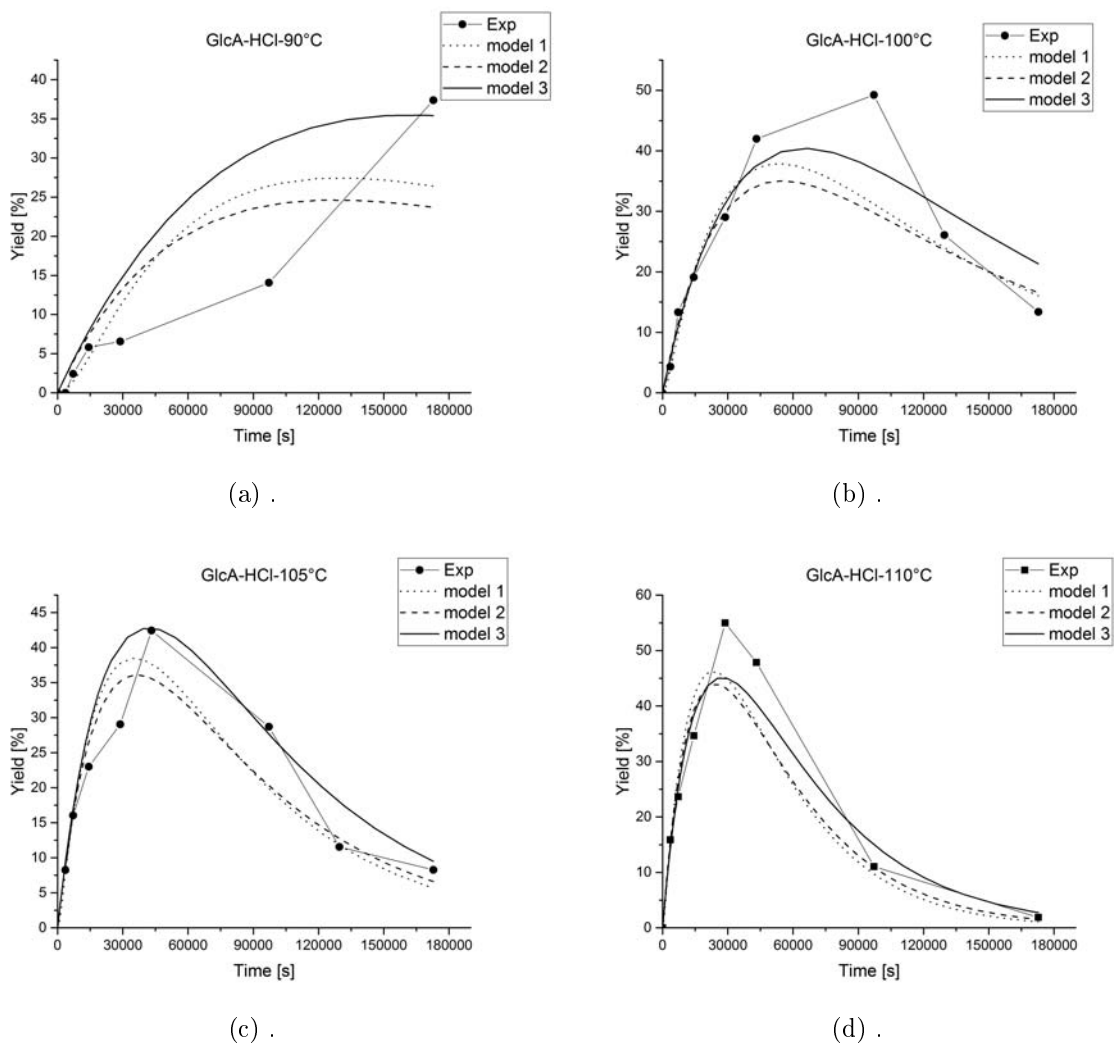


Figure 5.6: Modelling results for the homogeneous kinetic experimental data of GlcA

	model1		model2		model3	
T	R^2_{Rha}	R^2_{GlcA}	R^2_{Rha}	R^2_{GlcA}	R^2_{Rha}	R^2_{GlcA}
90	0.902	0.717	0.865	0.681	0.97	0.626
100	0.809	0.822	0.781	0.785	0.932	0.878
105	0.937	0.853	0.952	0.877	0.965	0.857
110	0.89	0.904	0.872	0.899	0.951	0.936

Table 5.1: Degree of explanations for the homogeneous models

model 1	A $\left[\left[\frac{m^3}{mol}\right]^{n-1} \frac{1}{s}\right]$	Ea [kJ/mol]
$R_1(n = 2)$	$(4.5 \pm 40)E10$	(126 ± 3.4)
$R_2(n = 2)$	$(5.86 \pm 373)E15$	(170 ± 2.39)
$R_3(n = 2)$	$(2.05 \pm 26)E6$	(95.1 ± 4.8)
$R_4(n = 2)$	$(1.01 \pm 12)E4$	(74.9 ± 4.5)
model 2		
$R_1(n = 3)$	$(1.88 \pm 14.3)E6$	(129 ± 2.88)
$R_2(n = 2)$	$(3.58 \pm 47)E5$	(89.8 ± 4.97)
$R_3(n = 2)$	$(7.71 \pm 95.6)E3$	(74.1 ± 4.68)
model 3		
$R_1(n = 3)$	$(3.21 \pm 0.104)E7$	(135 ± 0.0004)
$R_2(n = 3)$	$(1.22 \pm 0.00002)E5$	(118 ± 0.397)
$R_3(n = 2)$	$(2.53 \pm 31.8)E5$	(91.3 ± 39.7)
$R_4(n = 2)$	$(6.16 \pm 62.8)E5$	(83.8 ± 31.9)

Table 5.2: 95% IC for the homogeneous models parameters

lowest in Table 5.1. According to the results in Table 5.1, it can be concluded that the third model is able to better describe the experimental trends, indeed the values of R^2 for both Rha and GlcA are the highest among all the three models. It must be taken into account that the degree of explanation does not give any information about the suitability of the mechanism. Indeed, R^2 tells how well the experimental data used for the optimization has been described. Therefore, a high value for the degree of explanation does not ensure that the mechanism gives a good representation of the real chemical route.

In order to verify whether the parameters estimated by the MATLAB routines were well defined an estimation of the confidence interval was performed according to the equations (5.13). The results of the confidence interval estimations are reported in the Table 5.2.

The results, for the 95% interval of confidence in Table 5.2, suggest that the identification of the activation energies is rather precise for all the three model. Moreover, the absolute values for the activation energies in the formation reactions were comparable to the works of Kusema et al. and Jin [46][37] in which the acid hydrolysis of arabinogalactan and xylan has been studied. However, the 95% ICs results for the pre-exponential factors are typically one order of magnitude higher than the actual values of the optimized parameters. Therefore, it may be concluded that the collision factors are not well defined. There might be several reasons to explain the problem of the well identification of the parameter. For instance the quality and limited amount

of experimental observations can affect the confidence interval. Moreover, the three models were optimized only by taking into account the experimental trends of Rha and GlcA, which were the only ones available, even though other species appeared in the rate equations.

In summary three approaches were tested in order to model the kinetics for ulvan homogeneous acid hydrolysis according to the experimental data obtained in this thesis work. All the above-mentioned models were able to give a good representation of the experimental dataset, especially in the case of activation energy. However, the statistical analysis on the optimized parameters revealed that the pre-exponential factors are characterized by a very large 95% interval of confidence. Therefore, the values for the collision factors are not well defined. A higher amount of experimental data, including the ulvan, U^* and the decomposition products evolution, would be needed in order to better validate the kinetic parameters for the three models.

5.3 Heterogeneous reaction mechanisms

In the work of Wärnå et al. [84], the hydrolysis of O-acetyl-galactoglucomanan (GGM) catalysed by SMOPEX-101 was studied and a kinetic modelling was developed. The experimental kinetic data collected in the mentioned work suggested an addition of an autocatalytic effect in the kinetic model. The hemicellulose molecule which is far from linear has to randomly collide with the superficial active sites of the resin in order to be broken down. Consequently, as the reaction proceeds the structure of the hemicellulose becomes more open and the length of the chains is reduced. Therefore, the collision of the oligomers with the active sites may become easier and more frequent. This phenomenon results in the increasing of the hydrolysis reaction rate as the conversion increases.

As described for the homogeneous acid hydrolysis of hemicellulose (Section 5.1) the rate equations according to the mechanism depicted in Figure 5.7 can be written as follows.

$$\frac{dC_i}{dt} = k_i C_{i0} C_{H^+} C_{H_2O} \rho_b \quad (5.15)$$

Where the concentration of the unhydrolyzed i specie (C_{i0}) and the kinetic constant (k_i) can be expressed according to the following equations:

$$\begin{aligned} C_{0i} &= C_{i0} + C_i \\ k_i &= k_{0i}(1 + \beta X^\alpha) \end{aligned} \quad (5.16)$$

In equation (5.15) ρ_b represents the catalyst bulk density (m_{cat}/V) and in equa-

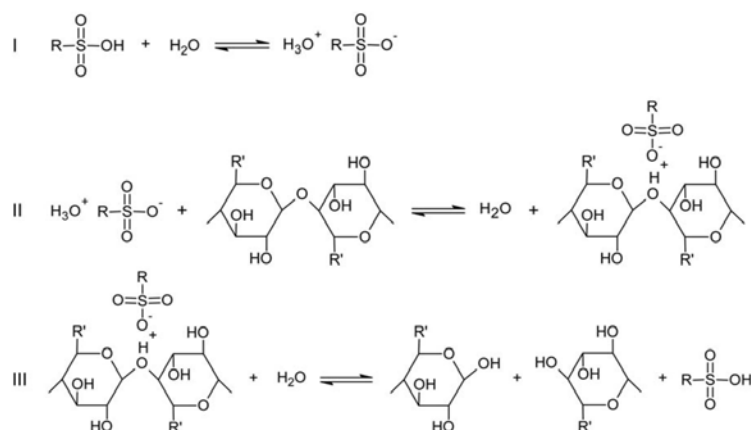


Figure 5.7: Homogeneous hydrolysis mechanism of hemicellulose in the work of Wärnä [84]

tion (5.16) X is the conversion and k_{0i} , β and α are the parameters to be estimated. The conversion is used in equation (5.16) in order to take into account for the observed autocatalytic behavior. Therefore, in this work no mass transfer limitations were considered, consequently the two phase (liquid-solid) system was simplified to a pseudo-homogeneous system in which no intraparticle mass and heat transfer phenomenon are considered. The pseudo-homogeneous hypothesis is anyhow supported by the fact that the SMOPEX-101 has a non porous structure (Section 3.3.2), so the active sites provided by the sulphonic groups are already available in the external surface of the fibers. Additionally, the reaction time was sufficiently long to neglect any possible external mass transfer limitations.

5.3.1 Heterogeneous mechanisms of ulvan hydrolysis

According to the experimental data presented in Section 4.2, no autocatalytic behavior was observed for ulvan heterogeneous acid hydrolysis. The glucuronic acid experimental trend revealed an unknown interaction between the sulfonic groups of the resin and the glucuronic acid cleaved from the ulvan backbone, which deeply decreased the yield of glucuronic acid to form lower molecular weight compounds. Therefore, the modelling of the heterogeneous hydrolysis of ulvan will be focused only on the rhamnose formation which is the most valuable compound among the two sugars. A pseudo-homogeneous mechanisms was tested in order to describe the kinetics of the reaction according to the experimental data.

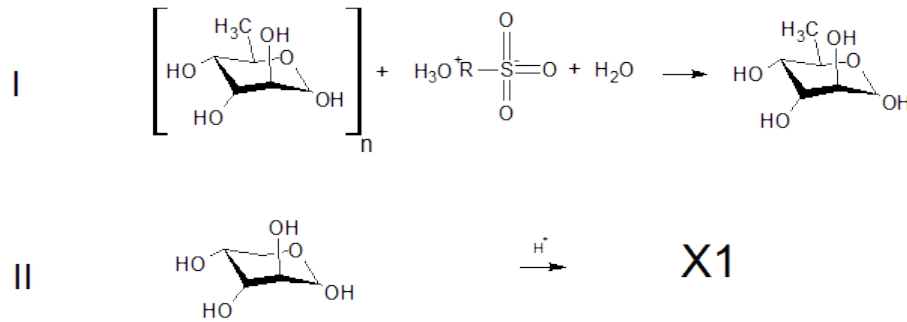


Figure 5.8: Suggested mechanism based on the work of Wörnå et al. [84]

Mechanism 1

The mechanism was based on the above-mentioned work of Wörnå and co authors [84]. The molecule of ulvan was considered to be formed only by a homopolymer of rhamnose units. According to the pseudohomogeneous assumption the reaction mechanism is depicted in Figure 5.8, in which the sulphonic groups of the resin bear the protons. The rate equations are defined as follow

$$\begin{aligned} R_I &= k_I C_{R0} C_{H^+} C_{H_2O} \\ R_{II} &= k_{II} C_{Rha} C_{H^+} \end{aligned} \quad (5.17)$$

As well as for the third homogeneous mechanism the rhamnose mass balance on allowed to calculate the concentration of unhydrolyzed rhamnose in the main chain.

$$C_{R0} = C_{0R} - C_{Rha} - C_{X1} \quad (5.18)$$

where C_{0R} represents the rhamnose concentration at time zero in the main chain. The general balance equations for an isothermal batch reactor at constant volume can be written as

$$\begin{aligned} \frac{dC_{Rha}}{dt} &= (R_I - R_{II})\rho_b \\ \frac{dC_{X1}}{dt} &= R_{II}\rho_b \end{aligned} \quad (5.19)$$

where ρ_b is the catalyst bulk density. As described in Section 5.2 the regression of the experimental kinetic data has been performed using a MATLAB algorithm according to the equations described. The three experimental kinetic data-set obtained at different temperatures were used together with the two data-set obtained at different acidity concentration in order to optimize the kinetic parameters.

	R^2
100°C-100mMH ⁺ eq	0.904
110°C-100mMH ⁺ eq	0.983
120°C-100mMH ⁺ eq	0.94
110°C-50mMH ⁺ eq	0.816
110°C-75mMH ⁺ eq	0.978

Table 5.3: Degree of explanations for the heterogeneous model

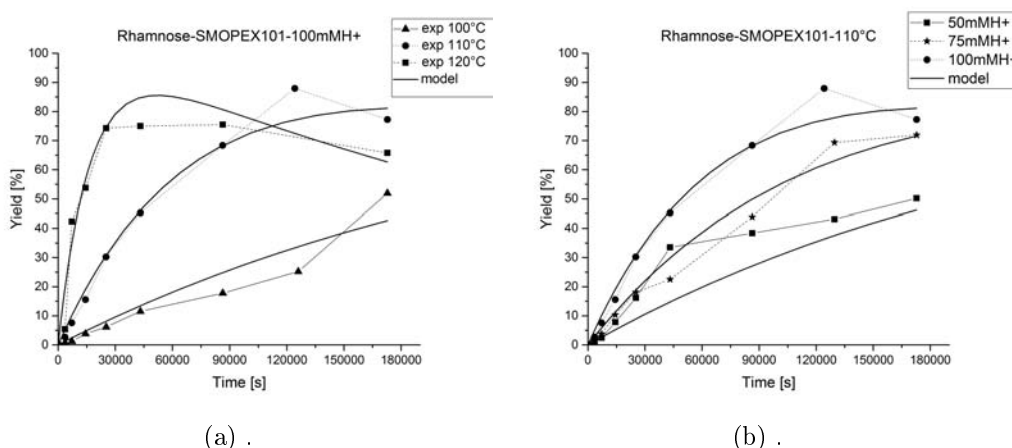


Figure 5.9: Modelling results for the heterogeneous kinetic experimental data of Rha

Parameters estimation results

The optimized parameters were assessed as reported in Section 5.2.1 for the homogeneous case.

The results for the parameter estimation are reported in Figure 5.9 and in Table 5.3, both the effect of temperature and the acid site concentration on the kinetic data are reported.

The values for the coefficient of determination (R^2), which are reported in Table 5.3, are typically above 90%. Therefore, the suggested model is able to give a proper representation of the experimental kinetic data. However, as mentioned earlier the values for R^2 are not necessarily a prove of a correct chemical-physical description of the phenomenon.

The wellness of the estimated parameters was checked according to the statistical equations introduced in Section 5.2.1 which results are reported in Table 5.4. The values for both the collision factor and the activation energy for the formation reaction (R_I) are well defined according to the results in Table 5.4. Indeed, the values of the lower and upper bound of the interval of confidence are smaller than the optimized parameters.

	A $\left[\left[\frac{m^3}{mol}\right]^{n-1} \frac{1}{s}\right]$	Ea [kJ/mol]
$R_1(n = 3)$	$(9.06 \pm 0.000323)E10$	(176 ± 0.007)
$R_2(n = 2)$	$(5.74 \pm 245)E7$	(126 ± 138)

Table 5.4: 95% IC for the homogeneous models parameters

Contrarily, the obtained confidence of interval obtained for the degradation reaction for both the pre-exponential factor and the activation energy were not satisfactory. Indeed, the absolute values for both the optimized parameters were lower than the values of the ICs.

The relatively small amount of data and the scattering behavior that occurred in the kinetic trend may explain the poor results obtained for the degradation reaction. Moreover, it should be noticed that only the kinetic trend obtained at 120°C was made-up of both formation and decomposition of rhamnose, whereas the rhamnose formation reaction is the only one that clearly occurs for the ulvan hydrolysis reaction evaluated at lower temperatures. Therefore, the lack of decomposition data can be another reason for the poorly defined parameters of this reaction.

To conclude, a pseudohomogeneous strategy was used to model kinetic data of acid hydrolysis of ulvan in this work. The model was able to give a good representation of the experimental data according to the values of the calculated coefficient of determination (Table 5.3). However, as well as in the homogeneous case, the statistical analysis revealed that the values for both the activation energy and the frequency factor were not well defined for the decomposition reaction (R_{II}). A larger amount of experimental data, including the ulvan and the decomposition products evolution would be needed in order to better validate the kinetic parameters of the model.

Conclusions

The acid hydrolysis of ulvan, a polysaccharide extracted from the green algae *Ulva rigida*, was studied in this master thesis project. The carbohydrate was successfully hydrolyzed into rhamnose, which is the most valuable constituents of the ulvan backbone. Different hydrolysis approaches were evaluated in order to hydrolyse ulvan into its monomeric constituent rhamnose (Rha) and glucuronic acid (GlcA). The performance of the homogeneous acid hydrolysis, the traditional route used in the hydrolysis of biomass, were compared with the heterogeneous acid hydrolysis. Accordingly, the homogeneous acid hydrolysis experiments were catalysed with HCl, whereas two commercial resin (SMOPEX101 and Amberlyst 70) bearing sulfonic groups were used as catalysts in the heterogeneous acid hydrolysis experiments. With the aim to study the kinetics of the hydrolysis of ulvan, different conditions were evaluated namely temperature (90-120°C), acidity (50-100mMH⁺eq) and type of catalyst. In addition, different reaction mechanism were tested in order to model the experimental kinetic data.

The experimental kinetic results showed that the hydrolysis of ulvan was affected by both temperature and acidity in the case of heterogeneous acid hydrolysis. Specifically the higher the temperature the faster the formation rate of monomers. As far as the acidity is concerned, the correlation was not well defined as in the case of the temperature. The maximum yield of rhamnose observed was around 90% (SMOPEX101-110°C/120C-100mMH⁺eq) whereas the glucuronic acid yield was much lower, the maximum value observed was around 10% (SMOPEX101-110°C-50mMH⁺eq). The wide difference in terms of yields among the two monomers was unexpected. Indeed, according to the earlier composition analysis of the unhydrolyzed mixtures, a ratio $1 : 1 = Rha : GlcA$ was found. An unknown interaction between the formed glucuronic acid and the sulfonic groups of the resin was suggested as the potential cause for the yield difference among Rha and GlcA. A number of different unknown molecules were detected in the hydrolyzates when analyzed in HPLC, presumably from the decomposition of GlcA. As far as the Amberlyst 70 experiments was concerned, a definitely poorer performance in terms of yield was obtained with respect to SMOPEX101. The lower yields obtained were most likely due to the internal mass transfer limitation

caused by the porosity of the catalyst. Eventually, the reutilization of the best solid catalyst (SMOPEX101) has revealed that a sharp drop in the catalyst activity occurred from the first to the second use. The maximum value for the yield of rhamnose dropped from 88% in the case of SMOPEX101 to 31% when Amb70 was used as a catalyst.

The homogeneous acid hydrolysis revealed that using an homogeneous catalysis gives comparable yield (80%), in terms of rhamnose yield, with respect to the heterogeneous acid hydrolysis, but with a much higher rate. In turn, the glucuronic acid yields obtained were much higher in the case of homogeneous hydrolysis (55%) compared to the heterogeneous one. As well as for the heterogeneous hydrolysis, the homogeneous hydrolysis was importantly dependent on the temperature. The higher the temperature the faster the formation rate of the monomers. However, in the homogeneous case, an appreciable decomposition trend was also observed for both rhamnose and glucuronic acid and these rates increased if the temperature increased. Since, with the homogeneous approach a higher GlcA yield was obtained, the hypothesis of an unknown interaction that occurred between the GlcA and the sulfonic group of the resin might be reasonable. Other evidence for this hypothesis were found in the hydrolysis experiments performed with pure GlcA using both the HCl and the resin (SMOPEX101). The experiments confirmed that the decomposition of GlcA was more severe if the reaction was catalysed by the resin. Nevertheless, a more detailed study would be needed in order to confirm this hypothesis and the possible interaction that uronic acid molecules might have with the resin.

Three reaction mechanisms were supposed for the homogeneous hydrolysis of ulvan. The models were able to give a suitable representation of the experimental kinetic data according to the relatively high values for the degree of explanation. Notwithstanding, the kinetic pre-exponential factors optimized were typically non-well defined. The coarse confidence interval for the mentioned parameters may be reduced by increasing the number of experimental data including the concentration evolution of the decomposition products. The heterogeneous hydrolysis of ulvan was treated according to a pseudo homogeneous model. Moreover, the unknown interaction between the sulfonic group of the resin and the formed GlcA drove the modelling to focus only on the rhamnose description. Therefore, a reaction mechanism for the hydrolysis of rhamnose from ulvan backbone was supposed. As well as for the homogeneous kinetic modelling, the values for the degree of explanation were relatively high, thus the model described well the kinetic experimental data. However, the lack of experimental data involving decomposition products hindered the kinetic parameter estimation. Indeed, the confidence interval for both activation energy and collision factor for the degradation reaction, were accordingly higher than the optimized values of the parameters. Therefore, the parameters were non-well defined for this reaction. The results for the modelling lead

to conclude that a larger amount of experimental data is needed in order to validate the supposed mechanism. Specifically, experimental data regarding the decomposition products of the monomers has to be quantified. Therefore it is suggested to performed the methanolysis analysis on the samples withdrawn throughout the reaction time, in order to close the mass balances for both Rha and GlcA and consequently estimate the carbon fraction that was converted into degradation products.

The main issues to be further studied in the future would be the detailed study of the glucuronic acid decomposition in order to detect all the decomposition products involved in the decomposition mechanism. Additionally, the study of the interaction between glucuronic acid and the sulfonic groups of the solid catalyst is the key in order to give a better understanding of the phenomena. Accordingly, this study might provide more information for the design of more suitable catalyst for the hydrolysis of carbohydrates bearing uronic acids. Besides, the study of the deactivation of the resin in order to reduce the loss of efficiency among different reaction batches is the key for industrial applications of this kind of process. Consequently, more temperature tolerant resins are required to successfully achieve the hydrolysis of this kind of carbohydrates. Furthermore, the increase of the quality and the number of experimental kinetic data is important to better validate the reaction mechanism suggested in this thesis work. Eventually the evaluation of an efficient strategy in order to collect and purify the monomer produced from the reaction media, as an intermediate step prior to further processing of the sugars is very important for a future industrial implementation of the production process.

Acknowledgments

I would like to express my gratitude to my supervisor Professor Paolo Canu for the precious advices, remarks and comments that have allowed to snake throughout the difficulties of this thesis project. Furthermore, to have given me the possibility to experience the thesis project abroad. My thankfulness goes also to Professor Jyri-Pekka Mikkola and Dr. Päivi Mäki-Arvela, for giving me the possibility to work on this specific topic and for their valuable help. Above all, a special thanks goes to Ricardo Pezoa Conte, my mentor and colleague who shared his scientific knowledge and experience, and he guided me through the entire exchange period.

A hearty thank goes to all the friends and colleagues I have met in Finland. To my flatmates, Helene, Tom, Violeta, Sophie and Elena for all the good foods and the moments of life we shared. To my colleagues in the lab, Nemanja, Maria, Shu, Erfan, Adriana, Silvia and Masoud for the coffee breaks, the evenings and the gym time we spent together.

A thought must go to all my Italian friends, in particular to Giovanni, Lorenzo, Alice, Paola, Giovanna, Sacha (Satta), Ilaria (I-LA) e Alessandro (Gatto) with which I have spent five years through the university journey. We have shared party, traveling and study time, and I will remember all those beautiful moments for the rest of my life.

I would like to say thanks to my family, my mum, my dad, my brother and all my relatives, for their unconditional love and support throughout the years. This work wouldn't have been possible without your care, patience and belief in me.

Last but not least, I would like to express my true gratitude and love to Giulia the girl that has been enduring me for three years so far. We have lived an arduous year of forced distance, but we have managed to stay together in spite of the few times we have seen each other and all the stiffness of a distance relationship. You are unique and special.

Appendix A

A.1 Total carbohydrates content

A.1.1 Methanolysis protocol

- Day 1

- Transfer 100 μL of sample to a pressure resistant pear-shape flask with a skrew cap
- Freeze the sample
- Allow the sample to dry in the freeze-dryer over night

- Day 2

- Add 1 mL of a carbohydrate calibration solution to two different pear-shaped flasks.
- Evaporate to dryness under nitrogen in a thermostatic bath at 50°C the calibration flasks.
- Add about 2mL of methanolysis reagent (HCl 2M in MEOH) to both the calibration and the freeze-dried samples.
- The samples are put in the oven at 100°C for 3h, and shaken every hour.
- After 3h the samples are allowed to cool down to room temperature, then the excess of HCl is neutralized by adding 200mL of pyridine.
- 1mL of internal standard solution (0.1mg mL⁻¹ sorbitol and resorcinol in MeOH) is added to the samples and the calibration samples.
- The methanol is evaporated under nitrogen in a thermostatic bath at 50°C.
- The samples are further dried for 20min in a vacuum dessiccator.
- The samples are silylated.

The calibration solution was formed by 0.1mg/mL of arabinose, rhamnose, xylose, mannose, galactose, glucose, glucuronic and galacturonic acid in a 9 : 1 = *MeOH* : H_2O solution.

A.1.2 Silylation protocol

- Add 150mL of pyridine to the samples, cap and shake the tubes.
- the tubes are further immersed for a few seconds in an ultrasonic bath.
- Add 150mL of HMDS to the samples, cap and shake the tubes.
- Add 75mL of TMCS to the samples, cap and shake the tubes.
- the tubes are further immersed for a few seconds in an ultrasonic bath.
- The flask are put in the oven at 70°C for 45min.
- The silylated samples are transferred to GC autosampler vials using clean Pasteur pipette. Try to avoid trasfering any of the precipitate to prevent clogging the injection needle.

A.2 Monomer analysis content (Heterogeneous samples)

- **Day 1**
 - Transfer 200 μ L of sample to a pressure resistant pear-shape flask with a skrew cap
 - Freeze the sample
 - Allow the sample to dry in the freeze-dryer over night
- **Day 2**
 - Add 1 mL of a carbohydrate calibration solution to two different pear-shaped flasks.
 - Add 1mL of xylitol (0.1 mg mL^{-1} in *MeOH*) to the freeze-dried samples as well as the calibration tubes.
 - Evaporate to dryness under nitrogen in a thermostatic bath at 50°C all the flasks.

- The samples are further dried for 20min in a vacuum dessicator.
- The samples are silylated as described in section A.1.2. However, in this case the samples are not treated in the oven but they are let stay overnight at room temperature.

Appendix B

B.1 Ulvan extraction

Some results regarding the ulvan extraction procedure are reported in Table B.1. According to the values for the washing pretreatment, specifically U_{fresh} , U_{solid} which is the solid phase after the washing and U_{liquid} which is the liquid phase after the washing, almost 20% of the alga weight is lost after the washing procedure. Moreover, it can be noticed that the weight loss is mostly due by the removing of the ashes content. Comparing the values for U_{solid} , which is the starting material for the extraction procedure and the values for $U_{extract}$ which is the final product, it can be noticed that more than 80% of the initial amount of both rhamnase and glucuronic acid can be recovered through the hot water extraction process.

B.2 HPLC Calibration

In Table B.2 the results for the calibration data, in terms of Elution time, Area and slope of the relatively calibration curve, are reported. The experimental points, needed to obtain the calibration curves, were produced with the HPLC program described in Section 3.4.4. Different mixture, at different concentration of the analytes reported in

sample	Glc [mg/galgae]	GlcA [mg/galgae]	Rha [mg/galgae]	Xyl [mg/galgae]	Ash [mg/galgae]	Mass loss [wt%]
$U_{extract-4h-90^{\circ}C}$	31.55	62.02	57.71	10.27		
$U_{liquid-washed}$	7.07	3.60	5.94	1.99		
$U_{solid-washed}$	166.70	75.83	67.88	35.56	64.85	19.24
U_{fresh}	170.33	82.77	75.65	37.03	178.00	

Table B.1: Results for the ulvan (U) mass balance on the washing procedure (fresh, solid, liquid), and values for the liquid phase after 4h of hot water extraction (unpublished data)

Compound	Elution time [min]	Area					slope mg mL ⁻¹ Area ⁻¹
		1mg/mL	0.75mg/mL	0.5mg/mL	0.25mg/mL	mg mL ⁻¹ Area ⁻¹	
GlcA	15.6	699.308	525.831	377.190	194.313	1.41E-03	
MalicA	16.5	1219.923	909.648	646.928	332.631	8.12E-04	
Glc	17.9	1224.255	907.335	650.199	349.078	8.08E-04	
Xyl	19.3	1109.749	815.309	576.035	301.454	8.99E-04	
GlcA-YL	21.8	524.112	376.992	279.431	161.884	1.90E-03	
FoA	28.1	385.462	299.589	220.079	115.098	2.50E-03	
HMF	64.4	1245.181	927.589	619.640	298.104	8.06E-04	
Furfural	97.6	629.079	473.677	299.067	151.665	1.60E-03	
LvA	32.7	696.119	495.510	344.062	168.770	1.46E-03	
ButyricA	44.2	671.162	484.317	362.928	169.842	1.49E-03	
GlycolicA	24.7	632.689	473.240	312.628	157.988	1.58E-03	
Compound	Elution time [min]	Area	Area	Area	Area	slope mg mL ⁻¹ Area ⁻¹	
		3mg/mL	2.25mg/mL	1.5mg/mL	0.75mg/mL		
Rha	20.5	3191.924	2409.646	1637.660	848.718	9.33E-04	
SuccA	23.6	1305.325	979.026	655.073	324.489	1.53E-03	
		0.5mg/mL	0.375mg/mL	0.25mg/mL	0.125mg/mL		
LacticA	25.6	227.110	175.895	112.201	57.5576	2.18E-03	

Table B.2: Calibration results for the compounds analyze in HPLC

Table B.2, were loaded into the instruments. Eventually, the output chromatograms were manually integrated with the default HPLC post-processing software in order to obtain the values for the area of the peaks. The manual integration was needed because of the partial overlapping of the peaks. A linear regression relating the area and the known concentration was finally obtained with Excel.

Appendix C

C.1 TEM results

The cross section of the fresh SMOPEX-101 and of the resin after the second hydrolysis run are reported in Figure C.1 and Figure C.2, respectively. The darkest area is the catalyst whereas the lightest one is the polymeric tape used to stick the resin slice on the TEM specimen. It can be noticed that a layer of about $1\mu\text{m}$ appears in both the fresh and the used catalyst, consequently it is intrinsic to the resin structure. To conclude, not noticeable difference were observed with the TEM analysis among the fresh and the reused catalyst, though a visible change in the color of the resin was observed.

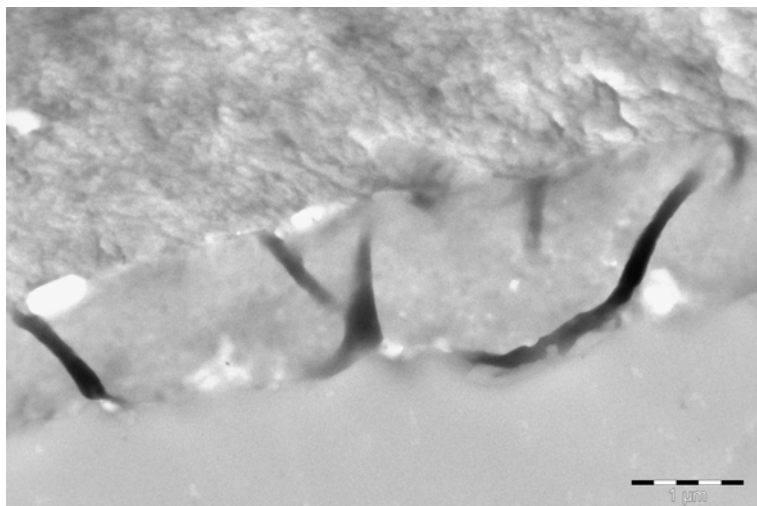


Figure C.1: TEM image of the cross section of the fresh SMOPEX101

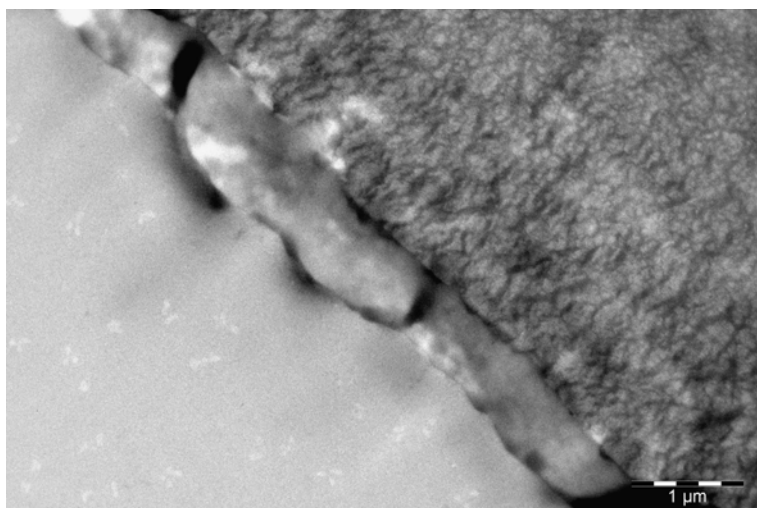


Figure C.2: TEM image of the cross section of the SMOPEX101 after the second run

Bibliography

- [1] Bjarne Holmbom Anna Sundberg, Kenneth Sundberg, Camilla Lillandt. “Determination of hemicelluloses and pectins in wood and pulp fibres by acid methanolysis and gas chromatography”. In: *Nordic Pulp and Paper Research Journal* 11.04 (1996), pp. 216–219. ISSN: 0283-2631. DOI: 10.3183/NPPRJ-1996-11-04-p216-219.
- [2] Eric V Anslyn and Dennis A Dougherty. *Modern Physical Organic Chemistry*. ISBN: 9781891389313.
- [3] J. J. BURNS et al. *GLUCURONIC ACID Free and Combined*. Ed. by GEOFFREY J. DUTTON. New York: Academic Press, 1966, p. 631.
- [4] Laura Barsanti and Paolo Gualtieri. *Algae: Anatomy, Biochemistry, and Biotechnology*. Ed. by CRC Press. second. 2014, p. 361. ISBN: 9788578110796. DOI: 10.1017/CB09781107415324.004. arXiv: arXiv:1011.1669v3.
- [5] F. Bertaud, A. Sundberg, and B. Holmbom. “Evaluation of acid methanolysis for analysis of wood hemicelluloses and pectins”. In: *Carbohydrate Polymers* 48.3 (2002), pp. 319–324. ISSN: 01448617. DOI: 10.1016/S0144-8617(01)00249-1.
- [6] Henry R. Bungay. *Energy, the biomass options*. New York: Jonh Wiley & Sons, 1981.
- [7] Faizal Bux and Yusuf Chisti. *Algae Biotechnology*. 2016. ISBN: 978-3-319-12333-2. DOI: 10.1007/978-3-319-12334-9. URL: <http://link.springer.com/10.1007/978-3-319-12334-9>.
- [8] Matthew N Campbell. “Biodiesel : Algae as a Renewable Source for Liquid Fuel”. In: *Guelph Engineering Journal* 1 (2008), pp. 2–7. ISSN: 19161107.
- [9] F Cavani et al. *Chemicals and Fuels from Bio-Based Building Blocks*. v. 1. Wiley, 2016. ISBN: 9783527338979. URL: <https://books.google.fi/books?id=6wWmCgAAQBAJ>.

- [10] Animesh Chakrabarti and M. M. Sharma. "State-of-the-Art Report Cationic ion exchange resins as catalyst". In: *Reactive Polymers* 20 (1993), pp. 1–45. ISSN: 09231137. DOI: 10.1016/0923-1137(93)90064-M.
- [11] Francesco Cherubini. "The biorefinery concept: Using biomass instead of oil for producing energy and chemicals". In: *Energy Conversion and Management* 51.7 (2010), pp. 1412–1421. ISSN: 01968904. DOI: 10.1016/j.enconman.2010.01.015. arXiv: /dx.doi.org/10.1016/j.enconman.2010.01.015 [http:]. URL: <http://dx.doi.org/10.1016/j.enconman.2010.01.015>.
- [12] Federica Chiellini and Andrea Morelli. "Ulvan: A Versatile Platform of Biomaterials from Renewable Resources". In: *Biomaterials* (2011), pp. 75–98. DOI: 10.5772/24901. URL: <http://cdn.intechweb.org/pdfs/22917.pdf> \backslash\$nh<http://www.intechopen.com/books/biomaterials-physics-and-chemistry/ulvan-a-versatile-platform-of-biomaterials-from-renewable-resources>.
- [13] Yusuf Chisti. "Biodiesel from microalgae". In: *Biotechnology Advances* 25.3 (May 2007), pp. 294–306. ISSN: 0734-9750. DOI: <http://dx.doi.org/10.1016/j.biotechadv.2007.02.001>. URL: <http://www.sciencedirect.com/science/article/pii/S0734975007000262>.
- [14] Jim Clark. *GAS-LIQUID CHROMATOGRAPHY*. 2007. URL: <http://www.chemguide.co.uk/analysis/chromatography/gas.html>.
- [15] Carina Costa et al. "Characterization of ulvan extracts to assess the effect of different steps in the extraction procedure". In: *Carbohydrate Polymers* 88.2 (2012), pp. 537–546. ISSN: 01448617. DOI: 10.1016/j.carbpol.2011.12.041.
- [16] G. Charles Dismukes et al. "Aquatic phototrophs: efficient alternatives to land-based crops for biofuels". In: *Current Opinion in Biotechnology* 19.3 (2008), pp. 235–240. ISSN: 09581669. DOI: 10.1016/j.copbio.2008.05.007.
- [17] David S Domozych et al. "The Cell Walls of Green Algae: A Journey through Evolution and Diversity." In: *Frontiers in plant science* 3.May (2012), p. 82. ISSN: 1664-462X. DOI: 10.3389/fpls.2012.00082. URL: <http://www.ncbi.nlm.nih.gov/pubmed/22639667> \backslash\$nh<http://www.pubmedcentral.nih.gov/articlerender.fcgi?artid=PMC3355577>.
- [18] Severian Dumitriu. *Polysaccharides: Structural Diversity and Functional Versatility*. Ed. by 2nd. Vol. 1. New York: Marcel dekker, 2004, p. 1223. ISBN: 9788578110796. DOI: 10.1017/CB09781107415324.004. arXiv: arXiv:1011.1669v3.

- [19] Kelly J Dussán et al. “Dilute-acid Hydrolysis of Cellulose to Glucose from Sugarcane Bagasse”. In: *Chemical Engineering Transactions* 38 (2014), pp. 433–438. ISSN: 9788895608297.
- [20] M Ehteshami et al. “Kinetic study of catalytic hydrolysis reaction of methyl acetate to acetic acid and methanol”. In: *Iranian Journal of Science & Technology* 30 (2006), pp. 595–606.
- [21] Sergey N. Fedorov et al. “Anticancer and cancer preventive properties of marine polysaccharides: Some results and prospects”. In: *Marine Drugs* 11.12 (2013), pp. 4876–4901. ISSN: 16603397. DOI: 10.3390/md11124876.
- [22] Valentina Fiorenzato. “BILANCI DI POPOLAZIONE DI UNA COLTURA MICROALGALE IN FOTOBIOREATTORI : SIMULAZIONI”. MA thesis. University of Padua, 2014, p. 146.
- [23] Edwin R Gilliland, Harris J Bixler, and Joseph E OConnell. “Catalysis of Sucrose Inversion in Ion- Exchange Resins”. In: *Industrial Engineering Chemistry Fundam.* 10.2 (1971), pp. 185–191.
- [24] Yulia Gladysenko. “Extraction of Hemicelluloses By Acid Catalyzed Hydrolysis”. In: *Thesis* (2011).
- [25] Linda E Graham et al. *Algae*. 2000, p. 25. ISBN: 0136603335.
- [26] A Haug. “The influence of borate and calcium on the gel formation of a sulfated polysaccharide from *Ulva lactuca*.” In: *Acta Chem Scand B.* 30.6 (1976), pp. 562–566. ISSN: 0904-213X. DOI: 10.3891/acta.chem.scand.30b-0562.
- [27] Jan Hendrik Hehemann, Alisdair B. Boraston, and Mirjam Czjzek. “A sweet new wave: Structures and mechanisms of enzymes that digest polysaccharides from marine algae”. In: *Current Opinion in Structural Biology* 28.1 (2014), pp. 77–86. ISSN: 1879033X. DOI: 10.1016/j.sbi.2014.07.009. URL: <http://dx.doi.org/10.1016/j.sbi.2014.07.009>.
- [28] F G Helfferich. *Ion Exchange*. Dover science books. Dover, 1962. ISBN: 9780486687841. URL: <https://books.google.fi/books?id=F90QMEA88CAC>.
- [29] Víctor Alberto Sifontes Herrera. “Hydrogenation of L-arabinose, D-galactose, D-maltose and L-rhamnose”. PhD thesis. Åbo Akademi University, 97, p. 2012.
- [30] G. Hilpmann et al. “Acid hydrolysis of xylan”. In: *Catalysis Today* 259 (2014), pp. 376–380. ISSN: 09205861. DOI: 10.1016/j.cattod.2015.04.044. URL: <http://dx.doi.org/10.1016/j.cattod.2015.04.044>.

- [31] Qiang Hu et al. "Microalgal triacylglycerols as feedstocks for biofuel production : perspectives and advances". In: *The Plant Journal* 54 (2008), pp. 621–639. DOI: 10.1111/j.1365-313X.2008.03492.x.
- [32] E. Husemann. "Book Review: Chemistry and Enzymology of Marine Algal Polysaccharides. By E. Percival and R. H. McDowell". In: *Angewandte Chemie International Edition in English* 7.9 (Sept. 1968), pp. 746–746. ISSN: 0570-0833. DOI: 10.1002/anie.196807463. URL: <http://doi.wiley.com/10.1002/anie.196807463>.
- [33] Latife Ceyda Irkin and Hüseyin Erdugan. "Chemical composition of *Ulva rigida* C. Agardh from the Çanakkale Strait (Dardanelles), Turkey". In: *Journal of Black Sea / Mediterranean Environment* 20.2 (2014). ISSN: 1304-9550.
- [34] Gwi Taek Jeong, Sung Koo Kim, and Don Hee Park. "Application of solid-acid catalyst and marine macro-algae *Gracilaria verrucosa* to production of fermentable sugars". In: *Bioresource Technology* 181 (2015), pp. 1–6. ISSN: 18732976. DOI: 10.1016/j.biortech.2015.01.038. URL: <http://dx.doi.org/10.1016/j.biortech.2015.01.038>.
- [35] Gwi-taek Jeong and Don-hee Park. "Effect of Reaction Factors on Reducing Sugar Production from *Enteromorpha intestinalis* Using Solid Acid Catalyst". In: *Korean Chemical Engineering Research* 53.4 (2015), pp. 478–481.
- [36] Guangling Jiao et al. "Chemical Structures and Bioactivities of Sulfated Polysaccharides from Marine Algae". In: *Mar. Drugs* 9.2 (2011), pp. 196–223. DOI: 10.3390/md9020196.
- [37] Qiang Jin et al. "Kinetic characterization for hemicellulose hydrolysis of corn stover in a dilute acid cycle spray flow-through reactor at moderate conditions". In: *Biomass and Bioenergy* 35.10 (2011), pp. 4158–4164. URL: <http://dx.doi.org/10.1016/j.biombioe.2011.06.050>.
- [38] M. A. Khan. "Hydrolysis of hemicellulose by commercial enzyme mixtures". PhD thesis. 2010, pp. 1–28. ISBN: 1402-1552 - ISRN: LTU-DUPP-10/040-SE. DOI: 1402-1552- ISRN: LTU-DUPP--10/040--SE. URL: <http://epubl.ltu.se/1402-1552/2010/040/LTU-DUPP-10040-SE.pdf>.
- [39] Ali O Kiliç et al. "Comparative Study of Vaginal Lactobacillus Phages Isolated from Women in the United States and Turkey: Prevalence, Morphology, Host Range, and DNA Homology". In: *Clinical and Diagnostic Laboratory Immunology* 8.1 (Jan. 2001), pp. 31–39. ISSN: 1071-412X. DOI: 10.1128/CDLI.8.1.31-39.2001. URL: <http://www.ncbi.nlm.nih.gov/pmc/articles/PMC96007/>.

- [40] Se-Kwon Kim and Katarzyna Chojnacka. *Marine Algae Extracts*. Vol. 1, 2. WILEY-VCH, 2015. ISBN: 9788578110796. DOI: 10.1017/CB09781107415324.004. arXiv: arXiv:1011.1669v3.
- [41] Se-kwon Kim. *Handbook of Marine Macroalgae Handbook of Marine Macroalgae Biotechnology and Applied Phycology*. John Wiley & Sons, 2012. ISBN: 9780470979181.
- [42] Youngmi Kim et al. “Plug-flow reactor for continuous hydrolysis of glucans and xylans from pretreated corn fiber”. In: *Energy and Fuels* 19.5 (2005), pp. 2189–2200. ISSN: 08870624. DOI: 10.1021/ef0501061.
- [43] Stefan Kraan. *Algal Polysaccharides , Novel Applications and Outlook*. Ed. by Chuan-Fa Chang. Intech, 2012. ISBN: 978-953-51-0864-1. DOI: 10.5772/51572.
- [44] H. D. Kumar and Hriday Narain Singh. *A Textbook on Algae*. Ed. by Affiliated East-West Press. 1971, p. 200. ISBN: 9788578110796. DOI: 10.1017/CB09781107415324.004. arXiv: arXiv:1011.1669v3.
- [45] Bright T. Kusema et al. “Acid hydrolysis of O-acetyl-galactoglucomannan”. In: *Catal. Sci. Technol.* 3.1 (2013), pp. 116–122. ISSN: 2044-4753. DOI: 10.1039/C2CY20314F. URL: <http://xlink.rsc.org/?DOI=C2CY20314F>.
- [46] Bright T. Kusema et al. “Kinetics of acid hydrolysis of Arabinogalactans”. In: *International Journal of Chemical Reactor Engineering* 8.1 (Jan. 2010). URL: <http://www.bepress.com/cgi/viewcontent.cgi?article=2118&context=ijcre>.
- [47] Bright T. Kusema et al. “Selective hydrolysis of arabinogalactan into arabinose and galactose over heterogeneous catalysts”. In: *Catalysis Letters* 141.3 (2011), pp. 408–412. ISSN: 1011372X. DOI: 10.1007/s10562-010-0530-x.
- [48] Bio-Rad Laboratories. *Aminex® Carbohydrate Analysis Columns*. URL: <http://www.bio-rad.com/it-it/product/aminex-carbohydrate-analysis-columns>.
- [49] M. Lahaye and M. A V Axelos. “Gelling properties of water-soluble polysaccharides from proliferating marine green seaweeds (*Ulva* spp.)” In: *Carbohydrate Polymers* 22.4 (1993), pp. 261–265. ISSN: 01448617. DOI: 10.1016/0144-8617(93)90129-R.
- [50] Marc Lahaye. “NMR spectroscopic characterisation of oligosaccharides from two *Ulva rigida* ulvan samples (*Ulva*les, Chlorophyta) degraded by a lyase”. In: *Carbohydrate Research* 314.1-2 (1998), pp. 1–12. ISSN: 00086215. DOI: 10.1016/S0008-6215(98)00293-6.

- [51] Marc Lahaye and Bimalendu Ray. "Cell-wall polysaccharides from the marine green alga *Ulva "rigida"* (Ulvales, Chlorophyta) - NMR analysis of ulvan oligosaccharides". In: *Carbohydrate Research* 283 (1996), pp. 161–173. ISSN: 00086215. DOI: 10.1016/0008-6215(95)00407-6.
- [52] Marc Lahaye and Audrey Robic. "Structure and Functional Properties of Ulvan, a Polysaccharide from Green Seaweeds". In: *Biomacromolecules* 8.6 (2007), 1765–1774.
- [53] Michelle A LeRoux, Farshid Guilak, and Lori A Setton. "Compressive and shear properties of alginate gel : Effects of sodium ions and alginate concentration ". In: *Journal Biomedical Material Research* 47.1 (Nov. 1999), pp. 46–53. DOI: 10.1002/(SICI)1097-4636(199910)47.
- [54] C. E. Timberlake M. L. Wolfrom, A. Thompson. "Comparative hydrolysis rates of the reducing disaccharides of d-glucopyranose". In: *American Association of Cereal Chemists* 40 (1963), pp. 82–86.
- [55] Päivi Mäki-Arvela et al. "Recent Progress in Synthesis of Fine and Specialty Chemicals from Wood and Other Biomass by Heterogeneous Catalytic Processes". In: *Catalysis Reviews: Science and Engineering* 49.3 (2007), pp. 197–340. ISSN: 0161-4940. DOI: 10.1080/01614940701313127.
- [56] Päivi Mäki-Arvela et al. "Synthesis of sugars by hydrolysis of hemicelluloses- A review". In: *Chemical Reviews* 111.9 (2011), pp. 5638–5666. ISSN: 00092665. DOI: 10.1021/cr2000042.
- [57] J. P. McKinnell and Elizabeth Percival. "Structural investigations on the water-soluble polysaccharide of the green seaweed *Enteromorpha compressa*". In: *Journal of the Chemical Society (Resumed)* 0 (1962), pp. 3141–3148. ISSN: 0368-1769. DOI: 10.1039/JR9620003141. URL: <http://dx.doi.org/10.1039/JR9620003141>.
- [58] Taku Michael et al. "Production of organic acids from alginate in high temperature water". In: *The Journal of Supercritical Fluids* 65 (2012), pp. 39–44. ISSN: 0896-8446. DOI: 10.1016/j.supflu.2012.02.021. URL: <http://dx.doi.org/10.1016/j.supflu.2012.02.021>.
- [59] Emyr Alun Moelwyn-Hughes. "The kinetics of the hydrolysis of certain glucosides, part III.; [small beta]-methylglucoside, cellobiose, melibiose, and turanose". In: *Transactions of the Faraday Society* 25.0 (1929), pp. 503–520. ISSN: 0014-7672. DOI: 10.1039/TF9292500503. URL: <http://dx.doi.org/10.1039/TF9292500503>.

- [60] Andrea Morelli and Federica Chiellini. “Ulvan as a new type of biomaterial from renewable resources: Functionalization and hydrogel preparation”. In: *Macromolecular Chemistry and Physics* 211.7 (2010), pp. 821–832. ISSN: 10221352. DOI: 10.1002/macp.200900562.
- [61] Jerry D. Murphy et al. “A Perspective on algal biomass”. In: *IEA Bioenergy* (2015), pp. 1–38.
- [62] D Murzin and O Simakova. *Biomass Sugars for Non-Fuel Applications*: RSC Green Chemistry. Royal Society of Chemistry, 2015. ISBN: 9781782621133. URL: <https://books.google.fi/books?id=a5UBCwAAQBAJ>.
- [63] Andrea Pérez Nebreda et al. “Acid hydrolysis of O-acetyl-galactoglucomannan in a continuous tube reactor: a new approach to sugar monomer production”. In: *Holzforschung* 0.0 (2015). ISSN: 1437-434X. DOI: 10.1515/hf-2014-0314. URL: <http://www.degruyter.com/view/j/hfsg.ahead-of-print/hf-2014-0314/hf-2014-0314.xml>.
- [64] Tetsuko Noguchi et al. *Atlas of Plant Cell Structure*. ISBN: 9784431549406.
- [65] Ondřej Novotný, Karel Cejpek, and Jan Velišek. “Formation of carboxylic acids during degradation of monosaccharides”. In: *Czech Journal of Food Sciences* 26.2 (2008), pp. 117–131. ISSN: 12121800.
- [66] Francis Orata. *Derivatization reactions and reagents for gas chromatography analysis, Advanced Gas Chromatography Progress in Agricultural, Biomedical and Industrial Applications*. Intech, 2012, pp. 83–156. ISBN: 978-953-51-0298-4. DOI: 10.5772/33098. URL: <http://forensicscienceeducation.org/wp-content/uploads/2013/02/Analytical-derivatization-.pdf>.
- [67] Gaio Paradossi et al. “A physico-chemical study on the polysaccharide ulvan from hot water extraction of the macroalga *Ulva*”. In: *International Journal of Biological Macromolecules* 25.4 (1999), pp. 309–315. ISSN: 01418130. DOI: 10.1016/S0141-8130(99)00049-5.
- [68] Yu Pengzhan et al. “Antihyperlipidemic effects of different molecular weight sulfated polysaccharides from *Ulva pertusa* (Chlorophyta)”. In: *Pharmacological Research* 48.6 (2003), pp. 543–549. ISSN: 10436618. DOI: 10.1016/S1043-6618(03)00215-9.
- [69] Elizabeth Percival. “The polysaccharides of green , red and brown seaweeds : Their basic structure , biosynthesis and function”. In: *British Phycological Journal* 14.2 (June 1979), pp. 103–117. DOI: 10.1080/00071617900650121.

- [70] Elizabeth Percival. “The polysaccharides of green, red and brown seaweeds: Their basic structure, biosynthesis and function”. In: *British Phycological Journal* 14.2 (1979), pp. 103–117. ISSN: 0007-1617. DOI: 10.1080/00071617900650121.
- [71] Víctor Pérez Martínez. “ACID HYDROLYSIS OF HEMICELLULOSES FROM HARDWOOD AND SOFTWOOD WITH HOMOGENEOUS AND HETEROGENEOUS CATALYSTS”. MA thesis. UNIVERSIDAD DE VALLADOLID, Åbo Akademi University, 2015, p. 163.
- [72] R. Pezoa-Conte et al. “Deconstruction of the green alga *Ulva rigida* in ionic liquids: Closing the mass balance”. In: *Algal Research* 12 (2015), pp. 262–273. ISSN: 22119264. DOI: 10.1016/j.algal.2015.09.011.
- [73] Camila L Pires et al. “Sulfated polysaccharide extracted of the green algae *Caulerpa racemosa* increase the enzymatic activity and paw edema induced by sPLA2 from *Crotalus durissus terri fi cus* venom”. In: *Revista Brasileira de Farmacognosia - Brazilian Journal of Pharmacognosy* 23.4 (2013), pp. 635–643. ISSN: 0102-695X. DOI: 10.1590/S0102-695X2013005000050. URL: <http://dx.doi.org/10.1590/S0102-695X2013005000050>.
- [74] A M Prokhorov. *Great Soviet Encyclopedia: A Translation of the 3rd Edition, Index to*. Great Soviet Encyclopedia. publisher not identified, 1981. URL: <https://books.google.fi/books?id=N0o-YgEACAAJ>.
- [75] Huimin Qi et al. “Antioxidant activity of different sulfate content derivatives of polysaccharide extracted from *Ulva pertusa* (Chlorophyta) in vitro”. In: *International Journal of Biological Macromolecules* 37.4 (2005), pp. 195–199. ISSN: 01418130. DOI: 10.1016/j.ijbiomac.2005.10.008. URL: http://ac.els-cdn.com.ezproxy.uct.ac.za/S0141813005002333/1-s2.0-S0141813005002333-main.pdf?{_}tid=d9c1c7cc-84e6-11e5-a8cf-0000aacb35f{\&}acdnat=1446856453{_}eac4db7230195404220ae80db1a8e827.
- [76] Huimin Qi et al. “In vitro antioxidant activity of acetylated and benzoylated derivatives of polysaccharide extracted from *Ulva pertusa* (Chlorophyta)”. In: *Bioorganic and Medicinal Chemistry Letters* 16.9 (2006), pp. 2441–2445. ISSN: 0960894X. DOI: 10.1016/j.bmc1.2006.01.076.
- [77] B. Quemener, M. Lahaye, and C. Bobin-Dubigeon. “Sugar determination in *ulvans* by a chemical-enzymatic method coupled to high performance anion exchange chromatography”. In: *Journal of Applied Phycology* 9.2 (1997), pp. 179–188. ISSN: 09218971. DOI: 10.1023/A:1007971023478.

- [78] Julie Bordonaro Rebecca Carrier. *Chromatography - Equipment*. 1994. URL: <http://www.rpi.edu/dept/chem-eng/Biotech-Environ/CHROM0/chromequip.html>.
- [79] Audrey Robic et al. "Ultrastructure of Ulvan: A polysaccharide from green seaweeds". In: *Biopolymers* 91.8 (2009), pp. 652–664. ISSN: 00063525. DOI: 10.1002/bip.21195.
- [80] G Roesijadi, S B Jones, and Y Zhu. "Macroalgae as a Biomass Feedstock : A Preliminary Analysis". In: *Pacific Northwest National Laboratory, Richland* (Sept. 2010), pp. 1–50. ISSN: PNNL-19944; Other: BM0204010; TRN: US201106%%96. URL: http://www.pnl.gov/main/publications/external/technical_reports/PNNL-19944.pdf.
- [81] Kara Rogers. *Fungi, Algae and Protist*. Britannica Educational Publishing. ISBN: 9781615304639.
- [82] A. I. Ruiz-Matute et al. "Derivatization of carbohydrates for GC and GC-MS analyses". In: *Journal of Chromatography B: Analytical Technologies in the Biomedical and Life Sciences* 879.17-18 (2011), pp. 1226–1240. ISSN: 15700232. DOI: 10.1016/j.jchromb.2010.11.013. URL: <http://dx.doi.org/10.1016/j.jchromb.2010.11.013>.
- [83] Dinabandhu Sahoo and Joseph Seckbach. *The Algae World*. Vol. 26. 2015. ISBN: 978-94-017-7320-1. DOI: 10.1007/978-94-017-7321-8. URL: <http://link.springer.com/10.1007/978-94-017-7321-8>.
- [84] Tapio Salmi et al. "Kinetic modeling of hemicellulose hydrolysis in the presence of homogeneous and heterogeneous catalysts". In: *AIChE Journal* 60.3 (2014), pp. 1066–1077. ISSN: 1547-5905. DOI: 10.1002/aic.14311. URL: <http://dx.doi.org/10.1002/aic.14311>.
- [85] Gour Gopal Satpati and Ruma Pal. "Biochemical composition and lipid characterization of marine green alga *Ulva rigida*- a nutritional approach". In: *Journal of Algal Biomass Utilization* 2.4 (2011), pp. 10–13.
- [86] Sheffield Hallam University. *Chromatography: Introductory theory*. 2015. URL: <http://teaching.shu.ac.uk/hwb/chemistry/tutorials/chrom/chrom1.htm>.
- [87] Sigma-Aldrich Co. "HMDS+TMCS+Pyridine Product Specification". In: *Product Specification* 3 (1997), pp. 1–2.

- [88] Ralph Sims et al. “From 1st to 2nd Generation Bio Fuel Technologies: An overview of current industry and RD&D activities”. In: *IEA Bioenergy* November (2008), pp. 1–124.
- [89] Bhaskar Singh, Kuldeep Bauddh, and Faizal Bux. *Algae and Environmental Sustainability*. Ed. by Springer. 2015. ISBN: 9788132226390.
- [90] P. F. Siril, H. E. Cross, and D. R. Brown. “New polystyrene sulfonic acid resin catalysts with enhanced acidic and catalytic properties”. In: *Journal of Molecular Catalysis A: Chemical* 279.1 (2008), pp. 63–68. ISSN: 13811169. DOI: 10.1016/j.molcata.2007.10.001.
- [91] Eero Sjostrom and Raimo Alen. *Analytical Methods in Wood Chemistry, Pulp- ing, and Papermaking*. Ed. by T. E. Timell. Springer, 1998, p. 327. ISBN: 9783642640711. DOI: 10.1007/978-3-662-08986-6.
- [92] D A Skoog, F J Holler, and S R Crouch. *Principles of Instrumental Analysis*. International student edition. Thomson Brooks/Cole, 2007. ISBN: 9780495012016. URL: <https://books.google.fi/books?id=Gr0sQgAACAAJ>.
- [93] Robert V. Stick and Spencer J. Williams. *Carbohydrates: The Essential Molecules of Life*. 2009, pp. 413–443. ISBN: 9780240521183. DOI: 10.1016/B978-0-240-52118-3.00012-0. URL: <http://www.sciencedirect.com/science/article/pii/B9780240521183000120>.
- [94] Inn Shi Tan, Man Kee Lam, and Keat Teong Lee. “Hydrolysis of macroalgae using heterogeneous catalyst for bioethanol production”. In: *Carbohydrate Polymers* 94.1 (2013), pp. 561–566. ISSN: 01448617. DOI: 10.1016/j.carbpol.2013.01.042. URL: <http://dx.doi.org/10.1016/j.carbpol.2013.01.042>.
- [95] Eindhoven University of Technology. *Systems Biology and Metabolic Diseases*. 2012. URL: http://bmi.bmt.tue.nl/sysbio/parameter_estimation/parameter_estimation.html.
- [96] Brijesh K Tiwari and Declan J Troy. *Seaweed Sustainability Food and Non-Food Applications*. Elsevier, 2015, p. 470. ISBN: 9780124186972.
- [97] Chisako Usuki, Yukitaka Kimura, and Shuji Adachi. “Degradation of pentoses and hexouronic acids in subcritical water”. In: *Chemical Engineering and Technology* 31.1 (2008), pp. 133–137. ISSN: 09307516. DOI: 10.1002/ceat.200700391.
- [98] Léa Vilcoq et al. “Hydrolysis of oligosaccharides over solid acid catalysts: A review”. In: *ChemSusChem* 7.4 (2014), pp. 1010–1019. ISSN: 18645631. DOI: 10.1002/cssc.201300720.

- [99] R Wang et al. “Degradation Kinetics of Glucuronic Acid in Subcritical Water”. In: *Bioscience, biotechnology, and biochemistry* 74.3 (2010), pp. 601–605. ISSN: 0916-8451. DOI: 10.1271/bbbJI0S. URL: <http://www.tandfonline.com/doi/abs/10.1271/bbb.90818>.
- [100] Cassie Welker et al. “Engineering Plant Biomass Lignin Content and Composition for Biofuels and Bioproducts”. In: *Energies* 8.8 (2015), pp. 7654–7676. ISSN: 1996-1073. URL: <http://www.mdpi.com/1996-1073/8/8/7654/>.
- [101] Isuru Wijesekara, Ratih Pangestuti, and Se Kwon Kim. “Biological activities and potential health benefits of sulfated polysaccharides derived from marine algae”. In: *Carbohydrate Polymers* 84.1 (2011), pp. 14–21. ISSN: 01448617. DOI: 10.1016/j.carbpol.2010.10.062. URL: <http://dx.doi.org/10.1016/j.carbpol.2010.10.062>.
- [102] Charles E Wyman. *Aqueous Pretreatment of Plant Biomass for Biological and Chemical Conversion to Fuels and Chemicals* (Google eBook). 2013, p. 568. ISBN: 0470975822. URL: <http://books.google.com/books?hl=en&lr=&id=TI7XbVsiyEEC&pgis=1>.
- [103] Charles E Wyman et al. “Hydrolysis of Cellulose and Hemicellulose”. In: *Polysaccharides: Structural Diversity and Functional Versatility* (2005), pp. 994–1033. DOI: 10.1201/9781420030822.ch43.
- [104] Hela Yaich et al. “Effect of extraction conditions on the yield and purity of ulvan extracted from *Ulva lactuca*”. In: *Food Hydrocolloids* 31.2 (2013), pp. 375–382. ISSN: 0268005X. DOI: 10.1016/j.foodhyd.2012.11.013.
- [105] Bin Yang et al. “Enzymatic hydrolysis of cellulosic biomass”. In: *Biofuels* 2.4 (2011), pp. 421–450. ISSN: 1759-7269. DOI: 10.4155/bfs.11.116.

